

STATUS OF THESIS

Title of thesis

Investigation on CO₂ Induced Asphaltene Precipitation Using Baronia
Oil Samples

ALI FIKRET MANGI ALTA'EE

Hereby allow my thesis to be placed at the information Resource Center (IRC) of Universiti Teknologi PETRONAS (UTP) with the following conditions:

1. The thesis becomes the property of UTP
2. The IRC of UTP may make copies of the thesis for academic purposes only.
3. The thesis is classified as:
 Confidential
 Non-confidential

If this thesis is confidential, please state the reason:

PETRONAS related interest

The contents of the thesis will remain for _____ years.

Remarks on Disclosure:



ALI FIKRET MANGI ALTA'EE
Universiti Teknologi PETRONAS
Malaysia.

Date: 15th June 2009

Endorsed by



ISMAIL MOHD. SAAID
Universiti Teknologi PETRONAS
Malaysia.
Assoc. Prof. Dr. Ismail M Saaid
Faculty Member
Geoscience & Petroleum Engineering Department
Universiti Teknologi PETRONAS

Date: 15th June 2009

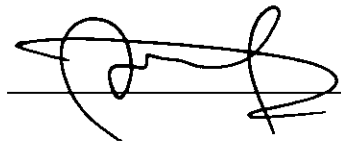
UNIVERSITI TEKNOLOGI PETRONAS

Approval by Supervisor (s)

The undersigned certify that they have read, and recommend to the Postgraduate Studies Programme for acceptance, a thesis titled "Investigation on CO2 induced Asphaltene Precipitation using Baronia Oil Samples" submitted by (Ali Fikret Mangi Alta'ee) for the fulfillment of the requirements for the degree of Master of Science in Petroleum Engineering.

Date

Signature

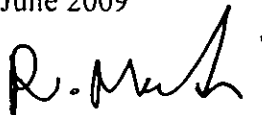
:  _____

Main Supervisor

: AP. Dr. Ismail Mohd. Saaid
Assoc. Prof. Dr. Ismail M Saaid
Faculty Member
Geoscience & Petroleum Engineering Department
Universiti Teknologi PETRONAS

Date

: 15th June 2009



Co-Supervisor

: AP. Dr. Rahim Masoudi

TITLE PAGE

UNIVERSITI TEKNOLOGI PETRONAS

Investigation on CO₂ Induced Asphaltene Precipitation Using Baronia Oil

Samples

By

Ali Fikret Mangi Alta'ee

A THESIS

SUBMITTED TO THE POSTGRADUATE STUDIES PROGRAMME

AS A REQUIREMENT FOR THE
DEGREE OF MASTER OF SCIENCE

PETROLEUM ENGINEERING

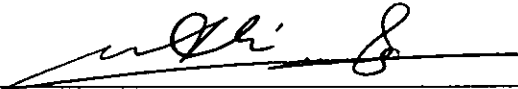
BANDAR SERI ISKANDAR,

PERAK

JUNE, 2009

DECLARATION

I hereby declare that the thesis is based on my original work except for quotations and citations which have been duly acknowledge. I also declare that it has not been previously or concurrently submitted for any other degree at UTP or other institutions.

Signature : 
Name : **Ali Fikret Mangi Alta'ee**
Date : **June 15th, 2009**

ACKNOWLEDGEMENT

All gratitude and thanks are due to “*ALLAH*” for his guidance throughout this work and for all the blessings he has bestowed upon me. This study would not have been done without the help of “*ALLAH*”.

I would like to thank my dear wife, for her support and her patient, she was the amazing supporter for me to finish this work successfully.

I would like to thank my supervisor Dr. Ismail Mohd. Saaid for his supervision and guidance throughout the whole work with this thesis. I greatly appreciate his encouragement to go ahead with my work.

Special thanks to my co-supervisor Dr. Rahim Masoudi, for his knowledge and technical guidance. I greatly appreciate his advices.

Thank you Dr. Anwar Raja, for giving me the opportunity to join PETRONAS Research Sdn Bhd (PRSB). Thank you as well for your supervision and encouragement during the early steps of this work.

Special thanks to my dear brother Mohamed Idrees Ali, your knowledge in this field and your support and guidance have been mainly responsible for the success of this work. It was an amazing learning experience that I will never forget.

Thank you to staff members of Sub-Surface and Facility Engineering Group in PETRONAS Research Sdn Bhd (PRSB), for making their laboratory available for me. Thank you as well for helping in the experimental work of this study.

Special thanks to Dr. Nasir Darman for giving me the opportunity to join this project, and thanks to the PMU staff and PCSB EOR group for the assistant.

Thank you to all staff members of the postgraduate studies program. Appreciation is acknowledged for the assistantship opportunity provided by UNIVERSITI TEKNOLOGI PETRONAS.

Finally thank you to my parents, for their prayers and support. Thank you to my friends and many other who have in a way or another helped me.

ABSTRACT

Asphaltene precipitation is one of the serious problems during the secondary and tertiary oil recovery in light oil reservoirs using CO₂ injection. Baronia RV2 light oil sample has been chosen to study the possibility of asphaltene precipitation during the contact of CO₂ with oil. When CO₂ is in contact with light oil, there is a tendency for asphaltene precipitation which might lead to serious production and reservoir problems such as permeability reduction, porosity alteration, and plugging of wellbore and possibility of blocking the whole production system.

The present research is to investigate the asphaltene precipitation phenomenon and to analyze the mechanism of asphaltene deposition during the CO₂ injection process. A laboratory study for crude oil characterization has been carried out to determine the properties of reservoir fluid. A routine and special PVT analysis using a high pressure and temperature visual cell has been carried out to examine the phase behavior of asphaltene and CO₂. Oil expansion test under CO₂ injection and micro- slim tube test have been carried out to investigate the swelling factor and minimum miscibility pressure and to identify the effect of different concentration of CO₂ on asphaltene precipitation. Static and dynamic asphaltene studies have been carried out to determine the asphaltene precipitation at different CO₂ concentrations and different pressures. Asphaltene precipitation was found during the static asphaltene test when the CO₂ concentration was changed under reservoir pressure and temperature. The results show that the amount of precipitated asphaltene increased with increasing the concentration of injected CO₂. However; in the dynamic test asphaltene precipitation fluctuated when both pressure and CO₂ concentration were changed simultaneously. Results from dynamic asphaltene test were analyzed using statistical analysis method to predict the asphaltene precipitation under the effect of both pressure and CO₂ concentration. Multiple regression analysis and analysis of variance (ANOVA) were used to get the multiple linear regression model of asphaltene precipitation for Baronia RV2. The model was tested by using different concentration of CO₂ at selected pressures to predict the asphaltene precipitation at any pressure and CO₂ concentration. Comparison was made between the measured and predicted asphaltene precipitation.

ABSTRAK

Pemendakan asfaltena merupakan salah satu dari masalah serius semasa perolehan minyak sekunder dan tertiar di reserbor minyak ringan menggunakan suntikan CO₂. Sampel minyak ringan Baronia RV2 telah dipilih untuk mengkaji kemungkinan berlakunya pemendakan asfaltena semasa berlakunya sentuhan antara CO₂ dengan minyak. Apabila CO₂ berada di dalam keadaan tersentuh dengan minyak ringan, terdapat kecenderungan untuk pemendakan asfaltena yang mungkin akan membawa kepada masalah reserbor dan pengeluaran yang serius seperti pengurangan kebolehtelapan, perubahan keliangan, dan penutupan lubang telaga dan kemungkinan menyekat keseluruhan sistem pengeluaran.

Kajian ini bertujuan untuk menyelidik fenomena pemendakan asfaltena dan menganalisa mekanisma pemendakan asfaltena semasa proses suntikan CO₂. Satu kajian makmal untuk pencirian minyak mentah telah dijalankan bagi menentukan sifat bendalir reserbor. Analisa PVT rutin dan khas menggunakan sel visual tekanan dan suhu tinggi telah dijalankan untuk mengkaji kelakuan fasa asfaltena dan CO₂. Ujikaji pengembangan minyak di bawah suntikan CO₂ dan ujikaji tiub langsing mikro telah dijalankan untuk menyelidik faktor pembengkakan dan tekanan ketercampuran minima dan untuk mengenalpasti kesan kepekatan CO₂ yang berbeza terhadap pemendakan asfaltena. Kajian asfaltena dinamik dan statik telah dijalankan untuk menentukan pemendakan asfaltena pada tekanan dan kepekatan CO₂ yang berbeza. Pemendakan asfaltena didapati berlaku semasa ujikaji asfaltena statik apabila kepekatan CO₂ diubah pada suhu dan tekanan reserbor. Keputusan menunjukkan bahawa jumlah asfaltena termendak bertambah apabila kepekatan CO₂ yang disuntik juga bertambah. Walau bagaimanapun, dalam ujikaji dinamik pemendakan asfaltena berubah-ubah apabila kedua-dua tekanan dan kepekatan CO₂ diubah serentak. Keputusan dari ujikaji asfaltena dinamik telah dianalisa menggunakan kaedah analisa statistikal untuk menjangka pemendakan asfaltena di bawah kedua-dua kesan tekanan dan CO₂. Analisa regresi berbilang dan analisa varians (ANOVA) telah digunakan untuk mendapat model regresi linear berbilang pemendakan asfaltena bagi Baronia RV2. Model tersebut telah diuji menggunakan kepekatan CO₂ yang pelbagai pada beberapa tekanan terpilih untuk menjangka

pemendakan asfaltena pada sebarang tekanan dan kepekatan CO₂. Perbandingan di antara pemendakan asfaltena yang diramal dan diukur telah dibuat.

TABLE OF CONTENTS

STATUS OF THESIS.....	I
APPROVAL PAGE	II
TITLE PAGE	III
DECLARATION.....	IV
ACKNOWLEDGEMENT.....	V
ABSTRACT.....	VI
ABSTRAK	VII
TABLE OF CONTENTS	IX
LIST OF TABLES	XII
LIST OF FIGURES.....	XIII
CHAPTER I: INTRODUCTION.....	1
1.1 ENHANCED OIL RECOVERY (EOR).....	1
1.2 CO ₂ FLOODING	2
1.3 CO ₂ FLOODING MECHANISMS.....	2
1.4 ASPHALTENE PRECIPITATION	3
1.5 THE DEPOSITION PROBLEM	4
1.6 RESERVOIR BACKGROUND.....	5
1.7 PROBLEM STATEMENT.....	5
1.8 RESEARCH OBJECTIVES.....	6
1.9 RESEARCH METHODOLOGY.....	6
CHAPTER II: LITERATURE REVIEW	8
2.1 DEFINITION OF ASPHALTENE.....	8
2.2 NATURE OF ASPHALTENE	9
2.3 ASPHALTENE-RESINS RELATIONSHIP	10
2.4 MECHANISM OF ASPHALTENE PRECIPITATION	11
2.4.1 Effect of Fluid Composition Changes.....	13
2.4.2 Effect of Electrokinetic Effects.....	13
2.4.3 Effect of Pressure and Temperature Change	14
2.4.4 Effect of CO ₂ Injection	15

2.5 MODELING ASPHALTENE PRECIPITATION.....	19
2.6 REMOVAL OF ASPHALTENE.....	21
2.7 SUMMARY OF THE LITERATURE REVIEW.....	22
CHAPTER III: METHODOLOGY.....	24
3.1 CRUDE OIL CHARACTERIZATION.....	24
3.1.1 Density Measurement.....	25
3.1.2 Asphaltene Content.....	26
3.1.3 Wax Content.....	29
3.1.4 Wax Appearance Temperature (WAT).....	30
3.1.5 Compositional Analysis of Stock Tank Oil (STO) up to C ₄₀₊	31
3.1.6 SARA Analysis.....	32
3.2 PHASE BEHAVIOR EXPERIMENTS.....	32
3.2.1 Compositional Analysis of Separator Oil and Separator Gas.....	33
3.2.2 Recombination of Separator Oil and Gas.....	34
3.2.3 Constant Composition Expansion Test (CCE).....	35
3.3 EOR EXPERIMENTS.....	37
3.3.1 Micro-Slim Tube Displacement (MST) Test.....	37
3.3.2 Swelling Test.....	40
3.4 ASPHALTENE PRECIPITATION EXPERIMENTS.....	41
3.4.1 Static Asphaltene Precipitation Test.....	41
3.4.2 Dynamic Asphaltene Precipitation Test.....	42
3.5 STATISTICAL ANALYSIS PROCEDURE.....	43
3.5.1 Analysis of Variance (ANOVA).....	45
CHAPTER IV: RESULTS AND DISCUSSION.....	47
4.1 CRUDE OIL CHARACTERIZATION.....	47
4.1.1 Compositional Analysis of STO up to C ₄₀₊	48
4.1.2 SARA Analysis.....	52

4.2 PHASE BEHAVIOR EXPERIMENTS.....	53
4.2.1 Compositional Analysis of Separator Oil	54
4.2.2 Compositional Analysis of Separator Gas	55
4.2.3 Calculation of recombined wellstream of Baronia RV2.....	56
4.2.4 Constant Composition Expansion (CCE)	59
4.3 EOR EXPERIMENTS	62
4.3.1 Micro-Slim Tube Displacement Test.....	62
4.3.2 Swelling Test	64
4.4 ASPHALTENE PRECIPITATION EXPERIMENTS	66
4.4.1 Static Asphaltene Precipitation Test	66
4.4.2 Dynamic Asphaltene Precipitation Test.....	68
4.5 STATISTICAL ANALYSIS FOR PREDICTION OF ASPHALTENE PRECIPITATION.....	72
4.5.1 Linear Regression Model.....	72
4.5.2 Analysis of Variance (ANOVA).....	73
4.5.3 Model Fitting and Statistical Analysis.....	73
4.5.4 Testing of Statistical Prediction of Asphaltene Precipitation	78
CHAPTER V: CONCLUSIONS AND RECOMMENDATIONS FOR FUTURE WORK	83
5.1 CONCLUSIONS.....	83
5.2 RECOMMENDATIONS FOR FUTURE WORK	84
REFERENCES.....	85
APPENDICES.....	91

LIST OF TABLES

Table	Title	Page
4.1	Crude oil characterization results	47
4.2	Composition of separator oil	54
4.3	Plus fraction properties of separator oil (Baronia RV2)	55
4.4	Composition of separator gas (Baronia RV2)	55
4.5	Composition of reservoir fluid (Baronia RV2)	56
4.6	Plus fraction properties for reservoir fluid (Baronia RV2)	57
4.7	Amount of CO ₂ added for Swelling Test	64
4.8	Results of CCE with different concentrations of CO ₂ at 204°F	65
4.9	Asphaltene precipitation with different pressures and CO ₂ concentrations	69
4.10	Results of regression analysis when $\beta_0 \neq$ zero	75
4.11	Results of regression analysis when $\beta_0 =$ zero	75
4.12	Results of the polynomial multiple regression model	81
4.13	Measured and predicted asphaltene precipitation	82

LIST OF FIGURES

Figure	Title	Page
2.1	The effect of solvent carbon number on asphaltenes precipitation	9
2.2	Asphaltenes-Resins Micelles	11
2.3	Pressure-composition and pressure-temperature asphaltene precipitation envelope	14
2.4	Comparison of the amount of carbon dioxide induced precipitation with the first and multiple contacts	18
3.1	PAAR DMA48 density meter	25
3.2	Reflux apparatus	27
3.3	GFD filter paper	28
3.4	Filtration apparatus	28
3.5	HP 5890 Series II High Temperature Gas Chromatography (HTGC) equipment	31
3.6	Gas Analyzer	33
3.7	Recombination Cell	34
3.8	High pressure visual PVT cell	36
3.9	Schematic diagram of Jefri phase behavior system	36
3.10	Micro-slim tube (MST) equipment	39
3.11	Schematic diagram of micro-slim tube (MST) equipment	39
4.1	Fingerprints of Baronia RV2 crude oil	49
4.2	Fingerprints of four different types of crude oil	49
4.3	Single Carbon Number of Baronia RV2 Stock Tank Oil	51
4.4	SARA analyses by liquid chromatographic separation using n-C ₅ (Baronia RV2)	52
4.5	Single carbon number distribution for Baronia RV2 reservoir fluid	58
4.6	Pressure vs. volume at 204°F for Baronia RV2 recombine oil	60
4.7	Single phase and 2-phase for Baronia RV2	61
4.8	Oil Recovery vs. Displacement Pressure	63

Figure	Title	Page
4.9	Cumulative asphaltene precipitation with different %mol of CO ₂ at 3008 psia and 204°F	67
4.10	Asphaltene precipitation with different %mol of CO ₂ and different pressures at 204°F	70
4.11	Three-dimension plot for measured and predicted asphaltene precipitation	78
4.12	Calculated asphaltene precipitation versus. CO ₂ concentration at different pressures	79
4.13	Calculated asphaltene precipitation versus. CO ₂ concentration at different pressures using equation 4.6	82

CHAPTER I

INTRODUCTION

Gas injection is one of the most practically used EOR methods to improve oil recovery (Green and Willhite, 1998). Recently, the use of non- hydrocarbon gases such as nitrogen (N₂) and carbon dioxide (CO₂) are becoming commonly applied to enhance the gas injection EOR (Martin, 1992; Sarma, 2003). CO₂ flooding in particular, is the second most common enhanced oil recovery process (i.e. next to steam flooding), which has resulted in significant recovery worldwide (Milind, 2002). Nevertheless mixing of CO₂ and reservoir oil might create multiple phase equilibria, which includes a solid phase precipitation such as asphaltene (Sarma, 2003).

1.1 ENHANCED OIL RECOVERY (EOR)

Oil recovery generally can be divided into three stages: primary, secondary and tertiary. These stages described the oil production from a reservoir depending on the production duration and the natural energy in the reservoir (Green and Willhite, 1998).

Enhanced oil recovery (EOR) usually considered in the tertiary recovery processes after the secondary recovery became uneconomically. EOR involved the injection of fluids into a reservoir. The injected fluids supplement the natural energy of the reservoir lead to displace the remaining oil toward the producing well due to interact between the injected fluids and the reservoir rock-oil system which create suitable conditions for oil recovery. These interacts might be resulted in oil swelling, interfacial tension reduction, decreasing oil viscosity, or wettability modification (Green and Willhite, 1998).

1.2 CO₂ FLOODING

CO₂ flooding is one of the gases used in EOR to displace the residual oil after the waterflooding (Mungan, 1979; Green and Willhite, 1998). When oil and water contain a significant amount of dissolved CO₂, their viscosities, densities, and compressibilities are modified in a direction which helps increase the oil recovery efficiency. Therefore, the use of CO₂ in oil recovery should be considered where CO₂ is available in sufficient quantities and is economically priced (Mungan, 1979).

There are several factors that have to be considered for CO₂ flooding (Mungan, 1979; Green and Willhite, 1998):

- CO₂ must flow through the reservoir above its minimum miscibility pressure (MMP).
- CO₂ is most effective with light oils, those with oil gravity greater than 25° API.
- Since CO₂ flows through the reservoir more easily than oil, it also does best in reservoir with low heterogeneity. (If some layers of the reservoir are distinctly more permeable than others, CO₂ will flow there preferentially, rather than maintaining uniform front and high sweep efficiency).
- Stratification and fracturing can cause loss of CO₂ and reduce oil recovery.

1.3 CO₂ FLOODING MECHANISMS

CO₂ flooding process can be classified as immiscible or miscible, even though CO₂ and crude oils are not actually miscible upon first contact in the reservoir (Martin and Taber, 1992). Whether it is carried out as a miscible or an immiscible displacement, the following mechanisms play some roles in increasing the oil recovery by CO₂ flooding (Mungan, 1979; Martin and Taber, 1992):

- Reduction of oil viscosity
- Swelling of oil
- Extraction or vaporization of oil
- Miscibility effects

-
- Reduction of interfacial tension
 - Solution gas drive or blow-down recovery
 - Increase in injectivity

In miscible CO₂ displacement, the vaporization of crude oil, and reduction of interfacial tension are important mechanisms (Fred and Stalkup, 1983). On the other hand, reduction of crude oil viscosity and its swelling are important mechanisms in immiscible carbon dioxide displacement (Mungan, 1979).

In miscible displacement, CO₂ is effective in recovering oil for a number of reasons. First, CO₂ being soluble in crude oil at reservoir pressure, swells the net oil volume and reduces oil viscosity long before miscibility is achieved by a vaporizing-gas-drive mechanism (Fred and Stalkup, 1983). Second, when miscibility has been approached, the oil-CO₂ phase contains many of the intermediate hydrocarbon components that flow together. Third, the oil-CO₂ phase has relatively low interfacial tension and high apparent volume as compared with the water phase (Fred and Stalkup, 1983). As a result, high oil recovery may occur at pressures below those required for the generation of miscibility. The generation of miscibility between oil and CO₂ is still considered to be the most important mechanism and this will occur in most CO₂/crude-oil system when the pressure is high enough (Fred and Stalkup, 1983; Martin and Taber, 1992).

1.4 ASPHALTENE PRECIPITATION

The precipitation of asphaltene during CO₂ miscible flooding can reduce the permeability of the reservoir rocks near the well-bore region causing formation damage (Sim *et al.*, 2005), and tubing plug-up (Kokal and Sayegh, 1995; Sim *et al.*, 2005) leading to production losses. It was reported that the amount of asphaltene in crude oil is not the main reason of asphaltene precipitation (Kokal and Sayegh, 1995; Sarma, 2003). The main reason of asphaltene precipitation was reportedly due to disturbance of the thermodynamic equilibrium of the asphaltene-resins micelles by changing the pressure, temperature and oil composition (Leontaritis, and Mansoori, 1987; Saram, 2003; Buenrostro-Gonzalez *et al.*, 2004).

Extensive field and laboratory data have shown that the lighter the oil, the lower the asphaltene solubility (Sarma, 2003). Asphaltene would precipitate relatively more easily from light oil than from heavy oil, in spite of the heavier oil might have much higher asphaltene content. For example, the heavier Venezuelan Boscan crude with 17.2 %wt asphaltene was produced nearly problem-free, on the other hand the light crude of Hassi-Messaoud in Algeria with 0.15 %wt asphaltene encountered many production problems due to asphaltene precipitation (Sarma, 2003).

Asphaltene is a highly condensed polyaromatic structure or molecule, consisting primarily of carbon, hydrogen and minor proportion of hetero elements such as sulfur, nitrogen, oxygen (Mansoori, 1997; Sarma, 2003). The injected CO₂, could cause changes in the fluid behavior, equilibrium conditions and also alter the asphaltene-to-resin ratio of crude oil which favors precipitation of organic solids, mainly asphaltenes (Buenrostro-Gonzalez *et al.*, 2004). Once asphaltenes have been precipitated from oil during CO₂ flooding, they may continue to flow as suspended particles or they may deposit onto the rock surface causing plugging and altering the wettability of reservoir matrix, which can severely reduce recovery efficiency and cause formation damage (De Boer *et al.*, 1995; Buenrostro-Gonzalez *et al.*, 2004).

1.5 THE DEPOSITION PROBLEM

In many cases, deposition of asphaltenes could occur in the reservoir, in the well tubing or it can be carried through the flow lines into the separators and other down stream equipment. The cost of cleaning asphaltenes from equipments can be very expensive and significantly affect the economics of a project (Kokal and Sayegh, 1995).

Many studies have suggested that asphaltenes precipitation might be caused by changes in thermodynamic conditions of temperature, pressure and oil composition (Kokal and Sayegh, 1995; Mansoori, 1997; Sarma, 2003; Buenrostro-Gonzalez *et al.*, 2004). Previous observations indicated that destabilized colloidal system of crude oil can lead to asphaltene precipitation. CO₂ injection process is thought as one of the causes of destabilizing the colloidal system of crude oil (Mansoori, 1997). The

injected CO₂ caused changes in the reservoir fluid composition, pressure and temperature that could lead to precipitation of asphaltene.

1.6 RESERVOIR BACKGROUND

Baronia RV2 is one of the major oil reservoirs located in Baronia field in the Baram Delta in water depth of 250 ft below MSL (Mean Sea Level) in block SK15 of the Baram Delta, approximately 40 kilometers offshore NW of Lutong, Sarawak. It was discovered in July 1967 by well BN-1 and production started in May 1972 with an estimated STOIIP of 711 MMSTB and ultimate recovery of 322 MMSTB. The Baronia RV2 reservoir is a sandstone with an average porosity of approximately 19% and average permeability of 70 mD. Since no gas was seen on logs, RV2 was assumed to be under-saturated reservoir at the initial pressure of 3420 psi and temperature of 194° F when production started 1972. The oil gravity is around 42° API, and oil viscosity of 0.3 cP. The current reservoir temperature is 204° F, and the initial reservoir pressure has depleted to become 3008 psia. Baronia RV2 is under water injection since 1994. A reservoir simulation study carried out in 2001 predicted that the water injection had an excellent volumetric sweep efficiency, which was supported by a very favorable mobility ratio of less than 1 (Nor Idah, 2005). The findings suggest that any further recovery improvement in the RV2 reservoirs should be focused on the application of EOR process that can further reduce the remaining oil (Nor Idah, 2005).

1.7 PROBLEM STATEMENT

The problem of asphaltene precipitation during CO₂ injection in light oil reservoirs is one of the serious problems facing the oil production (Kokal and Sayegh, 1995; Mansoori, 1997; Sarma, 2003; Buenrostro-Gonzalez *et al.*, 2004). The precipitation of asphaltene during CO₂ flooding for light oil reservoirs could cause formation plugging and wettability reversal which could lead to reduced recovery efficiencies. In many cases, the precipitated asphaltene can plug up well tubing and it also may go to the well head and downstream separators.

The Baronia RV2 reservoir, which produces light oil with very low asphaltene content, has been identified by PETRONAS for water alternating CO₂ injection as a tertiary recovery process (Nor Idah, 2005). Asphaltene precipitation could be anticipated since other reservoirs with similar quality of crude oil as that of Baronia RV2 has problem of asphaltene precipitation. In addition, many researchers seemed to agree that the mechanism of asphaltene deposition is still not fully understood and rather dependent on the composition, pressure and temperature of the reservoir. Therefore, for the case of Baronia RV2 reservoir, there is a need to identify factors that could potentially cause precipitation of asphaltene during the CO₂ injection process. Information from this study would be beneficial in the long term project planning and implementation which could lead to efficient oil recovery and substantial monetary savings.

1.8 RESEARCH OBJECTIVES

This study aims to:

1. Characterize Baronia RV2 crude compositions and their tendency for asphaltene precipitation in the presence of CO₂.
2. Determine conditions of pressure and CO₂ concentration with minimum precipitation of asphaltene.
3. Propose a statistical correlation between CO₂ concentration and pressure for the prediction of asphaltene precipitation for the Baronia RV2 oil.

1.9 RESEARCH METHODOLOGY

A detailed experimental investigation on CO₂ induced asphaltene precipitation using Baronia RV2 oil samples has been carried out through a series of laboratory studies consisting of the followings:

1. Crude oil characterization using stock tank oil (STO).
2. Phase behavior experiments of recombined oil (live oil).
3. EOR experiments.

-
4. Asphaltene precipitation experiments.
 5. Statistical analysis of laboratory data (CO₂ concentration and pressure).

CHAPTER II

LITERATURE REVIEW

This chapter present report from the literature on the nature of asphaltene and its characteristics. Mechanisms of asphaltene precipitation and factors that lead to asphaltene precipitation during CO₂ injection are discussed.

2.1 DEFINITION OF ASPHALTENE

The term “asphaltene” is credited to a French scientist Boussngault who used it to describe certain constituents during distillation of asphalts in eastern France and Peru. These constituents were insoluble in alcohol but soluble in turpentine. However, because they resembled the parent asphalt itself in appearance; he referred them as “asphaltene” to signify their origin. In simple words, “asphaltene” and “asphalt” are not the same; rather, asphaltene is a constituent of asphalt (Mansoori, 1997; Sarma, 2003). Mansoori (1997) shows a summary of researchers about definition of asphaltene. Nellensteyn defined asphaltenes as the fraction insoluble in low boiling point paraffin hydrocarbons, but soluble in carbon tetrachloride and benzene, while Marcusson defined asphaltene as the insoluble fraction in light gasolines and petroleum ether. Pfeiffer defined it as the fraction insoluble in n-heptane but soluble in toluene (Mansoori, 1997). Mitchell and Speight (1973) defined asphaltene as the fraction separated from crude oil or petroleum products upon addition of hydrocarbon solvents such as n-heptane.

Chemists nowadays define asphaltene as the part precipitated by addition of low boiling paraffin solvents such as n-heptane and benzene soluble fraction whether it is derived from carbonaceous sources such as petroleum, coal or oil shale (Mansoori, 1997). In term of physical appearance, asphaltenes are dark brown to black friable solids with no definite melting point; they decompose on heating leaving a carbonaceous residue and volatile products (Sarma, 2003; Speight, 2004). They are obtained from petroleum by the addition of a non-polar solvent such as a hydrocarbon with a surface tension lower than 25 dyne cm⁻¹ at 25°C (Speight, 2004). Liquids used for this purpose are low-boiling petroleum naphtha, petroleum ether, n-pentane, iso-pentane, n-heptane, and the likes (Speight, 2004). Asphaltenes are soluble in liquids

with a surface tension above 25 dyne cm^{-1} , such as pyridine, carbon disulfide, carbon tetrachloride, and benzene. Asphaltenes are insoluble in liquefied petroleum gases, such as methane, ethane and propane; In fact, propane is used commercially in processing petroleum residues for asphaltene constituents and resin constituents (Speight, 2004). Asphaltene can be classified by particular paraffin used to precipitate them from crude oil. It has been shown that various solvents precipitate different amounts of asphaltene as shown in Figure 2.1 (Mitchell, 1973; Kokal and Sayegh, 1995).

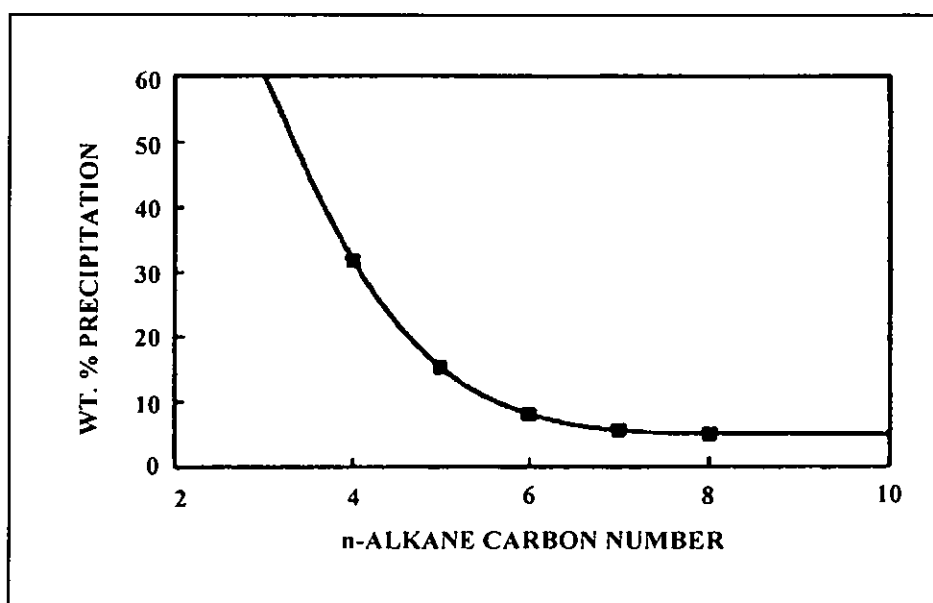


Figure 2.1 the effect of solvent carbon number on asphaltenes precipitation (Kokal and Sayegh, 1995)

2.2 NATURE OF ASPHALTENES

Generally crude oil is considered to be a colloidal system consisting primarily of hydrocarbons belonging to one of the following classes (McCain, 1990; Kokal and Sayegh, 1995; Nghiem, 1999; Alkafeef *et al.*, 2003; Speight, 2004):

- 1- Paraffins (or alkanes), that consist of chains of hydrocarbon segments ($-\text{CH}_2-$, $-\text{CH}_3$) that are connected by single bonds. Methane (CH_4) is the simplest and most common compound in petroleum reservoir fluids.
- 2- Naphtenes, which are hydrocarbons similar to paraffins, but containing one or more cyclic structures.

- 3- Aromatics, which contains one or more ring structures similar to benzene (C_6H_6). The atoms are connected by aromatic double bonds.
- 4- Resins and asphaltenes, which are large molecules consisting primarily of hydrogen and carbon, with one to three sulfur, oxygen, or nitrogen atoms per molecule. The basic structure is composed of rings, mainly aromatics, with three to ten or more rings per molecule. In addition to hydrocarbons, non-hydrocarbon compounds such as nitrogen (N_2), carbon dioxide (CO_2), and hydrogen sulfide (H_2S) are often found in petroleum mixtures (McCain, 1990).

The basic structures of resins and asphaltenes are similar (Mansoori, 1997; Speight, 2004). Both can be formed by oxidation of polycyclic aromatic hydrocarbons. On the other hand, both can be reduced to hydrocarbons by hydrogenation, which yields moderate to large hydrocarbon molecules, hydrogen sulfide, and water. Further, resins can be converted to asphaltenes by oxidation. The important difference between resins and asphaltenes is, asphaltenes do not dissolve in petroleum, but are dispersed as colloids, while resins dissolve easily in petroleum (McCain, 1990).

Asphaltene fractions are defined as dispersed colloids in the oil phase and are stable because the resins molecules are adsorbed by asphaltenes and act as protective bodies for asphaltene particles (Kokal and Sayegh 1995; Nghiem, 1999). Resins are defined as the fraction of the deasphalted oil that is strongly adsorbed by surface-active materials such as Fuller's earth, alumina or silica resins and can only be desorbed by a solvent such as pyridine or mixture of toluene and methanol (Buenrostro-Gonzalez *et al.*, 2004).

2.3 ASPHALTENES-RESINS RELATIONSHIP

Asphaltenes and resins are aromatic heterocompounds with aliphatic substitutions and they form the most polar fraction of crude oil; these resins and asphaltenes together are called micelles. Figure 2.2 shows asphaltenes-resins micelles (Leontaritis and Mansoori, 1987; Kokal and Sayegh, 1995; Fisher *et al.*, 2003; Buenrostro-Gonzalez *et al.*, 2004). Resins have a strong tendency to associate with asphaltenes. Such association to a large extent, determines, their solubility in crude oil (Buenrostro-Gonzalez *et al.*, 2004). The resins constituents play an important role in

the stability of petroleum and prevent separation of the asphaltene constituents (Speight, 2004). An important corollary of petroleum composition is that the mole fraction of resins is always larger than that of asphaltenes and hence the micelles are expected to be richer in resins (Speight, 2004).

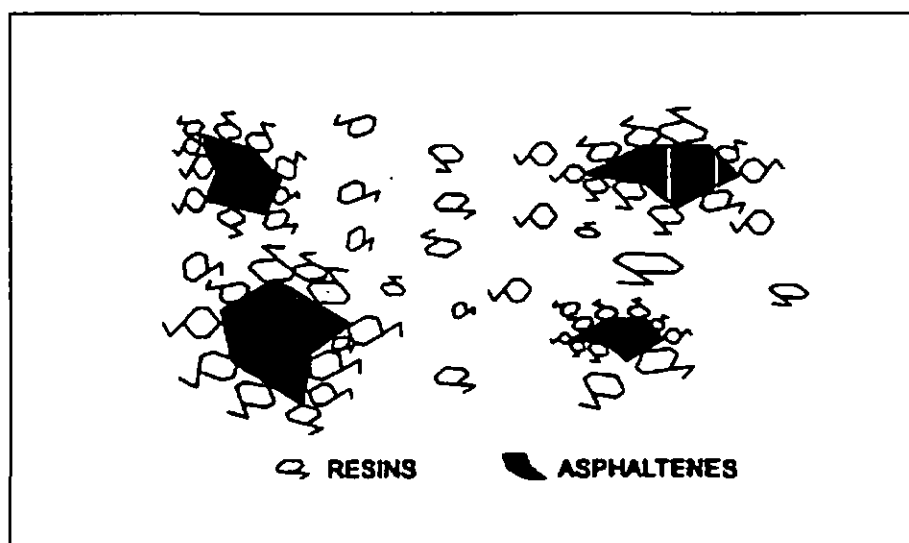


Figure 2.2 Asphaltene-Resins Micelles (Kokal and Sayegh, 1995)

The stability of petroleum can be represented by a three-phase system in which the asphaltene constituents, the aromatics (including the resins), and saturates are in a delicately balanced harmony (Speight, 2004). Mansoori (1997) suggested that there is a close relationship between asphaltenes, resins and high molecular weight polycyclic hydrocarbons. In nature, asphaltenes are hypothesized to be formed as a result of oxidation of natural resins. On the contrary, the hydrogenation of asphaltic compound products containing neutral resins and asphaltene produces heavy hydrocarbon oils i.e., neutral resins and asphaltenes are hydrogenated into polycyclic aromatic or hydroaromatic hydrocarbons. They differ, however, from polycyclic aromatic hydrocarbons by the presence of oxygen and sulfur in varied amounts (Mansoori, 1997).

2.4 MECHANISM OF ASPHALTENE PRECIPITATION

Reported studies seemed to agree that asphaltenes are heavy hydrocarbon molecules that are in colloidal suspension in the crude oil, stabilized by resins adsorbed on their surfaces (Hirschberg *et al.*, 1984; Leontaritis and Mansoori, 1987;

Nghiem, 1999). The precipitation of these heavy hydrocarbon molecules i.e., asphaltenes can cause serious problems in the reservoir such as permeability reduction and porosity alteration leading to formation damage, plugging of wellbore and blockage of production systems.

Changes in pressure, temperature and composition of reservoir fluids may alter the thermodynamic equilibrium of asphaltenes-resins micelles and subsequently cause asphaltene precipitation (Leontaritis and Mansoori, 1987; Kokal and Sayegh, 1995; Mansoori, 1997; Sarma, 2003). In this thesis, the term “precipitation” refers to the formation of asphaltene precipitate as a result of changes in thermodynamic equilibrium (imbalances), and “deposition” refers to the settling of the precipitated asphaltene onto the rock surface in a reservoir. Fisher and others (2003) reported that the process of asphaltene precipitation follow several important steps (Fisher *et al.*, 2003; Sim *et al.*, 2005).

- 1) The first step is precipitation; this is when the solid particles form a distinct phase as they come out of solution. The quantity and size of solid particles at this stage could be quite small.
- 2) The second step is flocculation, a process by which the small solid particles clump together and grow larger.
- 3) The third stage is deposition, a point at which the particles are so large that they can no longer be supported by the liquid and therefore settle out onto solid surfaces.

The mechanisms that lead to the precipitation of asphaltene, and its subsequent deposition are very complex, and not yet fully understood. However, it is widely proposed that some of the factors which may cause asphaltene precipitation are pressure drop, temperature changes, gas (HC and CO₂) injection, change in oil composition, pH shift due to the presence of acidic gases (CO₂, H₂S), acid stimulation, mixing of different crude oil streams, downhole shear and turbulence due to flow and, streaming potential (Sarma, 2003). In this chapter some of these factors will be discussed shortly, but the effect of gas injection (CO₂) will be discussed in details.

In few instances, the thermodynamic reversibility of the process has been reported (Sarma, 2003). However, laboratory results seem to suggest that in majority of cases, asphaltene precipitation process is irreversible (Mansoori, 1997; Sarma, 2003).

2.4.1 Effect of Fluid composition Changes

During the production life of a reservoir, the composition of reservoir fluid will change as the consequence of normal depletion during primary production of the reservoir. This will result in the loss of lighter components from the oil causing a decrease in the gas-oil ratio (GOR) and an increase in the density of the reservoir fluid. When oil loses its lighter-ends, more of the asphaltene content would go into solution with the oil. Therefore, would be expected a lesser asphaltene precipitation in older production reservoir (Kokal and Sayegh, 1995; Sarma, 2003). Addition of paraffinic compounds shifts the solubility of asphaltenes in the bulk oil because its solvent power affects the interactions among asphaltenes and resins. If the paraffinic compounds are good solvents for resins but not for asphaltenes, the interaction between resins and asphaltenes would be weak, which lead to asphaltenes precipitation (Buenrostro-Gonzalez *et al.*, 2004).

2.4.2 Electrokinetic Effects

Electrokinetic effects are due to the streaming electrical potential caused by in situ fluid flow in the reservoir could destabilize asphaltene micelles that are surrounded and peptized by resins. The asphaltene deposition problem has been found greater near the wellbores where the velocity is highest. To reduce deposition by electrokinetic effects the velocity of the fluids in the reservoir should be kept to a minimum. Large draw-downs should be avoided as these results in higher fluid velocities in the formation and wells. For asphaltic oils, the wells should be properly cleaned after periods of shut-ins or workovers. The flow rate should be kept small during the initial production stages and excessive opening of surface chokes avoided as it promotes asphaltene flocculation and deposition (Kokal and Sayegh, 1995; Sarma, 2003).

2.4.3 Effect of Pressure and Temperature Changes

Pressure depletion alone can destabilize asphaltenes and is likely the major reason for asphaltene deposition in well-bore pipes. As the density of crude oil decreases due to depressurization, the screening effect on asphaltene interactions arising from the pressure of oil components decreases, causing the interactions between asphaltenes to become stronger, which in turn induces the precipitation (Buenrostro-Gonzalez *et al.*, 2004). The formation of an asphaltene phase during natural production process depends on pressure and temperature. This behavior can be represented in a P-T diagram, where the onset points of asphaltene precipitation are localized, drawing asphaltene stability boundaries, similar to conventional hydrocarbon P-T phase diagram (Leontaritis, 1996, Buenrostro-Gonzalez *et al.*, 2004). This P-T diagram of asphaltenic fluids is called, the Asphaltene Precipitation Envelope (APE). The (APE) bounds the region where precipitation occurs. Figure 2.3 shows a typical pressure-composition APE and pressure-temperature APE (Leontaritis *et al.*, 1994; Leontaritis, 1996; Nghiem, 1999).

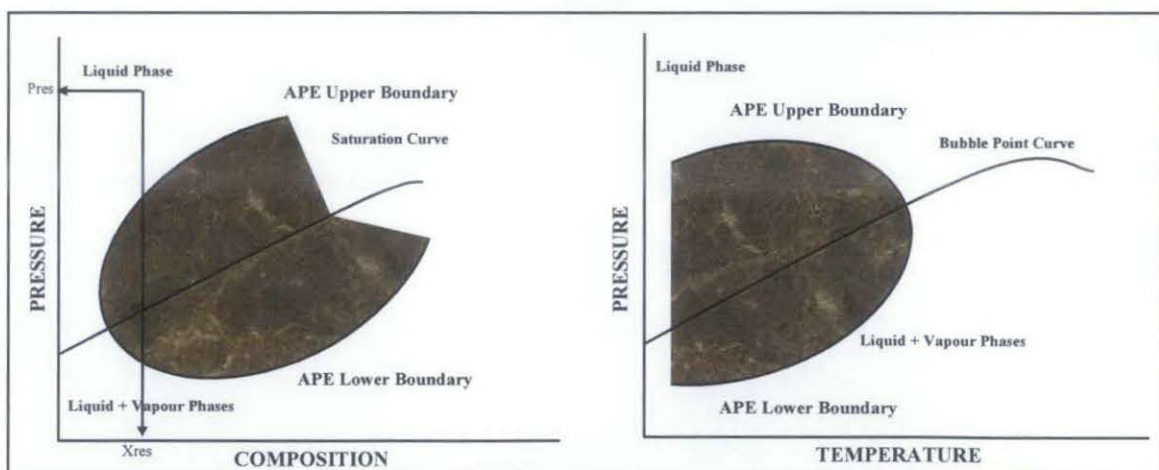


Figure 2.3 pressure-composition and pressure-temperature asphaltene precipitation envelope (Nghiem, 1999)

Buenrostro-Gonzalez *et al.* (2004) reported that the earliest experimental study on the effect of pressure in asphaltene precipitation was made in mixtures of bitumen with tetralin and *n*-pentane as precipitant. The study noted a consistent decrease in asphaltene precipitation as pressure increased. This observation was further validated

in mixtures of crude oil and hydrocarbons from methane to *n*-heptane. Later APEs were published by Leontaritis and Mansoori (1988) for the Prinos oil and by Leontaritis (1996) for South American and North American live oils. For these oils, it was observed that, as the temperature increases, the onset pressure decreases, requiring a bigger pressure change from the original reservoir *P–T* condition to initiate asphaltene precipitation (Buenrostro-Gonzalez *et al.*, 2004). The observation by Buenrostro-Gonzalez *et al.* (2004) of increased asphaltene solubility with temperature is in agreement with other observations by Andersen (1999), and Hirschberg *et al.* (1984). Hirschberg *et al.* (1984) presented an experimental study on temperature and pressure effects on the amount and nature of asphaltenic material precipitation. According to their results, high temperatures and pressures favored asphaltene solubility and further supported evidence on the reversibility of asphaltene precipitation (Hirschberg *et al.*, 1984; Buenrostro-Gonzalez *et al.*, 2004). Hammami *et al.* (2000) measured the APE for various Gulf of Mexico live oils through a series of isothermal pressure depletion experiments. Their results provided evidence of asphaltene precipitation above the saturation pressure and asphaltene redissolution below this pressure, and show that the pressure-depletion–induced asphaltene precipitation is a reversible process.

Fotland (1997) suggested that asphaltene precipitation is an irreversible process, especially when the crude oil is under conditions far from precipitation onset. On the other hand, Joshi *et al.* (2001) found that asphaltene precipitation in live oils is clearly reversible with pressure, although a subtle irreversibility may occur (Buenrostro-Gonzalez *et al.*, 2004). From previous observations, one can conclude that the pressure, composition of surrounding fluid and temperature are very important factors for asphaltene stability. It is generally believed that the effect of composition and pressure on asphaltene precipitation is stronger than the effect of temperature (De Boer *et al.*, 1995; Buenrostro-Gonzalez *et al.*, 2004)

2.4.4 Effect of CO₂ Injection

During gas flooding, e.g. CO₂ is injected into the reservoir to displace the residual oil left after water flooding. Miscibility of the solvent with the reservoir oil is a property that can also lead to the precipitation of asphaltene inside the reservoir matrix and its deposition on the reservoir rock. Most of the miscible solvents have the

potential for causing asphaltene flocculation. In this thesis the effect of CO₂ injection on asphaltene precipitation and the mechanisms that lead to asphaltene problems during CO₂ injection will be studied to avoid the asphaltene precipitation. The injected CO₂, when it is in contact with the reservoir oil, would cause changes in the fluid behavior and equilibrium conditions which favor precipitation of asphaltene (Kokal and Sayegh, 1995; Srivastava *et al.*, 1997; Sarma, 2003). Most of the oils in CO₂ flooding applications have relatively low asphaltene content, initially in the original oil. Asphaltene precipitation is one of the most serious production problems in the technological implementation of carbon dioxide flooding.

Sarma (2003) reported that during CO₂ tertiary flooding for medium gravity crude oil with 7%wt asphaltene content, asphaltene and wax deposition was serious problem. Analyses of laboratory and field data confirmed that gradual diffusion of CO₂ into the oil, which was being produced at low rate of about 100 BPD, had led to the precipitation of asphaltenes from the parent oil (Sarma, 2003). Kokal and Sayegh (1995) reported that asphaltene deposition also occurred in the well tubing in the Little Creek CO₂-flooding EOR pilot plant study in Mississippi.

The deposition is thought to have been caused by CO₂ which in the presence of water has an acidizing effect on the reservoir (Kokal and Sayegh, 1995). Reservoirs with even minute asphaltene content are susceptible to asphaltene precipitation due to not only pressure depletion during primary recovery, but also compositional change in the fluid during CO₂ injection (Mansoori, 1997; Srivastava, 1997; Moghadasi *et al.*, 2006). For instance Leontaritis *et al.* (1994) draw attention to the fact that the Boscan crude of Venezuela has not created any asphaltene problems, although it has over 17% by weight of asphaltenes. Whereas the Hassi-Massoud oil has severe asphaltene problems even though it has only a small fraction (0.1% by weight) of asphaltenes (Sarma, 2003).

2.4.4.1 Effect of CO₂ Concentration on Asphaltene Precipitation

Moghadasi *et al.* (2006) presented an experimental study on the effect of miscible CO₂ flood on asphaltene precipitation in Bangestan reservoir of Kupal field in south west of Iran. The asphaltene content of the recombined oil was 0.59 %wt and

the minimum pressure for CO₂ to be miscible with the oil at 160°F was 5300 psia. The study indicated that asphaltene began to precipitate at about 0.54 mole CO₂ concentrations and after that there was a linear increase in asphaltene precipitation with CO₂ concentration. The amount of asphaltene precipitation at the bubble point pressure was maximum. The study concluded that the amount of asphaltene precipitation due to CO₂ injection is dependent on the concentration of injected CO₂ gas, and the precipitation rapidly increase when the CO₂ concentration exceeds from one critical value (Moghadas *et al.*, 2006). Grau and Zana (1981) reported asphaltene precipitation in the extensive laboratory evaluation undertaken to evaluate the performance of a possible CO₂ tertiary project at Rangely Weber Sand Unit in Colorado. The precipitation occurred at gas concentration of 44 %mol or higher with an injected gas consisting of 95 %mol CO₂ and 5 %mol CH₄, while with a second gas (85 %mol CO₂, 5 %mol CH₄, and 10 %mol N₂), it occurred at gas concentration as low as 25 %mol (lowest gas concentration studied). The solid precipitation was estimated to be 2 to 5 %vol of the original reservoir oil (Parra-Ramirez *et al.*, 2001).

Ying *et al.* (2006) presented an experimental study on one oil field in China. The study indicated that with increasing injected CO₂, the precipitated asphaltene mass also increased. With 10 %mol CO₂ injection, the maximal asphaltene precipitation is 0.23 %mass, with 30 %mol CO₂ injection, the maximum is 0.44 %mass, with 50 %mol CO₂ injection, the maximum is 0.52 %mass and, with 60 %mol CO₂ injection, the maximum is 0.67 %mass. These phenomenon can be explained as the constant extraction effect of CO₂ of lighter hydrocarbons and some middle or heavier components from oil, which induces the content of heavier hydrocarbons, for example asphaltene, to increase (Ying *et al.*, 2006). Novosad and Constain (1990) observed precipitation at 40-50 %mol CO₂ concentrations (Novosad and Constain, 1990). Srivastava *et al.* (1995), indicated that asphaltene began to flocculate at about 42 %mol CO₂ concentration, and after that, there was a linear increase in asphaltene flocculation with CO₂ concentration (Parra-Ramirez *et al.*, 2001).

2.4.4.2 Effect of First and Multiple Contact of CO₂ on Asphaltene Precipitation

Carbon dioxide is highly soluble in oil and to a lesser extent in water. The miscibility between reservoir oil and CO₂ eliminates the interfacial tension and capillary forces, and thus improves oil recovery, in theory, all of the residual oil.

When the injected CO₂ and reservoir oil, mixed in any ratio, form a single phase, they are said to be first contact miscible. First contact miscibility can be achieved only for highly hydrocarbon rich gases, or at very high pressure for lean systems. Carbon dioxide is not in first contact miscible with most reservoir oils even at fairly high operating pressure. CO₂ can develop miscibility through multiple contacts under specific conditions of pressure and temperature, and specific oil compositions (Parra-Ramirez *et al.*, 2001). Parra-Ramirez *et al.* (2001) presented an experimental study on the effect of first and multiple contact for 34° API crude oil from Rangely field, Colorado. Rangely crude contains about 1.5 %wt asphaltene (as precipitated by n-heptane). It was determined that first-contact precipitation, at different carbon dioxide concentrations was negligible. Multiple contact experiments conducted to prove this hypothesis showed that multiple contact precipitation amounts were 3-5 times the first-contact precipitation values as shown in Figure 2.4 (Parra-Ramirez *et al.*, 2001).

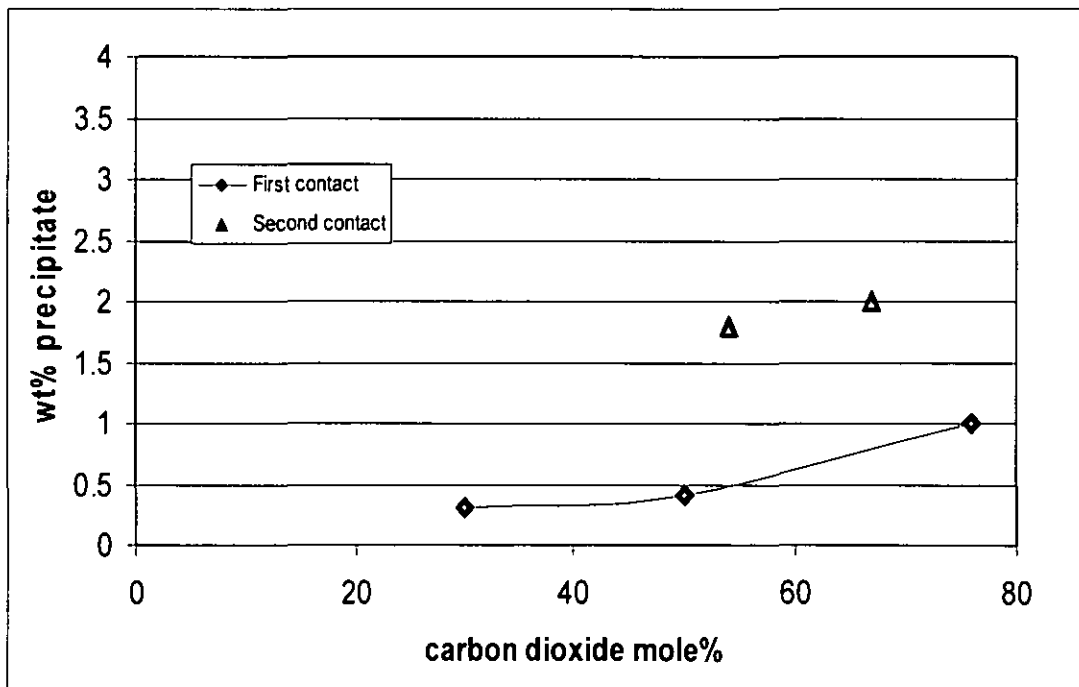


Figure 2.4 comparison of the amount of carbon dioxide induced precipitation with the first and multiple contacts (Parra-Ramirez *et al.*, 2001)

2.4.4.3 The Relationship Between Asphaltene Precipitation Mass Percent with Bubble point Pressure

Ying *et al.* (2006) observed from their experimental study that as pressure drops, the amount of dissolved gas increases. They observed that when the gas starts to dissolve into solution, there was highest asphaltene deposition. That is to say there was highest asphaltene deposition at the bubble point pressure. This can be explained as follows: as pressure drops, but before it reaches the bubble point pressure and with the increase of the lighter hydrocarbons in the oil, the solubility between resin and the lighter hydrocarbon components increases, which induces the resin to dissolve constantly. This caused the solubility of asphaltene to decrease consequently increased asphaltene deposition. At pressures below the bubble point pressure, further pressure drops caused some lighter components to evaporate into the vapor phase, thus making the oil heavier. The heavier oil favors asphaltene solubility, therefore asphaltene precipitation is reduced. Thus the maximal precipitated asphaltene is around the bubble point pressure (Ying *et al.*, 2006). Hirschberg *et al.* (1984), studied the influence of temperature and pressure on asphaltene precipitation during natural depletion. They found that when CO₂ was injected into the crude oil no precipitation was observed without addition of an intermediate hydrocarbon component such as decane. They also concluded that asphaltene precipitation is highest at the bubble point pressure (Hirschberg *et al.*, 1984; Parra-Ramirez *et al.*, 2001).

2.5 MODELING ASPHALTENE PRECIPITATION

Several approaches for modeling asphaltene precipitation have been reported in the petroleum literature such as the solubility model, thermodynamic colloidal model, thermodynamic micellization model, and solid model (Nghiem, *et al.*, 1993, Nghiem, 1999).

The existing asphaltene precipitation models fall into three classes, the first class is Molecular thermodynamic models in which asphaltene are dissolved in crude oil and crude oil forms a real solution, those models depending on the reversibility of asphaltene precipitation (Nghiem, 1999). The second class is Colloidal models in which asphaltene is suspended in crude oil and peptized by resins, in such models the

asphaltene precipitation is irreversible (Nghiem, 1999). The third class is Models based on scaling equation, in which the properties of complex asphaltene are not involved (Ashoori *et al.*, 2003).

The development of asphaltene precipitation models has been based mainly on two different conceptual descriptions of asphaltene solutions: (1) asphaltenes and resins are considered as molecular entities dissolved in crude oil; and (2) asphaltene and resin molecules from asphaltene-asphaltene and asphaltene-resin aggregates dispersed in an oil matrix (Buenrostro-Gonzalez *et al.*, 2004). The models corresponding to description (1) can be classified into three different categories. The first category uses the molecular solubility approach to describe an asphaltene-containing fluid as a mixture of asphaltenes and solvent in a true liquid state, whose thermodynamic properties can be calculated from a Flory–Huggins-type solution theory, using an energy interaction parameter estimated from Hildebrand’s solubility parameter (Hirschberg *et al.*, 1984; Kawanaka *et al.*, 1991; Buenrostro-Gonzalez *et al.*, 2004). The second category corresponds to models based on cubic equations of state (EOS) (Godbole *et al.*, 1992; Kohse *et al.*, 2000). The Godbole *et al.* (1992) and Kohse *et al.* (2000) models assume an asphaltene-containing crude oil as a multi-component mixture, where the heaviest component is split into two components: a nonprecipitating component related to resin/asphaltene micelles that remain in the oil, and a precipitating component related to asphaltenes and resin/asphaltene micelles that form the asphaltenic phase. The third category can be represented by the model developed by Ting *et al.* (2003), where asphaltenes are treated as molecules whose size and nonpolar van der Waals interactions dominate the asphaltene phase behavior (Buenrostro-Gonzalez *et al.*, 2004).

Examples of the models based on description (2) are a thermodynamic–colloidal model (Leontaritis and Mansoori, 1987) and a reversible micellization model (Pan and Firoozabadi, 1997). The basic assumption in these models is that a crude oil can be represented by three components: asphaltenes, resins, and the solvent. In the thermodynamic–colloidal model, asphaltene precipitation is modeled by solving for the equilibrium between the resins absorbed in asphaltenes and the resins that are present in the solvent. The micellization models apply the micellization theory proposed by Nagarajan and Ruckenstein (1991) (Buenrostro-Gonzalez *et al.*, 2004).

Nghiem *et al.* (1993, 1998, 2000) proposed a thermodynamic-colloidal model of asphaltene precipitation. This model is handy and efficient and it is a multiphase equilibrium model (gas-liquid-solid). This multiphase equilibrium thermodynamic model for asphaltic oil system during CO₂ injection satisfies the following requirements: (Nghiem *et al.* 1993, 1998, 2000; Ying *et al.*, 2006)

- Ability to make quantitative predictions.
- Compatibility with flash calculations using an equation of state.
- Small number of adjustable parameters.
- Computationally efficient for potential inclusion in a compositional model.

This model considers the precipitated asphaltene as a pure dense phase. This phase is referred to as the asphalt phase and can either be a liquid or solid.

2.6 REMOVAL OF ASPHALTENE

Many methods have been used for cleaning wells from asphaltene deposits (Kokal and Sayegh, 1995). In general, these methods can be classified into three methods namely mechanical, chemical and resinous additives. A fourth method, which is more of a preventive step, is the manipulation of the pressure, temperature and flowrate.

The mechanical method involves mechanical scraping and cleaning of the deposits inside the wells. The common one is by wireline which is slow and costly, particularly if the asphaltene plug is long and hard. Another technique is the drilling plug by using a coiled tubing unit but it is difficult because of the limitation of the coiled tubing operation. Another technique is by applying pressure to create a differential pressure, but all of these techniques are slow and costly.

Chemical cleaning is applied when the mechanical cleaning techniques failed. There are many solvents, additives and commercial chemicals available for dissolving deposited asphaltene. One method is the reverse and normal circulation of solvents with hot oil which have been tried but with mixed results. Hydrocarbon solvents such as toluene, xylene and other solvents such as pyridine and carbon disulphide are effective in dissolving asphaltene, but have limited usage because they are costly and

not safe due to their low flash points. In addition, these solvents also such as pyridine and carbon disulphide can create corrosion problems.

In some cases resinous additives have been found effective to prevent or reduce asphaltene precipitation but it is not common. More work needs to be done before this application can be made successful.

Since the removal of asphaltenes tend to create other related problems which could be unsafe and expensive, it is desirable to prevent or reduce its deposition. One of the ways to reduce asphaltene deposition inside wells is to monitor the operating pressure, temperature and/or production rates to avoid conditions where asphaltenes precipitate. For temperature control, a method using insulating annular fluids to avoid excessive heat losses and to maintain the fluid temperature has been used (Kokal and Sayegh, 1995). However, this method has limited application. A move towards low gas-oil ratio reduces flocculation, but most of these methods is not effective inside the reservoir but only in the tubings (Kokal and Sayegh, 1995). Therefore the simplest and least expensive method could be by selecting the optimum downhole conditions for the CO₂ injection to avoid asphaltene precipitation and deposition.

2.7 SUMMARY OF THE LITERATURE REVIEW

Asphaltene is the most heavy and polar component in crude oil, and it is precipitated by adding a low boiling paraffin solvent like n-heptane and benzene soluble fraction. Asphaltenes and resins are aromatic heterocompounds with aliphatic substitutions and they form the most polar fraction of crude oil; these resins and asphaltenes together are called micelles.

The precipitation of asphaltene can lead to formation damage due to permeability reduction and porosity alteration. The reason of asphaltene precipitation is destabilizing the asphaltene-resins micelles due to change in thermodynamic conditions of temperature, pressure and oil composition.

Many factors lead to asphaltene precipitation like fluid composition change due to natural depletion, electrokinetic effects, pressure and temperature changes, and

effect of CO₂ injection. When the injected CO₂ contacts the reservoir oil, can cause changes in the fluid behavior and equilibrium conditions which lead to asphaltene precipitation.

It has been observed that the amount of the asphaltene in crude oil is not the reason of the precipitation of asphaltene. Extensive field and laboratory data confirm that the lighter the oil, the lower is the asphaltene solubility. Asphaltene will precipitate more easily from light oil than from heavy oil, in spite of the heavier oil may have much higher asphaltene content. Most of the CO₂ flooding applications are for light oil which relatively has low asphaltene content.

The amount of asphaltene precipitation due to CO₂ injection is depending on the concentration of injected CO₂ gas, and the precipitation rapidly increases when the CO₂ concentration exceeds from one critical value. The asphaltene precipitation in the multiple contacts miscibility of CO₂ with oil is 3-5 times more than the first contact miscibility. The maximum amount of asphaltene precipitation is at the bubble point pressure.

Several approaches for modeling asphaltene precipitation have been reported in the petroleum literature. The existing models fall into three classes, the first class is: Molecular thermodynamic models in which asphaltene are dissolved in crude oil and crude oil forms a real solution, the second class is: Colloidal models in which asphaltene is suspended in crude oil and peptized by resins, the third class is: Models based on scaling equation, in which the properties of complex asphaltene are not involved.

Many methods have been used for cleaning wells from asphaltene deposits. In general, these methods can be classified into three methods namely mechanical, chemical and resinous additives. Since the removal of asphaltenes tend to create other related problems which could be unsafe and expensive, it is desirable to prevent or reduce its deposition. Therefore the best way to reduce asphaltene deposition is to avoid the conditions that lead to the precipitation by monitoring the operating pressure, temperature and the production rate.

CHAPTER III

METHODOLOGY

This chapter describes the experimental work conducted in this study, which consist of five parts:

- 3.1 Crude Oil Characterization
- 3.2 Phase Behavior Experiments (Routine PVT Analysis)
- 3.3 EOR Experiments
- 3.4 Asphaltene Precipitation Experiments
- 3.5 Statistical Analysis Procedure

3.1 CRUDE OIL CHARACTERIZATION

Crude oil characterization is one of the most important studies for oil industry to determine the crude oil properties. The objective of crude oil characterization for Baronia RV2 is to determine the reservoir fluid composition and properties, for further investigation on the effect of CO₂ on Baronia RV2 oil. This is due to the fact that in most cases, the injection of CO₂ into reservoir fluid is well known to lead to heavy hydrocarbons deposition such as wax and asphaltene, which will pose several production problems later. It has been accepted that crude oil is generally considered to be a colloidal system consisting primarily of hydrocarbons such as saturate, aromatics, resins, and asphaltene (McCain, 1990; Kokal and Sayegh, 1995; Nghiem, 1999; Alkafeef *et al.*,2003; Speight, 2004).

The crude oil characterization experiments included the following tests:

- 3.1.1 Density Measurement, using PAAR DMA48 density meter
- 3.1.2 Asphaltene Content, ASTM (D3279-07)
- 3.1.3 Wax Content, UOP-46

- 3.1.4 Wax Appearance Temperature (WAT), by cross polarization microscopy
- 3.1.5 Compositional Analysis up to C₄₀₊ by gas chromatography
- 3.1.6 SARA Analysis, by liquid chromatographic separation

3.1.1 Density Measurement

Density is a physical property of matter, as each element and compound has a unique density associated with it. Density is defined in a qualitative manner as the measure of the relative "heaviness" of objects with a constant volume. The density of crude oil was measured using PAAR DMA48 density meter equipment as shown in Figure 3.1.



Figure 3.1 PAAR DMA48 density meter

The density measurement was done using the stock tank oil (STO) sample of Baronia RV2. The calibration of the device was checked by measuring the density of a liquid of a known density at certain temperature, such as distilled water. The device was cleaned by Dichloromethane (DCM), and the temperature was set at 20°C. The oil sample was taken using a syringe and approximately 0.7 cc was injected into the device. After a stable reading was obtained, the density (g/cc) was recorded. The procedure was repeated 4 times until consistent readings were obtained.

3.1.2 Asphaltene Content

The asphaltene content was determined according to the ASTM D3279-07 test method shown in Appendix A. This test method is useful in quantifying the asphaltene content of petroleum asphalts, gas oils, heavy fuel oils, and crude petroleum. Asphaltene content is defined as those components not soluble in n-heptane.

The test was carried out by mixing 1 g of Baronia RV2 stock tank oil sample with 100 ml of n-heptane. The mixture was heated and secured under a reflux condenser as shown in Figure 3.2. The mixture was adjusted for gentle heating for 30 minutes then left to cool to room temperature for a period of 1 hour. Gooch crucible plus one thickness of the glass-fiber filter pad (GFD) as shown in Figure 3.3 were prepared and placed in the oven at 107°C for a period of 15 minutes, then kept in the desiccator for cooling for 15 minutes also. Then the crucible and filter paper were weighed to obtain the original weight before filtration.

A vacuum filter was prepared with a suction flask for filtration process after the mixture of oil sample and n-heptane has heated up again to 38-49 °C. The filtration apparatus is shown in Figure 3.4. The sample/solvent mixture was poured through the filter using a gentle vacuum. After the filtration, the crucible was placed in the oven for 15 minutes then kept in the desiccator for 15 minutes also. The weight of the crucible was recorded to obtain the weight after filtration. The difference of the weight before and after filtration represents the total mass of n-heptane insolubles. The calculation of the

mass percent of normal-heptane insolubles (*NHI*) as the percentage by weight of the original sample is as follows:

$$NHI \% = \frac{A}{B} \times 100 \quad (3.1)$$

Where:

- A* ≡ Total mass of insolubles, gram
B ≡ Total mass of sample, gram

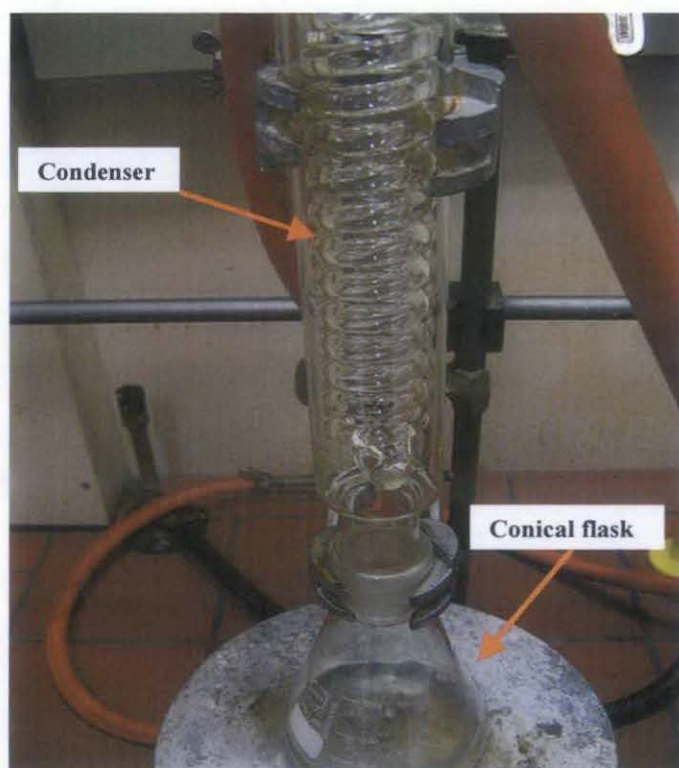


Figure 3.2 Reflux apparatus



Figure 3.3 GFD filter paper

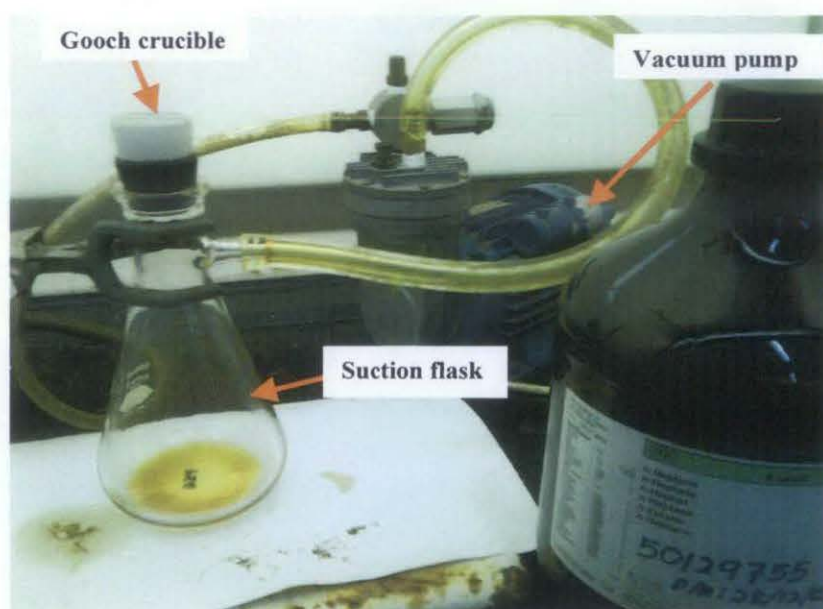


Figure 3.4 Filtration apparatus

3.1.3 Wax Content

The wax content measurement was conducted according to the method of Universal Oil Products (UOP-46) as shown in Appendix A, to determine the mass percent of wax in crude oil. The purpose of measuring the wax content in this research is to determine the wax content in Baronia RV2 crude oil for later study of wax-asphaltene co-precipitation. Studies conducted by previous researches have observed that asphaltene did not deposit alone but with paraffin. This indicates that asphaltene deposition lead to paraffin deposition too (Vazquez, and Mansoori, 2000).

In this test, 1 g of the oil sample was taken and mixed with 150-200 ml of petroleum spirit (ether 40-60°C). 15g of bole white powder (fuller earth) was added to the mixture to remove the black colour from the crude and make it yellow. The mixture was then filtered through two layers of No.4 filter using vacuum filtration. The filtrate was transferred into a round bottom flask and 200 ml of a mixture of 30% petroleum spirit and 70% acetone was added. The round bottom flask was placed at a Roto-vapor at 60°C and a speed of 90 rpm to reduce the volume of the filtrate/solvent mixture to 20 ml. and the 20 ml remains from the filtered, that 20 ml has been mixed with 200 ml of a mixture of 30% petroleum spirit and 70% of acetone. Then the mixture was kept in a cooling bath at (-17°C) for 2 hours and at the same time the Gooch-crucible with glass-fiber filter pad (GFD) were put in the freezer.

After 2 hours the mixture was taken out from the cooling bath and the crucible with the filter pad were taken out from the freezer. Then the mixture was filtered through the Gooch crucible using vacuum filtration. The wax is now trapped on the filter paper. A new round bottom flask was taken and kept to dry in a desiccator for 30 minutes. Then the weight of the empty round bottom flask was obtained. This is the initial weight of the round bottom flask. A 100 ml of petroleum spirit was measured and heated until boiling. Then, the boiled solvent was used to wash the trapped wax on the filter paper to re-dissolve the wax before transferring it into the round bottom flask that has been weighed earlier.

The round bottom flask now containing the re-dissolved wax was put at a rotovapour at 70°C and speed of 90 rpm until the wax solution became dry. Then the flask was put in the oven for 30 minutes followed by drying in the silica gel drying flask for another 30 minutes. The weight of the dry round bottom flask was taken again to obtain the final weight. The test was repeated 3 times to obtain correct wax content.

(Wax_{content} %) was calculated using the following formula:

$$Wax_{cont. \%} = \frac{weight_{final} - weight_{initial}}{weight_{sample}} \times 100 \quad (3.2)$$

3.1.4 Wax Appearance Temperature (WAT)

Wax appearance temperature is defined as the first temperature that wax starts to become solid and appears in crude oil. This test was conducted using the BX51/BX52 Olympus microscope system and BXP polarizing microscope, which uses liquid Nitrogen for cooling and heater for heating the sample.

The purpose of this test is to find out at what temperature wax will start to appear and become solid for Baronia RV2 oil to confirm if there will be any wax might be deposited with asphaltene or not.

A 10 micro liter sample of the Baronia RV2 oil was placed in the polarizing microscope. The heater temperature was set at 50°C and the cooling temperature at 1°C. The video cam and the screen were checked to be ready for capturing the video before running the test. The device was switched on and the sample start to be heated until the temperature reached the set heating temperature (50°C); then the device automatically started cooling down until reaching the set cooling temperature (1°C). During the cooling down process, the appearance of wax was monitored on the screen. The appearance of wax is observed as white spots on the screen. The temperature was recorded at the appearance of the first white spot on the screen, this temperature will be the wax appearance temperature.

3.1.5 Compositional Analysis of Stock Tank Oil (STO) up to C₄₀₊

The compositional analysis of stock tank oil was conducted using HP 5890 Series II high temperature gas chromatography (HTGC) equipment as shown in Figure 3.5. The chromatograph is used to identify the types of crude oil i.e. normal paraffinic, waxy, aromatic or naphthenic. The gas chromatograph (GC) separates the crude oil components according to the boiling points of each one. Helium gas was used as the carrier gas to carry the vapour of each separated component. The column used for this analysis was silica with length of 100 meter and diameter of 0.25 mm.

A 10 micro liter of stock tank oil sample was injected into the GC using a syringe. The test was run at an initial temperature of 30°C and final temperature of 350°C with a heating rate of 4°C/min. A single run of the GC analysis took approximately 2 hours. The fingerprint results were obtained from the computer that was connected to the GC equipment.



Figure 3.5 HP 5890 Series II High Temperature Gas Chromatography (HTGC) equipment

3.1.6 SARA Analysis

The composition of the soluble matter can be determined by liquid chromatographic separation, which separates the crude oil into saturated hydrocarbons (S), aromatic hydrocarbons (A), NSO compounds or resins (R) and asphaltenes (A). The SARA compositional data are useful in evaluating oil source quality and thermal maturation. An amount of soluble organic matter extract in chloroform was concentrated and n-pentane (in excess) was added. The precipitated asphaltenes were centrifuged off, dried and weighed. The remaining extract was dried to remove chloroform, and then successively resolubilised in hexane, benzene and benzene/methanol solution. The extracts were then run through a silica gel column to determine the % saturates % aromatics and % NSO compounds (resins).

3.2 PHASE BEHAVIOR EXPERIMENTS

Phase behavior experiments are very important for any reservoir engineering projects. The objectives of this study are to analyze the separator oil and separator gas compositions, to obtain representative live reservoir fluid by physical recombination of separator oil and separator gas to a specific gas-oil ratio, and bubble point measurement.

The Routine PVT analysis conducted for this research project included the tests listed below. The Differential Liberation test has been excluded since the data provided by this test are not necessary for the evaluation of asphaltene precipitation.

3.2.1 Compositional Analysis of Separator Oil and Separator Gas

3.2.2 Recombination of Separator Oil and Gas

3.2.3 Constant Composition Expansion Test (CCE)

3.2.1 Compositional Analysis of Separator Oil and Separator Gas

The separator gas cylinder was first heated to the separator temperature. A small amount of gas was then injected into the Natural Gas Analyzer as shown in Figure 3.6 for compositional analysis. The composition of the separator oil was analyzed by using a spike flash technique. The sample was flashed from separator conditions to atmospheric conditions to obtain stock tank gas and liquid at standard conditions. The evolved gas was circulated for a sufficient period of time until the stock tank oil and gas have achieved equilibrium. The gas-oil ratio (GOR) was then measured. The GOR was used later to calculate the composition of the separator oil.



Figure 3.6 Gas analyzer

The composition of the equilibrium gas (from C_1 to C_{12+} including N_2 and CO_2) was analyzed using the Natural Gas Analyzer (NGA). The equilibrium oil was analyzed using the High Temperature Gas Chromatography (HTGC) as shown in Figure 3.5, which gives detailed hydrocarbon compositions from C_3 to C_{33} . Then the composition of the separator

oil was obtained through mass balance calculation. The molecular weight of the equilibrium oil was derived from the HTGC results and density was measured using ANTON PAAR densitometer as shown in Figure 3.1. From the separator gas and separator oil composition, the composition of the recombination fluid was calculated by using the separator gas oil ratio (GOR).

3.2.3 Recombination of Separator Oil and Gas

The separator gas and separator oil were physically recombined using the recombination cell as shown in Figures 3.7 and 3.8, to the separator gas oil ratio of 750 scf/bbl, which is the original GOR of Baronia RV2 reservoir oil. The reservoir fluid exhibited a bubble point pressure of 2635 psig. This bubble point pressure believed to be not accurate because Baronia RV2 oil is volatile oil and need a visual cell to detect the bubble point. The resulting fluid was used for constant composition expansion test, EOR studies and asphaltene precipitation study.

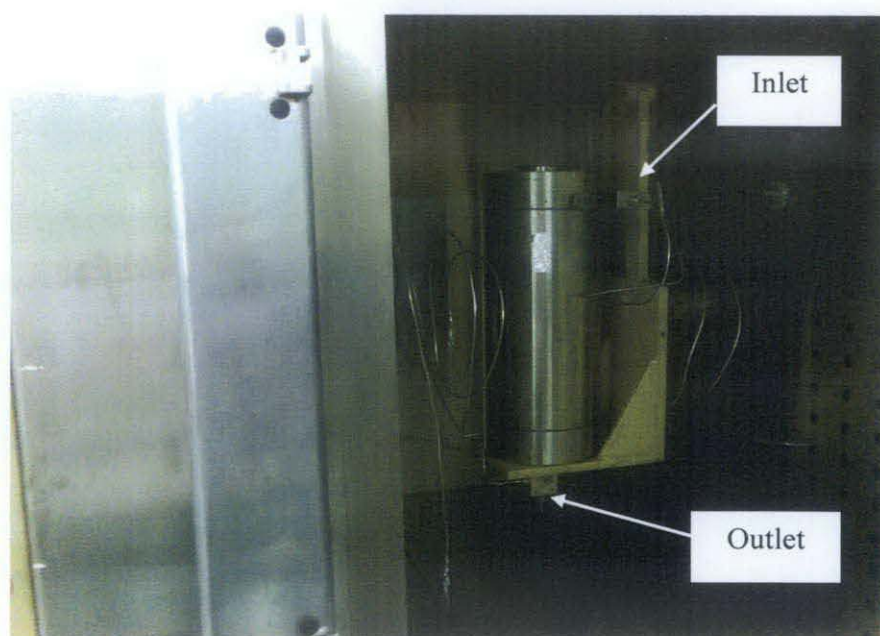


Figure 3.7 Recombination cell

3.2.3 Constant Composition Expansion Test (CCE)

A constant composition expansion or P-V relation is conducted to study the volumetric behavior of reservoir fluid at reservoir conditions. This test was performed at the visual PVT cell. A known volume of the reservoir fluid was charged isobarically into the high pressure visual PVT cell as shown in Figure 3.8. The sample was then heated to the reported reservoir temperature and the pressure was monitored to ensure the fluid is in single phase. After thermal equilibrium was established, the sample was subjected to a series of pressure drops. At each pressure reading, the volume of the sample was measured using the Camcorder Detection Measurement System. Then a graph of pressure versus volume was plotted and the bubble point pressure was determined by the intersection of the two lines on the PV graph. The visual PVT cell also allows for visual observation of the first appearance of gas of the reservoir fluid at simulated reservoir conditions. Visual observation gives a better indication of the bubble point region and the bubble point can be determined more accurately from the PV plot.

Other parameters which can be obtained from the P-V relation are saturation volume, fluid compressibility above bubble point, relative volume factor, Y-function and thermal expansion factor. Figure 3.9 shows the schematic diagram of the Jefri phase behavior system (PVT cell) used in this study.



Figure 3.8 High pressure visual PVT cell

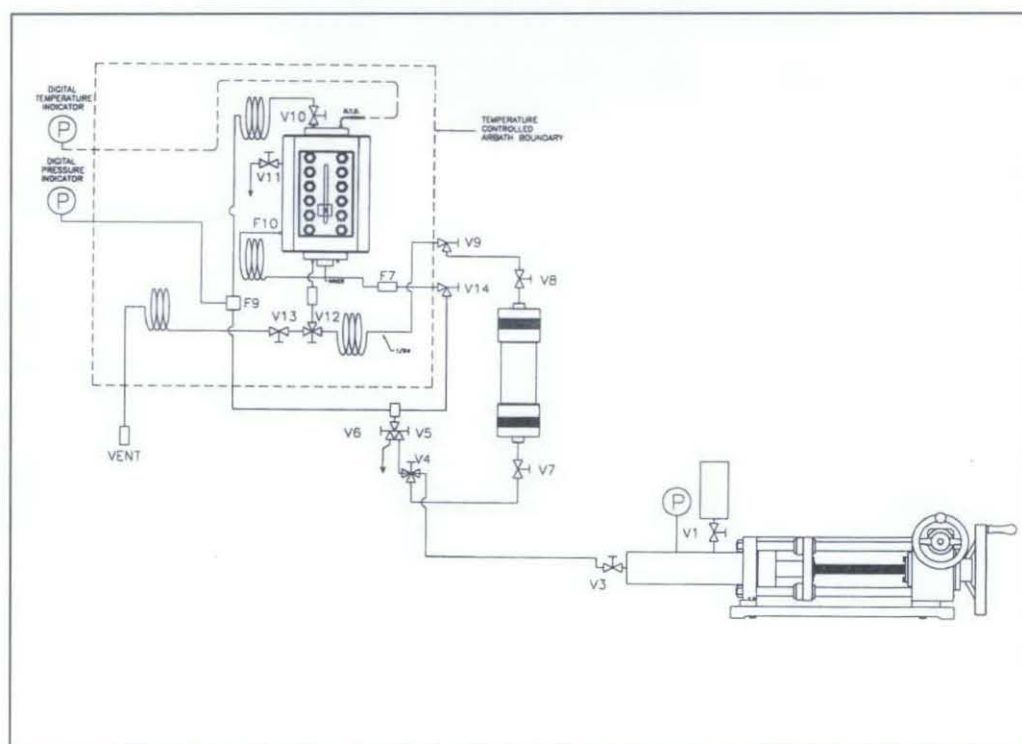


Figure 3.9 Schematic diagram of Jefri phase behavior system

3.2 EOR EXPERIMENTS

EOR laboratory studies have been conducted to study the effect of CO₂ on Baronia RV2 oil to evaluate the possibility of CO₂ injection process for Baronia RV2 reservoir.

The EOR experiments included the following tests:

- Micro-Slim Tube Displacement Test
- Swelling Test

3.3.1 Micro-Slim Tube Displacement (MST) Test

The objective of the micro-slim tube displacement test is to determine the minimum miscibility pressure (MMP) between the injection gas (CO₂) and Baronia RV2 recombined fluid at its reservoir temperature of 204 °F. The experiment was conducted using Micro-Slim Tube (MST) equipment as shown in Figure 3.10.

The MMP results from the micro-slim tube displacement test were used to distinguish between miscible or immiscible gas flooding at specified reservoir pressure. For optimal oil recovery, the gas flooding should be conducted at pressures equal to or greater than the MMP. Pure CO₂ (99.99%) were used as the injection gas in this test.

The displacement experiments were conducted in a 30 m x 0.53 mm unpacked coiled, stainless steel micro-slim tube (MST). It was housed in an oven and connected to a receiving pump that also functioned as a back-pressure regulator. The schematic diagram of the apparatus is presented in Figure 3.11. The supply of the injected gas and the recombined fluid sample was made via high-pressure syringe pumps. There were switching valves to determine the flow path of the fluid.

The pore volume (PV) was taken as the volume of sample required to fill up the MST and the associated lines as shown in Figure 3.11.

After thermal equilibration, the displacement was carried out at a constant CO₂ injection rate of 0.25 cc/min. The receiving pump was run at a similar reversed flow rate in order to maintain the pressure. The ultraviolet detector (UV) at the outlet end of the MST indicated the CO₂ breakthrough. The time at which the detector response changed abruptly, indicating breakthrough, was noted. The volume of CO₂ injected and the volume of displaced sample in the receiving pump at the onset of CO₂ breakthrough were also recorded.



Figure 3.10 Micro-slim tube (MST) equipment

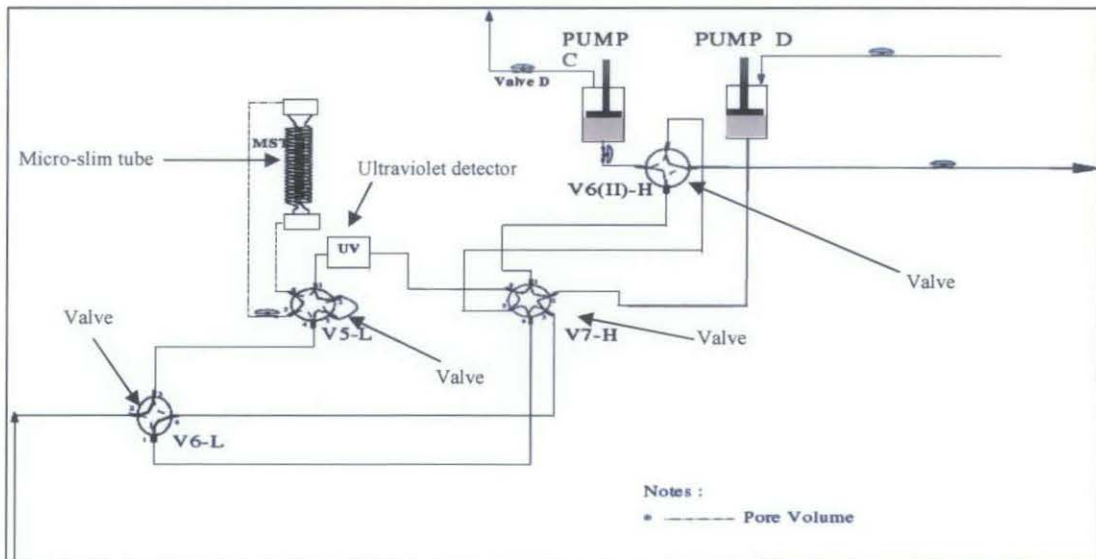


Figure 3.11 Schematic diagram of micro-slim tube (MST) equipment

3.3.2 Swelling Test

Swelling tests are also called single contact miscibility study, or oil expansion behavior under CO₂ injection. Solubility of the injected CO₂ in the reservoir oil is studied in these experiments by measuring the swelling factor, saturation pressure curve, liquid and gas volumes in the two-phase region (by constant mass expansion) for different mixtures of injected CO₂ and reservoir oil. A known amount of recombined samples was combined with a known amount of CO₂.

Baronia recombined sample was pressurized to single phase at a pressure of 5000 psig and about 20 cc of the single phase sample was transferred into the PVT cell. Then the sample was heated to reservoir temperature of 204 °F. The sample was then depressurized to reservoir pressure of 3008 psig.

CO₂ gas was pressurized to 3008 psig and heated to reservoir temperature in a separate cylinder. Then the required volume of CO₂, determined by calculation, was added into the recombined oil in the PVT cell to make the Oil-CO₂ ratio. The temperature and pressure of the mixture was monitored continuously and the PVT mixer was turned-on to ensure a proper mixing of CO₂ gas with the recombined sample. After the temperature and pressure of the mixture were observed stable, then the mixture was pressurized to 5000 psig with the temperature maintained at reservoir temperature.

The mixture was later subjected to a series of depressurization step and the gas and liquid level of the mixture were measured using CCD camera at each pressure step. The pressure and volume readings were plotted on a PV-relation graph to determine the bubble point and the swelling factor was calculated. The whole step was repeated for each different concentration of CO₂. A total of four CO₂ concentrations was used.

3.4 ASPHALTENE PRECIPITATION EXPERIMENTS

The asphaltene precipitation study included two experiments:

- Static Asphaltene Precipitation Test.
- Dynamic Asphaltene Precipitation Test.

The objectives of these experiments are to investigate the possibility of asphaltene precipitation when Baronia RV2 oil is in contact with CO₂ under static and dynamic conditions, and to study the asphaltene behavior changes with different concentrations of CO₂ at different pressures.

3.4.1 Static Asphaltene Precipitation Test

Static test indicates the most important factor of asphaltene precipitation i.e. the CO₂ concentration. This experiment was done at reservoir pressure of 3008 psia and temperature of 204°F (isobaric and isothermal) by adding different mol% of CO₂ (22%, 40%, 70%, 85%) to Baronia RV2 recombined oil to investigate the effect of different CO₂ concentrations on asphaltene precipitation. The experiment was done using the PVT cell system.

A known volume of Baronia RV2 recombined oil was transferred into the PVT cell at 5000 psi. Then the sample was depressurized to the reservoir pressure of 3008 psia and was left to reach equilibrium conditions at 3008 psia and 204°F. The volume of oil was measured after the sample has reached equilibrium.

The required volume of CO₂ was calculated depending on the volume of oil sample in the PVT cell by considering the transfer pressure and gas properties as shown in Appendix B.

After equilibrium has been achieved in the PVT cell, the calculated CO₂ volume was transferred into the PVT cell to combine with the oil sample. The transfer of CO₂ was

conducted isobarically at the reservoir pressure of 3008 psia. The oil sample was combined with the CO₂ and left to reach equilibrium conditions as indicated where no changes in the pressure and the temperature were observed.

When the combined CO₂ and oil mixture has reached equilibrium conditions, the volume of the mixture was recorded. Then a known volume of the mixture was flashed to atmospheric conditions while the PVT cell pressure was maintained constant at the reservoir pressure. The stock tank oil obtained from the flashed mixture was taken for asphaltene precipitation analysis following the ASTM D3279-07 method using n-Heptane.

After the flash process, the volume of oil-CO₂ mixture in the PVT cell was recorded and another calculated volume of CO₂ for a new CO₂ concentration was added to the oil-CO₂ mixture. The above procedures of reaching equilibrium conditions, volume measurement, flash process and asphaltene determination were repeated at the new CO₂ concentration.

A total of five different CO₂ concentrations was injected, and at each concentration, the asphaltene precipitation analysis was performed to study the effect of CO₂ concentration on asphaltene precipitation of Baronia RV2 oil sample.

3.4.2 Dynamic Asphaltene Precipitation Test

This experiment investigates the asphaltene precipitation under dynamic conditions during the displacement of oil by CO₂. It was carried out using different mol% of CO₂ at different pressures, at the reservoir temperature 204 °F (isothermal). This test was conducted using the Micro-Slim tube equipment during the measurement of MMP.

The test included several runs, each run was at different pressure and different CO₂ concentration. The test was conducted at the pressures of 1000, 1600, 2200, 2400, 3000, 3600 psi.

The experimental procedure is similar to the micro-slim tube test procedure mentioned in section 3.3.1. However in this test, at each CO₂ displacement run the injected volume of CO₂ was recorded to calculate the mol% of injected CO₂ that was in contact with Baronia RV2, using the general gas law and mass balance calculation. The calculation of CO₂ mol% for dynamic asphaltene test is shown in Appendix B.

When the displacement run was completed i.e. when there was no more oil recovered from the micro-slim tube, the recovered oil sample was taken for asphaltene precipitation analysis following the ASTM D3279-07 method.

The micro-slim tube was prepared for a new run by flushing the tube with n-heptane to remove any possible precipitated asphaltene that might be trapped inside it. Any residue trapped inside the micro-slim tube was taken for asphaltene precipitation analysis. If any precipitated asphaltene was found in the trapped residue sample, this amount of asphaltene (%wt) will be added to the asphaltene obtained from the recovered oil sample from the same test run. The amount of asphaltene from the recovered oil and from the trapped residue gives the total amount of precipitated asphaltene for that particular run. The test was repeated twice to ensure consistent results.

3.5 STATISTICAL ANALYSIS PROCEDURE

Regression analysis has been used to analyze the data gathered from dynamic asphaltene test to propose a correlation to predict asphaltene precipitation during the change of pressure and CO₂ concentration.

Regression analysis is a statistical technique that is very useful for getting the relationships between two or more variables (Montgomery and Runger, 2002). Usually, the investigator seeks to ascertain the causal effect of one variable upon another. However the data of dynamic asphaltene test contains two variables (pressure and CO₂ concentration) which affect asphaltene precipitation. Regression analysis tool was used to investigate the effect of each variable on asphaltene precipitation.

In general, suppose that there is a single dependent variable or response y that depends on k independent or regressor variables, for example, x_1, x_2, \dots, x_k . The relationship between these variables is characterized by a mathematical model called a regression model. The regression model is a fit to a set of sample data contains two or more variables. Regression methods are frequently used to analyze data from unplanned experiments, such as might arise from observation of uncontrolled phenomena or historical records (Montgomery, 2001).

The amount of asphaltene precipitation which obtained from the dynamic asphaltene test were analyzed using regression analysis statistical method to develop a correlation of asphaltene precipitation for Baronia RV2 oil sample. The correlation would be used to enable the prediction of asphaltene precipitation at reservoir temperature for any given pressure and CO₂ concentration. Microsoft excel 2003 has been used for the analysis.

The Regression analysis tool performs linear regression analysis by using the "least squares" method to fit a line through a set of observations. This can analyze how a two or more independent variables could affect a single dependent variable. The single dependent variable is represented by asphaltene precipitation. However the pressure and CO₂ concentration are represented as independent variables. The proposed correlation is based on the following equation (Montgomery, 2001):

$$y = \beta_0 + \beta_1 x_1 + \beta_2 x_2 + \dots + \beta_k x_k + \varepsilon \quad (3.3)$$

Where y is the dependent variable, x_1, \dots, x_k are the independent or explanatory variables, β_0 defines the intercept of the plane, β_1 and β_2 called the partial regression coefficients, because β_1 measures the expected change in y per unit change in x_1 when x_2 is held constant and β_2 measures the expected change in y per unit change in x_2 when x_1 is held constant, and ε is the disturbance or error term. The amount of asphaltene precipitation in the dynamic asphaltene test was input as y -axes. However the pressure input as x_1 and CO₂ concentration as x_2 . After run the regression analysis using Microsoft excel 2003, the regression coefficient β_0, β_1 , and β_2 will be calculated to complete the form of the correlation. The total error ε will be calculated also which represents the total

correlation error between the measured and predicted values. The adequacy of the correlation was checked by analysis of variance (ANOVA) statistical method (Montgomery, 2001).

3.5.1 Analysis of Variance (ANOVA)

This method could allow more than two sets of data to be examined at the same time. There are many different types of ANOVA, but they all use the same basic method of comparing the variance between different treatments with the variance within treatments (Clarke, G.M., and Kempson, 1997; Montgomery, 2001; Montgomery and Runger, 2002).

There are two assumptions for ANOVA to check the validity of the regression:

- Null Hypothesis (H_0): $\beta_1=\beta_2=0$, [the independent variables (pressure and CO₂) have no effect on dependent variable (asphaltene)].
- Alternative Hypothesis (H_A): At least one $\beta \neq 0$, [the independent variables (pressure and CO₂) have effect on dependent variable (asphaltene)].

Null hypothesis should be rejected to confirm the validity of the correlation, while the alternative hypothesis accepted, and that will depend on the following important factors:

1. F -statistic or F -value is the quality of the entire model, meaning with all independent variables included. The larger the F is the better and it'll be against null hypothesis. Once F -statistics calculated we compare it to a critical F value or F -table at significance level (α), which is normally 0.05. F -table is shown in Appendix C.
2. R -Square is another measure of the explanatory power of the model. In theory, R -square compares the amount of the error explained by the model as compared to the amount of error explained by averages. The higher the R -square the better and go against null hypothesis. Generally an R -Square above 0.5 is generally considered quite good.

-
3. Adjusted *R*-square is a modified version of *R*-Square, and has the same meaning, but includes computations that prevent a high volume of data points from artificially driving up the measure of explanatory power. An Adjusted *R*-Square above 0.20 is generally considered quite good (Montgomery, 2001).

The above factors play a role to accept or reject the null or the alternative hypothesis. The alternative hypothesis represents the reality of the assumption. In this research project the alternative hypothesis represents the effect of pressure and CO₂ concentration on asphaltene precipitation. Whereas the null hypothesis represents the non-effect of pressure and CO₂ concentration on asphaltene precipitation.

The measured density of the stock tank oil was 0.8180 g/cm^3 at 20°C , which corresponds to 41.5° API .

The measured asphaltene content for Baronia RV2 crude was found to be 0.117 \%wt , which is considered very low asphaltene content. Nevertheless it has been observed that the amount of the asphaltene in crude oil is not the reason of the precipitation of asphaltene.

The measured wax content of parent oil was 1.8661 \%wt . This value of wax content is very low, and therefore Baronia RV2 crude oil is not waxy oil. The WAT test found that measured WAT was at 16.3°C . This temperature is relatively very low considering that the reservoir temperature is at 95.6°C . If there is any decrease in the temperature during the CO_2 injection, the temperature might not drop to 16.3°C .

4.1.1 Compositional Analysis of STO up to C_{40+}

The chromatograph is used to identify the composition and types of crude oil i.e. normal paraffinic, waxy, aromatic or naphthenic. The fingerprints of Baronia RV2 crude oil in Figure 4.1 shows that the crude is between normal paraffinic and waxy oil by comparing it with the fingerprints of different types of crude oil. Figure 4.2 shows the four different types of crude oil (Danesh, 1998). As seen in Figure 4.2, normal paraffinic oil has large amounts of low carbon number compounds from C_8 and decreases steadily from C_8 until C_{30+} . While waxy oil contains large amount of intermediates in the range of $\text{C}_{10} - \text{C}_{20}$ that is mainly due n-paraffin that make up the wax. Aromatic and naphthenic oils contain more of lower carbon number compounds, which is due to the presence of high aromatic and naphthenic ring compounds.

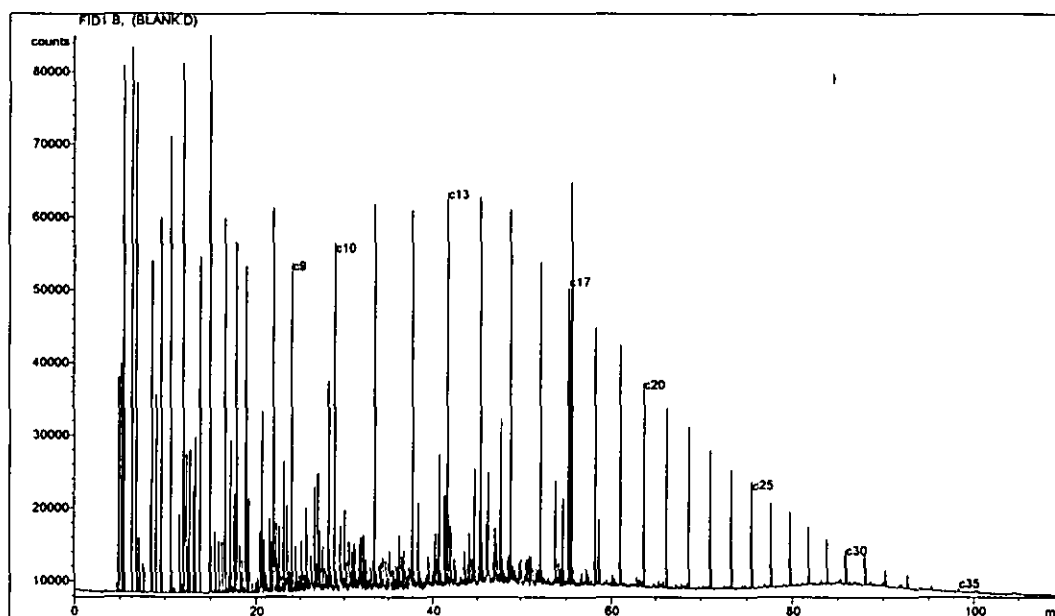


Figure 4.1 Fingerprints of Baronia RV2 crude oil

* The test was under atmospheric pressure and temperature from 86-662°F

** GC column length is 100m with diameter of 0.25 mm, material of column is silica

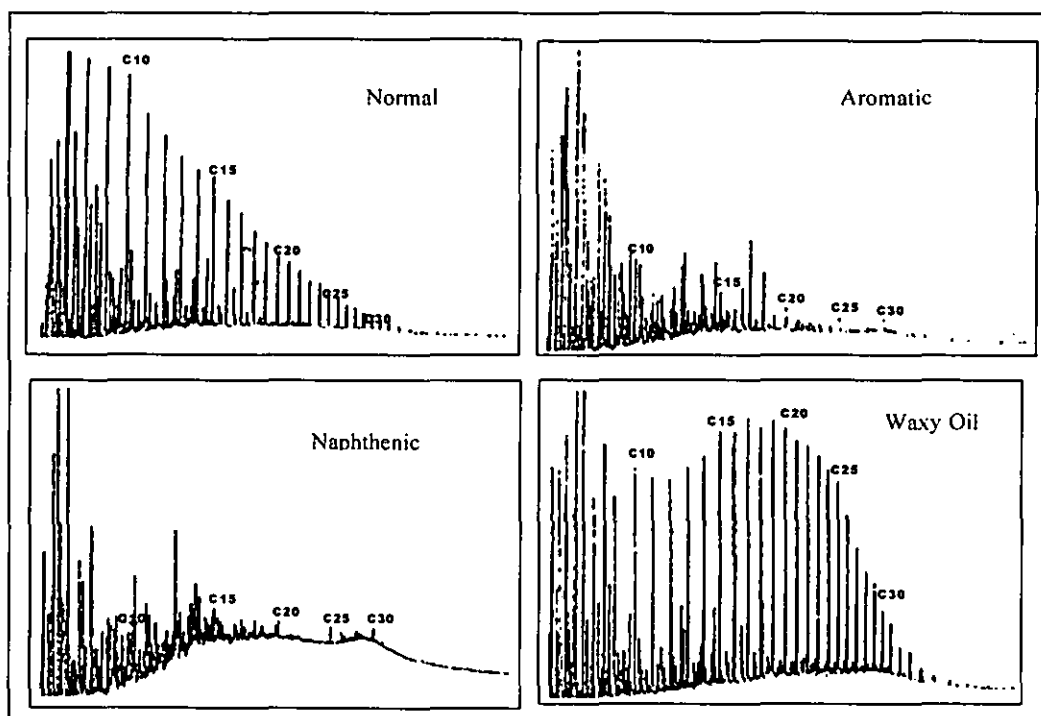


Figure 4.2 Fingerprints of four different types of crude oil, (Danesh, 1998)

Figure 4.3 shows the distribution of single carbon number (SCN) of Baronia RV2 stock tank oil from C₂-C₃₇₊. The weight percent of C₂ was only 0.048. The light components are not present since most has evolved into the gas phase. For the C₃₇₊ or the heavy end hydrocarbons, the weight percent was 0.02. This confirmed that Baronia RV2 is light oil, which is rich in light and intermediate components. The miscibility between the light oil and CO₂ will be achieved easily due to the CO₂ vaporization mechanism of the light and intermediate components leading to increased oil recovery (Fred and Stalkup, 1983).

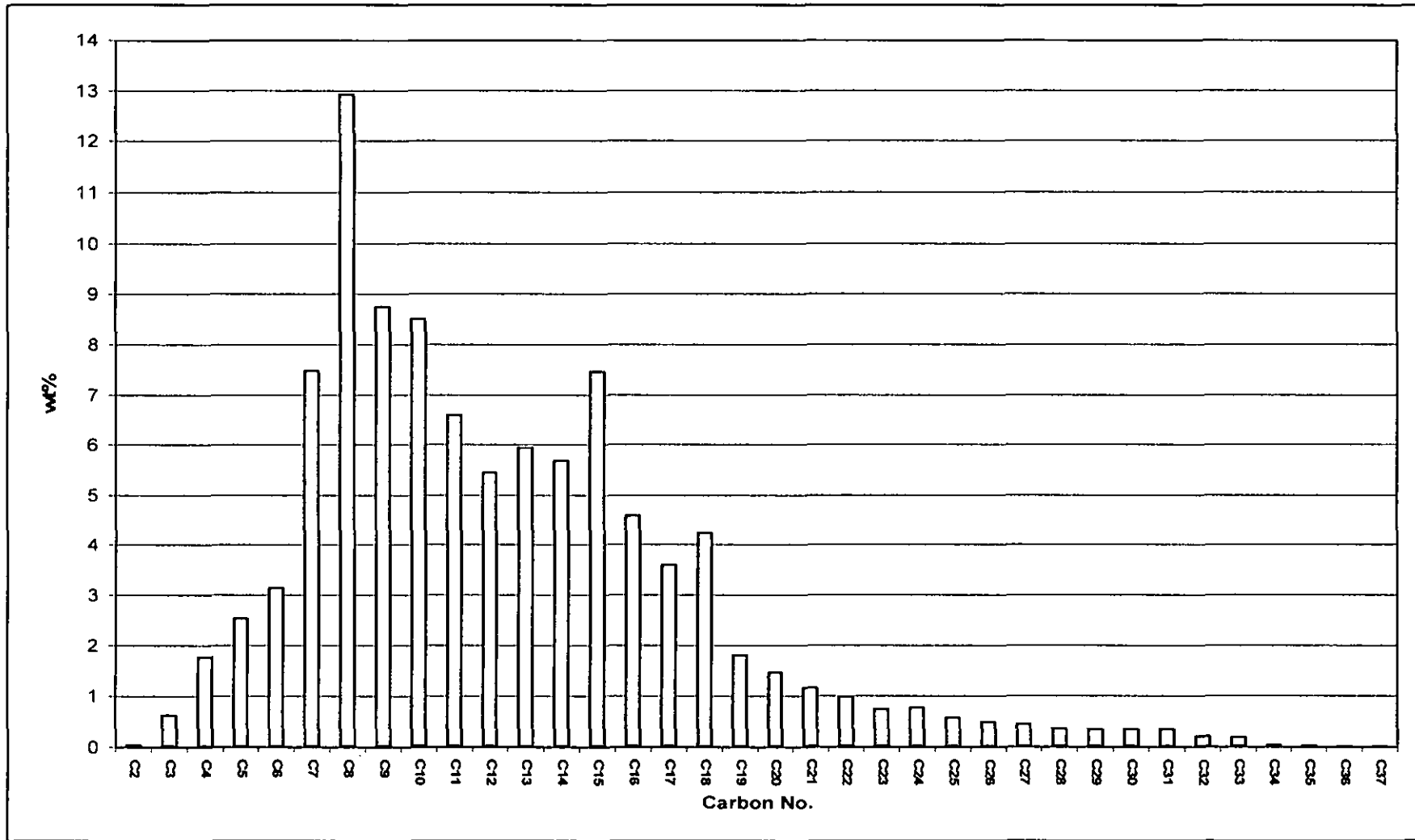


Figure 4.3 Single Carbon Number of Baronia RV2 Stock Tank Oil

* The test was under atmospheric pressure and temperature from 86-662°F

** GC column length is 100m with diameter of 0.25 mm, material of column is silica

4.4.2 SARA Analysis

SARA analysis was conducted on the crude oil to determine the composition of saturates, aromatics, resins, and asphaltenes by liquid chromatographic separation. This compositional data are useful in evaluating oil source quality and thermal maturation. Figure 4.4 shows the results of SARA analysis for Baronia RV2 stock tank oil.

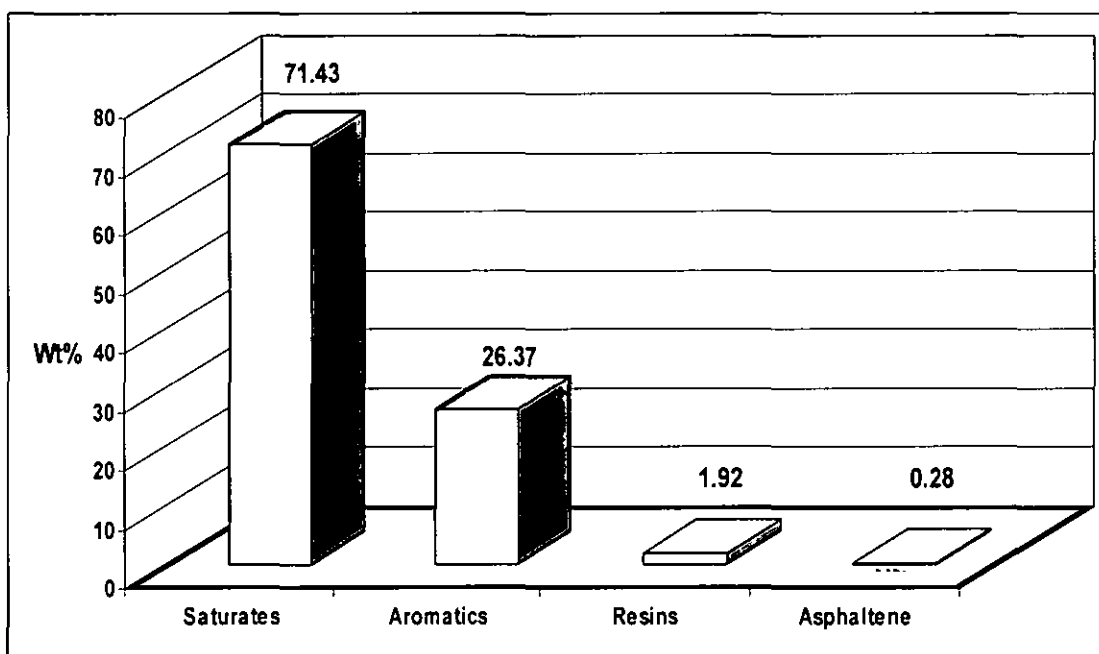


Figure 4.4 SARA analyses by liquid chromatographic separation using $n\text{-C}_5$ (Baronia RV2)

* Separation conditions: pressure of 10 mmHg and room temperature

Figure 4.4 shows that Baronia RV2 crude oil is rich in saturates fraction, low in aromatics fraction, and has very low resins and asphaltene fractions. It is generally known that asphaltene stability in crude oil depends on the ratio of aromatics to saturates from one side and from the other side depends on the ratio of asphaltenes to resins (Mansoori, 1997). Asphaltene is soluble in aromatic fractions such as toluene and benzene, and insoluble in saturate fractions such as n -pentane, n -hexane and n -heptane (Mitchell and Speight, 1973; Mansoori, 1997; Sarma, 2003; Speight, 2004).

High aromatic fraction in crude oil could increase the stability of asphaltene and thus decreases the probability of asphaltene precipitation. However, high

saturates fraction in crude oil leads to increase the probability of asphaltene precipitation and decrease the stability of asphaltene (Sarma, 2003). Baronia RV2 is rich in saturates fraction which might reduce the stability of asphaltene and might lead to asphaltene precipitation

The ratio of asphaltene to resins indicates the colloidal state of asphaltene in the oil. As mentioned earlier in chapter 2 in asphaltene-resins relationship section, resins stabilize asphaltene in the oil. Therefore, high asphaltene to resin ratio is generally expected to result in a low colloidal stabilization and lead to asphaltene precipitation (Mansoori, 1997; Sarma, 2003). However, some crudes do not follow that rule like the Venezuelan Boscan crude where asphaltene precipitation was not encountered in spite of its high asphaltene to resin ratio of 0.58. While the Algerian crude Hassi-Massaoud with asphaltene to resin ratio of 0.05 had severe problems of asphaltene precipitation (Mansoori, 1997). This indicates that there are other factors too that might affect asphaltene precipitation.

The SARA analysis results show that the asphaltene to resin ratio of Baronia RV2 crude is 0.14. This ratio is considered low. Based on this asphaltene to resin ratio, asphaltene precipitation is not expected for this oil. On the other hand, the SARA analysis results also show a relatively high saturates to aromatics ratio which might cause precipitation of asphaltene.

4.2 PHASE BEHAVIOR EXPERIMENTS

This part discusses the results obtained from the PVT experiments for Baronia RV2 separator oil and gas samples. The experiments included the compositional analysis up C₂₀₊ of separator oil and gas, physical recombination of separator oil and gas and constant composition expansion test (CCE). The phase behaviour study was carried out at simulated Baronia RV2 reservoir conditions of 3008 psia and 204°F.

4.2.1 Compositional analysis of separator oil

The separator oil sample was collected directly from the separator. It contained some amount of dissolved gas. Table 4.2 shows the composition of the separator oil calculated from the compositions of the stock tank oil and stock tank gas based on the measured gas oil ratio of 750scf/stb.

Table 4.2 Composition of separator oil (Baronia RV2)

Component	%Mol	%Wt	MW (g/mol)	Liquid Density (g/cc)
Nitrogen	0.12	0.03	28.01	0.81
Carbon Dioxide	0.07	0.02	44.01	0.82
Methane	3.17	0.38	16.04	0.30
Ethane	1.10	0.25	30.07	0.36
Propane	3.23	1.08	44.10	0.51
Iso-Butane	1.49	0.65	58.12	0.56
n-Butane	3.21	1.41	58.12	0.58
n-Pentane	0.02	0.01	72.15	0.60
Iso-Pentane	2.39	1.30	72.15	0.62
n-Pentane	2.37	1.29	72.15	0.63
Hexanes	4.81	3.13	86.18	0.66
Methylcyclopentane	2.32	1.47	84.16	0.75
Benzene	0.61	0.36	78.11	0.88
Cyclohexane	2.77	1.76	84.16	0.78
Heptanes	5.05	3.82	100.20	0.69
Methylcyclohexane	6.20	4.60	98.19	0.77
Toluene	0.27	0.19	92.14	0.87
Octanes	9.23	7.97	114.23	0.71
Ethylbenzene	1.04	0.84	106.17	0.87
meta+para-Xylene	0.53	0.43	106.17	0.87
ortho-Xylene	0.61	0.49	106.17	0.88
Nonanes	7.09	6.87	128.26	0.72
1,2,4 Trimethylbenzene	2.32	2.11	120.20	0.88
Decanes	5.84	6.27	142.29	0.73
Undecanes	5.50	6.49	156.31	0.74
Dodecanes	4.17	5.36	170.34	0.75
Tridacanes	4.40	5.85	176.00	0.81
Tetradecanes	3.91	5.61	190.00	0.82
Pentadecanes	4.77	7.36	204.00	0.83
Hexadecanes	2.75	4.53	218.00	0.84
Heptadecanes	2.03	3.55	232.00	0.84
Octadecanes	2.25	4.18	246.00	0.85
Nonadecanes	0.91	1.79	260.00	0.86
Eicosanes plus	3.45	8.54	327.77	0.86
Total	100.00	100.00		

Notes: The separator conditions were at pressure of 100 psi and temperature of 88°F

Calculated average molecular weight of oil=132.366 g/mol

GC column length is 100m with diameter of 0.25 mm, material of column is silica

The plus fraction was calculated using the grouping method for the heavy fractions (Danesh, 1998). Table 4.3 shows the plus fraction properties of Baronia RV2 separator oil.

Table 4.3 Plus fraction properties of separator oil (Baronia RV2)

Plus Fraction Properties	MW (g/mol)	Density (g/cc)	%Mol
C ₇₊	153.457	0.78	78.01
C ₁₂₊	216.203	0.83	28.64
C ₂₀₊	327.773	0.88	3.45

4.2.2 Compositional analysis of separator gas

The separator gas sample was collected at conditions of pressure 100 psi and temperature of 88°F. Table 4.4 shows that the separator gas of Baronia RV2 is rich in methane (76.30 %mol). Nitrogen and carbon dioxide are also present but their concentrations are very low. There is an absence of H₂S in Baronia RV2 oil. The average gas molecular weight is 22.73 g/mol, and the calculated gas gravity is 0.7836.

Table 4.4 Composition of separator gas (Baronia RV2)

Component	%Mol	%Wt	MW (g/mol)	Liquid Density (g/cc)
Nitrogen	0.31	0.38	28.01	0.81
Carbon Dioxide	0.80	1.55	44.01	0.82
Methane	76.30	53.85	16.04	0.30
Ethane	8.44	11.16	30.07	0.36
Propane	8.16	15.83	44.10	0.51
Iso-Butane	1.59	4.07	58.12	0.56
n-Butane	2.32	5.93	58.12	0.58
neo-pentane	0.00	0.00	72.15	0.60
Iso-Pentane	0.70	2.22	72.15	0.62
n-Pentane	0.53	1.68	72.15	0.63
Hexanes	0.43	1.63	86.18	0.66
Methylcyclopentane	0.12	0.44	84.16	0.75
Benzene	0.02	0.07	78.11	0.88
Cyclohexane	0.10	0.37	84.16	0.78
Heptanes	0.02	0.09	100.20	0.69
Methylcyclohexane	0.09	0.39	98.19	0.77
Toluene	0.02	0.08	92.14	0.87
Octanes	0.04	0.20	114.23	0.71
Nonanes	0.01	0.06	128.26	0.72
Total	100.00	100.00		

Note: The separator conditions were at pressure of 100 psi and temperature of 88°F

4.2.3 Calculation of recombined wellstream of Baronia RV2

The mass balance calculations were used in recombining the separator oil and separator gas compositions to obtain the complete composition of the reservoir fluid. Table 4.5 shows the composition of Baronia RV2 reservoir fluid calculated based on the compositions of the separator oil and gas, and separator GOR.

Table 4.5 Composition of reservoir fluid (Baronia RV2)

Component	%Mol	%Wt	MW (g/mol)	Liquid Density (g/cc)
Nitrogen	0.22	0.08	28.01	0.81
Carbon Dioxide	0.44	0.25	44.01	0.82
Methane	40.28	8.42	16.04	0.30
Ethane	4.83	1.89	30.07	0.36
Propane	5.73	3.29	44.10	0.51
Iso-Butane	1.54	1.17	58.12	0.56
n-Butane	2.76	2.09	58.12	0.58
neo-pentane	0.01	0.01	72.15	0.60
Iso-Pentane	1.53	1.44	72.15	0.62
n-Pentane	1.44	1.35	72.15	0.63
Hexanes	2.59	2.91	86.18	0.66
Methylcyclopentane	1.20	1.32	84.16	0.75
Benzene	0.31	0.32	78.11	0.88
Cyclohexane	1.41	1.55	84.16	0.78
Heptanes	2.50	3.26	100.20	0.69
Methylcyclohexane	3.10	3.96	98.19	0.77
Toluene	0.14	0.17	92.14	0.87
Octanes	4.57	6.80	114.23	0.71
Ethylbenzene	0.51	0.71	106.17	0.87
meta+para-Xylene	0.26	0.36	106.17	0.87
ortho-Xylene	0.30	0.41	106.17	0.88
Nonanes	3.50	5.85	128.26	0.72
1,2,4 Trimethylbenzene	1.14	1.79	120.20	0.88
Decanes	2.87	5.33	142.29	0.73
Undecanes	2.71	5.51	156.31	0.74
Dodecanes	2.05	4.56	170.34	0.75
Tridacanes	2.17	4.97	176.00	0.81
Tetradecanes	1.92	4.77	190.00	0.82
Pentadecanes	2.35	6.25	204.00	0.83
Hexadecanes	1.36	3.85	218.00	0.84
Heptadecanes	1.00	3.02	232.00	0.84
Octadecanes	1.11	3.55	246.00	0.85
Nonadecanes	0.45	1.52	260.00	0.86
Eicosanes plus	1.70	7.26	327.77	0.86
Total	100.00	100.00		

Notes: Separator conditions: Pressure of 100 psi and temperature of 88° F
 Calculated average molecular weight of the reservoir fluid = 76.72 g/mol

Figure 4.5 shows that the fluid is rich in light and intermediate components (C_1 - C_{16}), while the heavy components in C_{20+} is very low. This further confirms that Baronia RV2 is light oil. The calculation of recombined wellstream of Baronia RV2 will be important for any simulation study for Baronia RV2 reservoir in the future specially for a complete dynamic fluid flow simulation to study the effect of asphaltene precipitation in different regions in the reservoir. However the plus fraction has been calculated as C_{7+} , C_{12+} , and C_{20+} to be used for the simulation study, while simulation study the bigger the plus fraction used the most accurate results will be gained. Table 4.6 shows the plus fraction properties for Baronia RV2 reservoir fluid.

Table 4.6: Plus fraction properties for reservoir fluid (Baronia RV2)

Plus Fraction Properties	MW (g/mol)	Density (g/cc)	%Mol
C_{7+}	153.12	0.78	38.64
C_{12+}	216.20	0.83	14.11
C_{20+}	327.77	0.88	1.70

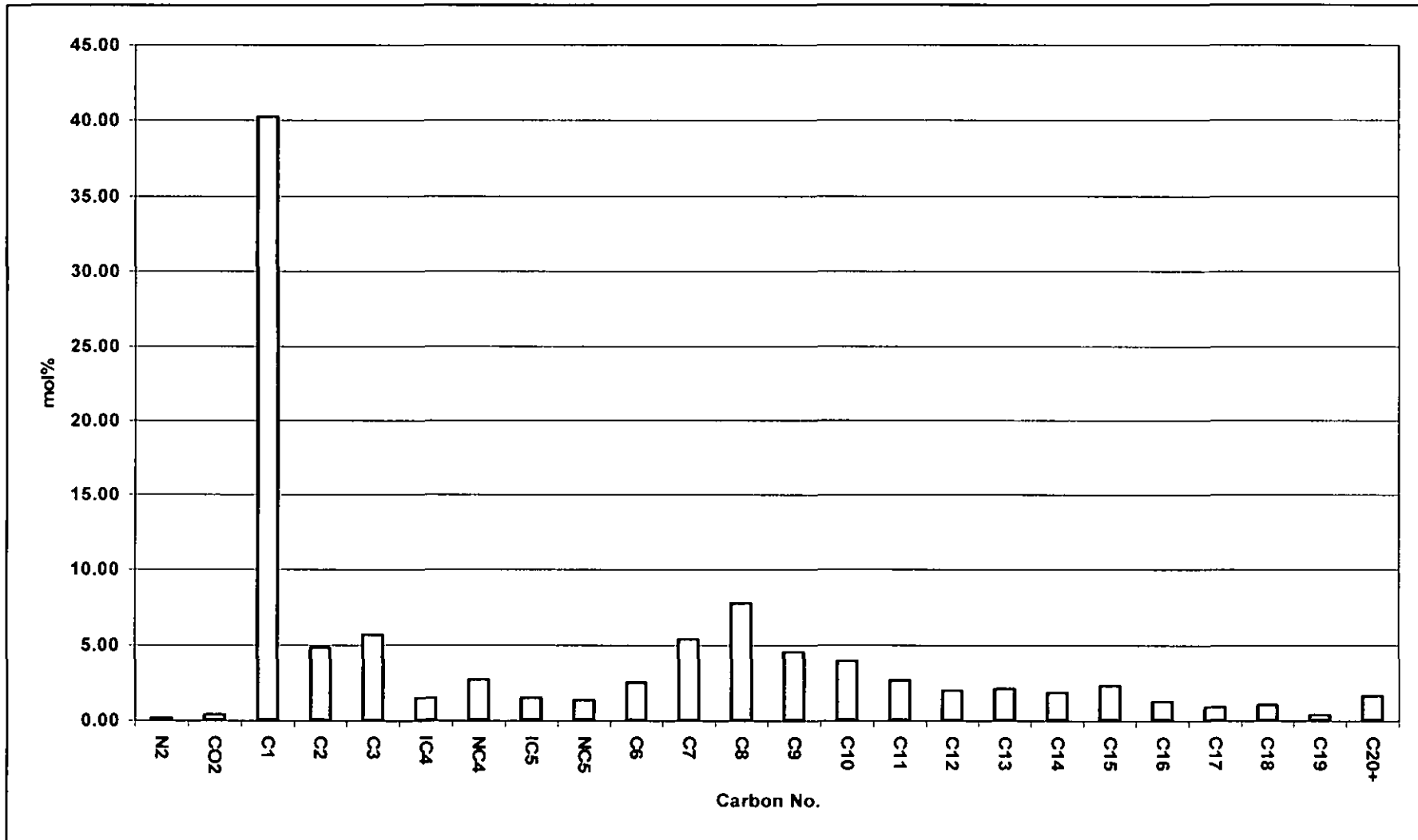


Figure 4.5 Single carbon number distribution for Baronia RV2 reservoir fluid

4.2.4 Constant Composition Expansion (CCE)

The test was conducted at reservoir temperature of 204°F using visual PVT cell. In the case of visual cell, the bubble point pressure range could be determined by visual observations of cell content (Dandekar, 2006). The initial observation indicated that the bubble point pressure, P_b was below 2700 psi and above 2600 psi because at 2700 psi the fluid was still in single phase, while at 2600 psi a gas cap was observed. After completion of the test, the pressure-volume (PV) data were plotted. A PV relationship is shown in Figure 4.6.

The Baronia RV2 crude oil is considered a volatile oil due to the high methane content, which is also responsible for the slight deviation in its PV -relation. In the case of normal black oil, distinct straight lines are usually observed in the PV -relation. However, in the case of Baronia RV2 this was not observed making it somewhat difficult to determine the P_b by the intersection of two straight lines. This behaviour is similar to volatile oils, where the change of slope at the bubble point pressure is less, almost like a curve and a sharp break is not clearly shown. This is because volatile oil is relatively more compressible than non-volatile oil; therefore some uncertainty remains in determining the bubble point from the PV relationship (Dandekar, 2006). However, visual observations of the first gas cap appearance of the reservoir fluid at simulated reservoir conditions enable a good estimation of the bubble point pressure from the PV -relation data. The PV relationship for Baronia RV2 was plotted using a straight line representing the single-phase region and a polynomial curve representing the 2-phase region. Figure 4.6 shows that the 2-phase region was plotted using a polynomial curve for two reasons:

- 1- The visual cell shows that the bubble point pressure is above 2600 psi and below 2700 psi as shown in Figure 4.7. The test was repeated 3 times to confirm the bubble point pressure range and each time the same result was obtained
- 2- The general gas law of $PV = ZnRT$ is not a straight line relationship because the z -factor is changing depending on the gas composition. The 2-phase region shows that the pump reading reduced (cell volume increased) by the pressure decreases. However, each reduced pressure will release more gas especially

Baronia RV2 is rich in C_1 , leading to change the gas composition and change the z -factor. However the volatile nature of the oil due to high content of C_1 which causes more gas components to come out of solution even at a slight pressure reduction. The presence of large amount of gaseous components makes the fluid more compressible below the P_b thus the polynomial behaviour. A polynomial curve with second degree order gives a good representation of the 2-phase region.

The measured P_b of Baronia RV2 was 2650 psig as determined from Figure 4.6, and this is supported by the P_b measurement by the visual observation of cell content that shows it was above 2600 psi and below 2700 psi. The intersect of two straight lines gives a bubble point of 2328 psi, which is shown high gas content in the cell as observed visually.

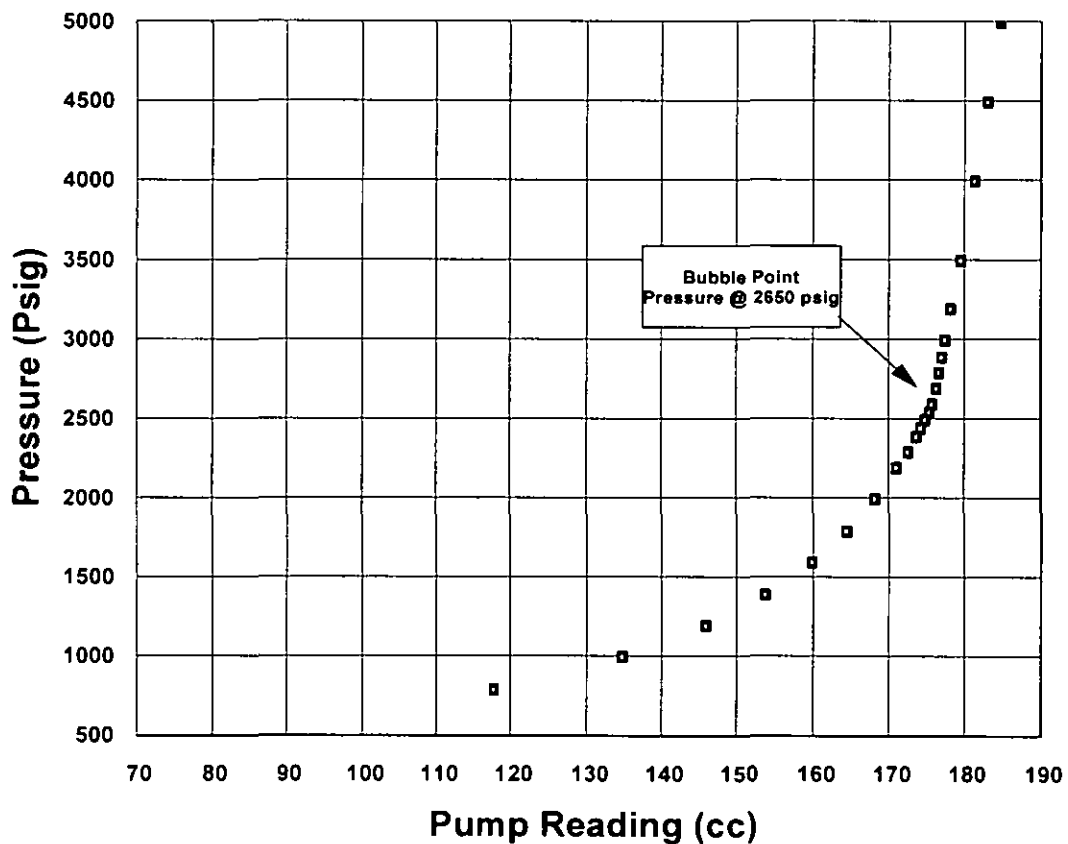


Figure 4.6 Pressure vs. volume at 204°F for Baronia RV2 recombine oil

Figure 4.7 shows four images for the PVT cell during the CCE test. Figure 4.7a shows the single phase at pressure of 2700 psig. By reducing the pressure slowly below 2700 psig, the first gas bubble started to appear as shown in Figure 4.7b. The gas bubble became bigger when the pressure decreased to 2600 psig as shown in Figure 4.7c. The gas phase became apparent when the pressure reached 2500 psig. The images of Figure 4.7 for the PVT cell confirmed that bubble point pressure for Baronia RV2 was below 2700 psig and above 2600 psig which is supported the bubble point calculation of Figure 4.6.

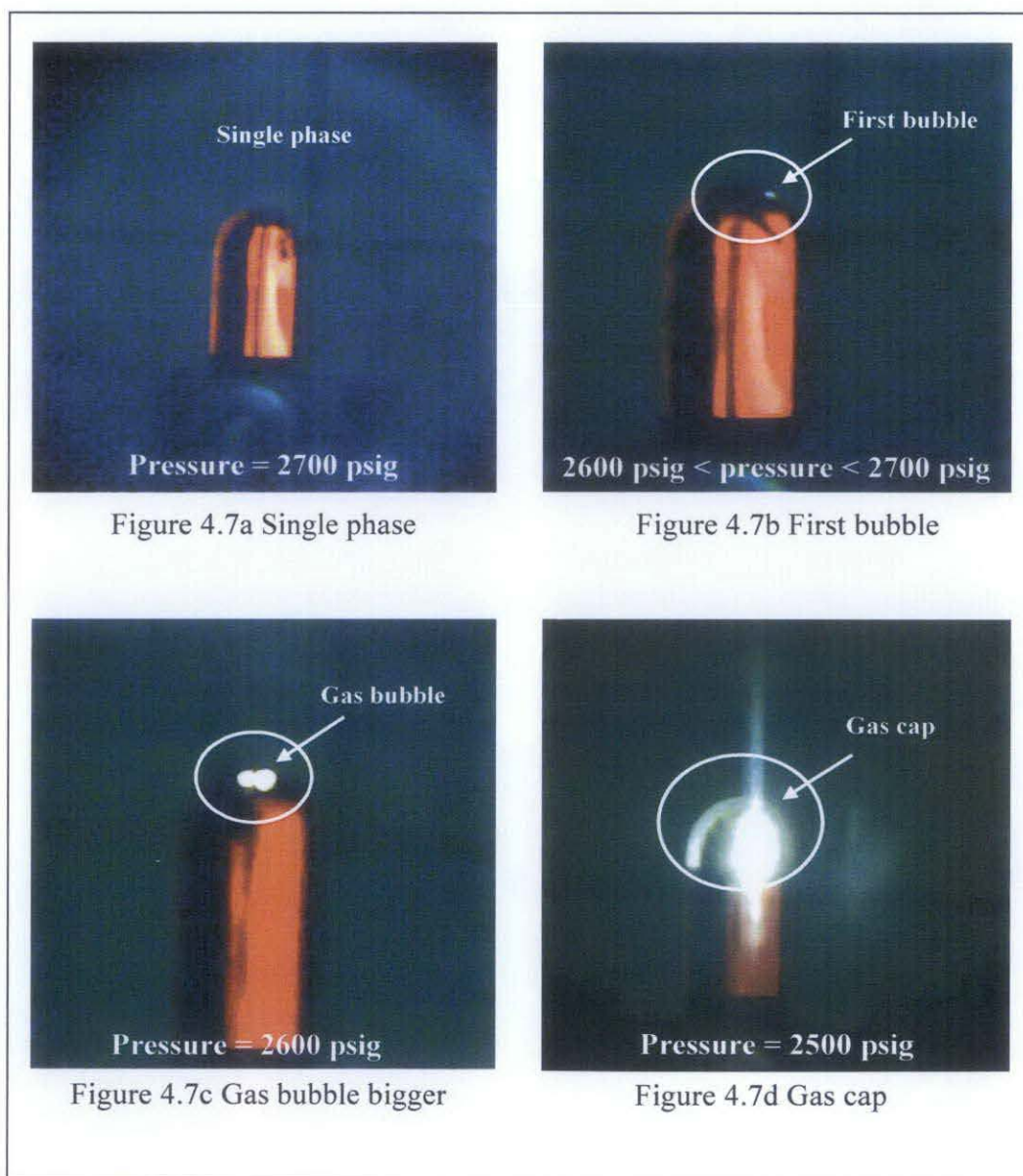


Figure 4.7 Single phase and 2-phase for Baronia RV2

The first PVT analysis for Baronia RV2 crude oil was done in 1976 by Sarawak Shell; the bubble point measurement was 3420 psi at GOR of 1212 scf/bbl (Nor Idah, 2005). The current result shows that the bubble point has decreased by about 770 psi after 32 years of production. The GOR has also been reduced to 750 scf/bbl from the original GOR of 1212 scf/stb due to the release of some gaseous components from the reservoir fluid. That makes the present Baronia RV2 reservoir fluid slightly heavier from its original fluid. Asphaltene precipitation expected to be higher for the GOR 1212 scf/stb due to the exists of light fractions. However the GOR now dropped to 750 scf/stb and asphaltene precipitation expected to be lesser than before due to the reduced of light fractions of crude oil.

4.3 EOR EXPERIMENTS

The aim of the EOR experiments is to evaluate the effectiveness of CO₂ gas injection in the Baronia RV2 reservoir. This EOR studies include the Micro-Slim tube displacement test and oil expansion behavior under CO₂ injection or swelling test.

4.3.1 Micro-Slim Tube Displacement Test

The objective of this experiment is to determine the minimum miscibility pressure (MMP) between injected CO₂ and Baronia RV2 reservoir fluid at its reservoir temperature of 204 °F. MMP results from the micro-slim tube test would be used to distinguish between miscible or immiscible displacements and the effect of pressure on displacement efficiency. For optimal oil recovery, the gas flooding should be conducted at a pressure equal to or greater than the MMP to ensure that miscibility can be achieved (Fred and Stalkup, 1983).

A series of displacement experiments was carried out on Baronia RV2 reservoir fluid with injected CO₂ at a series of pressures ranging from 1000 psig- 3600 psig. The volume of displaced oil at the gas breakthrough was calculated based on the time at which breakthrough occurred and the displacement rate. The recovery was then calculated as the percentage of the oil produced at CO₂ breakthrough (B/T).

$$\text{Recovery \%} = \frac{\text{Vol. of reservoir fluid produced @ Breakthrough}}{\text{Pore volume}} \times 100\% \quad (4.1)$$

Figure 4.8 shows the recovery % versus displacement pressure obtained from MMP test. The recovery gradually increases with displacement pressure, and then gradually level off after a certain pressure. Figure 4.8 shows that MMP for Baronia RV2-CO₂ is at 2435 psig.

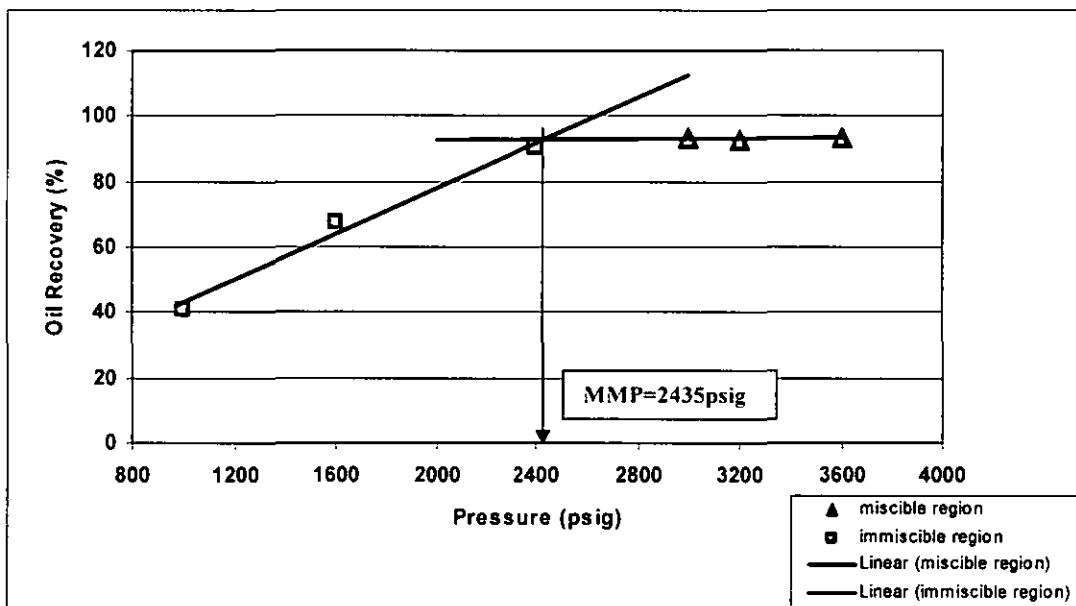


Figure 4.8 Oil Recovery vs. Displacement Pressure

The two regions of miscible and immiscible shown in Figure 4.8 were chosen, in accordance with the reported recommendation (Holm and Josendal, 1980). The study suggested that a displacement is considered miscible when more than 80% of oil in place is recovered at CO₂ breakthrough (Holm and Josendal, 1980).

The MMP of CO₂ with Baronia RV2 reservoir fluid is 2435 psig at the reservoir temperature 204 °F. However the bubble point pressure is 2650 psig which is higher than the MMP. Usually miscibility is developed by a purely vaporizing gas drive mechanism; in which case the MMP is always equal or greater than the bubble point pressure (Lars and Whitson, 2000). However when the injected gas contains light-intermediate components (C₂-C₅) or CO₂, the miscibility conditions are usually developed by condensing/vaporizing mechanism which make the MMP often less

than the bubble point pressure (Lars and Whitson, 2000). The miscibility of CO₂ with Baronia RV2 reservoir fluid is expected to be achieved quite easily due to high reservoir pressure of 3008 psia. When CO₂ mixed with Baronia RV2 reservoir fluid, the former will be at a pressure higher than the pressure needed to achieve miscibility with the reservoir fluid. Therefore CO₂ flooding in Baronia RV2 is expected to be a miscible process because the indicated MMP is lower than the reservoir pressure of 3008 psia

4.3.2 Swelling Test

Swelling test was carried out to investigate the oil expansion behavior under CO₂ injection. The solubility and effect of injected CO₂ in the reservoir oil were analyzed in these experiments by measuring the swelling factor, saturation pressure curve, liquid and the two-phase region (by constant mass expansion) for different mixtures of injected CO₂ and reservoir oil. Swelling test was carried out with four different concentrations of CO₂. The calculated amount (%mol) of CO₂ was based on material balance calculations by considering the transfer pressure and temperature from the CO₂ cylinder to the PVT cell. Table 4.7 shows the CO₂ concentration and %mol of CO₂ added to Baronia RV2 reservoir fluid.

Table 4.7 Amount of CO₂ added for swelling test

CO ₂ added (%mol)	Vol. of CO ₂ added @ 5000 psig (cc)
20	2.30
40	3.82
60	7.64
80	23.10

A Constant Composition Expansion (CCE) or bubble point pressure measurement was carried out on the mixture at each different concentration of CO₂ to examine the effect of CO₂ on the phase behavior of reservoir fluid. The results are shown in Table 4.8. Asphaltene precipitation has been observed during swelling test, the images of asphaltene precipitation has been attached in Appendix D.

Table 4.8 Results of CCE with different concentrations of CO₂ at 204°F

% CO ₂	Bubble Point Pressure (psig)	Swelling Factor
0	2650	1
20	2802	1.280
40	3025	1.303
60	3370	1.731
80	3880	3.260

Table 4.8 shows that both the bubble point pressure and the swelling factor increase with increasing concentration of CO₂ in the mixture. Pressure versus volume plot at different CO₂ concentration has been attached in Appendix E. These results suggest that CO₂ increases the volume of reservoir fluid trapped in the pores leading to swelling of the oil and displace it forward (Martin and Taber, 1992). The swelling factor shown in Table 4.8 represents the volume at saturation pressure of CO₂-oil mixture divided by the volume at saturation pressure of virgin oil. At 0% CO₂ i.e. virgin oil, the swelling factor is defined as 1. When CO₂ concentration increases, the swelling factor starts to increase because the oil volume becomes larger than the volume of the virgin oil. The dissolving CO₂ seems to expand the oil volume which leads to higher oil recovery (Fred and Stalkup, 1983).

In a similar study, Fred and Stalkup (1983) reported that the bubble point pressure increased due to the extraction of light and intermediate components of reservoir fluid by CO₂. The extraction of light and intermediate components from the reservoir fluid also caused a disturbance in the thermodynamic equilibrium of asphaltene-resins (Sarma, 2003). CO₂ affects the swelling factor and expands the oil volume. One of the advantages of CO₂ in EOR is the expansion of oil volume when CO₂ is mixed with the reservoir oil which will push the oil forward and affects higher recovery.

4.4 ASPHALTENE PRECIPITATION EXPERIMENTS

Asphaltene precipitation study consists two types of experiments: the static test (isobaric and isothermal) with different %mol of CO₂, and the dynamic test at different pressures and different %mol of CO₂ (isothermal).

4.4.1 Static Asphaltene Precipitation Test

The static test was carried out to assess the controlling factor, CO₂ concentration form asphaltene precipitation. This test was carried out at reservoir pressure of 3008 psia and temperature of 204°F (isobaric and isothermal) by adding different %mol of CO₂ (22%, 40%, 70%, 85%) to the live oil. The test was to investigate the effect of CO₂ concentration on asphaltene precipitation, as well as calculating cumulative asphaltene precipitation that might occur when the oil is in contact with fresh CO₂.

Figure 4.9 shows the graph of asphaltene precipitation versus CO₂ %mol obtained from the static test. At constant pressure the precipitation of asphaltene increases with increasing concentration of CO₂. This phenomenon can be explained by the constant extract effect of CO₂ of lighter hydrocarbons and some middle or heavier components from oil, which might alter the asphaltene-resins ratio causing asphaltene precipitation (Kokal and Sayegh, 1995; Srivastava *et al.*, 1997; Sarma, 2003). Results of static and dynamic asphaltene tests by Srivastava *et al.* (1999) during their study on Weyburn light crude oil for CO₂ injection suggest that CO₂ concentration could have very significant impact on asphaltene precipitation. There was a direct and linear relationship between CO₂ concentration and asphaltene precipitation, with increasing CO₂ concentration, asphaltene precipitation increased linearly (Srivastava *et al.*, 1999).

Observation during experiment shows that asphaltene precipitation increases with increasing amount of injected CO₂. Ying *et al* (2006) observed that when CO₂ increased, the precipitated asphaltene also increased. The study reported that CO₂ extracted light and intermediate components from the oil will and caused more disturbance to the asphaltene-resins ratio should lead to higher asphaltene precipitation (Parra-Ramirez *et al.*, 2001; Ying *et al.*, 2006).

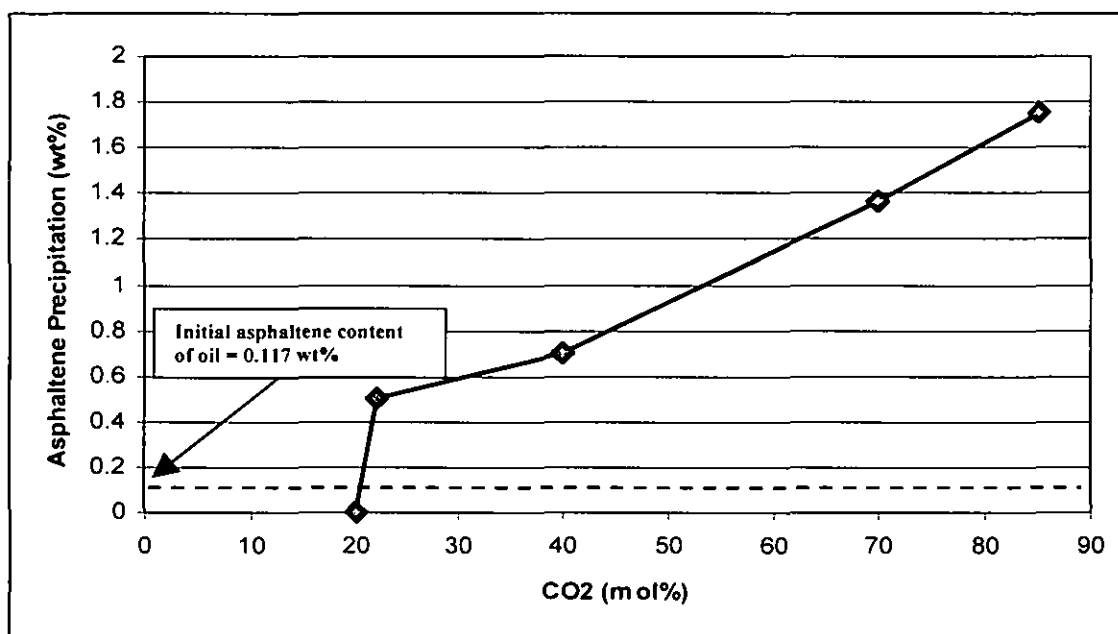


Figure 4.9 Cumulative asphaltene precipitation with different %mol of CO₂ at 3008 psia and 204°F

Observation from the present study shows that asphaltene starts to precipitate at the concentration of 22 %mol of CO₂, and increases slowly until 40 %mol CO₂. After 40 %mol CO₂ there was a linear increase of asphaltene precipitation with amount of injected CO₂. Srivastava *et al* (1995), reported in their study on light oil that asphaltene began to flocculate at about 42 %mol of CO₂ and after that there was a linear increase of asphaltene (%wt) with amount of injected CO₂ (%mol) (Srivastava *et al.*, 1995; Parra-Ramirez *et al.*, 2001). Novosad and Constain (1990), observed precipitation at 40-50 %mol CO₂ concentrations during their study on Midale light oil in Canada (Novosad and Constain, 1990). Monger and Fu (1987) and, Monger and Trujillo (1991), observed asphaltene precipitation in the mixtures of light oil containing 70 and 96 %mol of CO₂ (Monger and Fu, 1987; Monger and Trujillo, 1991).

These reported observations suggest that there is no consensus on the CO₂ concentration that will induce asphaltene precipitation. Each type of crude oil has its own different properties that might have some influence on asphaltene precipitation too. Therefore, at present the asphaltene precipitation study is limited to case study only and could not be a general study yet.

Baronia RV2 has a very low asphaltene content of 0.117 %wt. In spite of that, the possibility of asphaltene precipitation cannot be ruled out because the injection of CO₂ into a reservoir might cause changes in the fluid behavior and equilibrium conditions which favor the precipitation of asphaltene (Kokal and Sayegh, 1995; Srivastava *et al.*, 1997; Sarma, 2003). This necessitates the need to perform a dynamic asphaltene precipitation test.

4.4.2 Dynamic Asphaltene Precipitation Test

The Dynamic asphaltene test is to investigate the asphaltene precipitation under dynamic conditions during the displacement of oil by CO₂. In any asphaltene precipitation study, dynamic test is conducted to confirm the existence of asphaltene precipitation during fluid flow conditions. In static test, CO₂ contacted the oil without any flow which gives more time to the CO₂ to extract the intermediate and light components from oil. However, in dynamic test, CO₂ contacted the oil during the injection which let CO₂ contacted fresh oil each time which might not lead to any asphaltene precipitation. Burke *et al.* (1990) has shown that in static tests, asphaltene flocculation usually occurs, whereas in dynamic tests, precipitation of asphaltene might not occur (Parra-Ramirez *et al.*, 2001).

Dynamic asphaltene test was carried out using different concentrations of CO₂ and at different pressures, at reservoir temperature 204 °F (isothermal). This test was conducted using the Micro-Slim tube equipment to allow wider of pressure change to examine asphaltene precipitation.

A total of six experimental runs were carried out to investigate the amount of asphaltene precipitation. The effect of CO₂ concentration and pressure were studied. This study would allow the determination of conditions of pressure and CO₂ concentration with minimum asphaltene precipitation that will be beneficial to avoid any precipitation problems. The volume of injected CO₂ was calculated by multiplying the time of actual contact of CO₂ with oil by the flow rate of 0.25 cc/min. The calculation details of CO₂ %mol is given in Appendix B.

Table 4.9 shows the asphaltene precipitation that collected from the oil recovery during the MMP test and the asphaltene precipitation from the residue that trapped inside the micro-slim tube which collected after the cleaning by n-Heptane. The final asphaltene precipitation (%wt) was calculated by the summation of asphaltene weight (g) from the recovery and residue to get the final weight and then calculate the asphaltene precipitation (%wt)

Table 4.9 Asphaltene precipitation with different pressures and CO₂ concentrations

Pressure (psi)	CO ₂ (%mol)	Asphaltene Precipitation (g) from Recovery	Asphaltene Precipitation (g) from Residue	Asphaltene Precipitation (%wt)
1000	9.00	0.0008	0.0025	0.06
1600	37.65	0.0061	0.0019	0.14
2200	53.32	0.0545	0.0006	0.96
2400	50.06	0.0279	0.0021	0.52
3000	56.03	0.0651	0.0002	1.14
3600	57.43	0.0159	0.0021	0.31

Table 4.9 shows a fluctuating asphaltene precipitation, which might be due to a combined effect of changing CO₂ concentration and pressure together. On the other hand, in the static test where only the CO₂ concentration was varied, the asphaltene precipitation increased when the concentration of CO₂ was increased. In the static test, the increase in asphaltene precipitation was due to the effect of increasing CO₂ concentration only.

A three-dimension surface plot of the results from Table 4.9 is made to illustrate the behavior of asphaltene precipitation for Baronia RV2 under simultaneous changes in pressure and CO₂ concentration. Figure 4.10 shows the three-dimension surface graph of asphaltene precipitation and the measured asphaltene precipitation with different CO₂ concentrations at different pressures. The measured values showed as (x, y, z) axis. Figure 4.10 shows that the asphaltene precipitation increased by increasing the CO₂ concentration and pressure decrease.

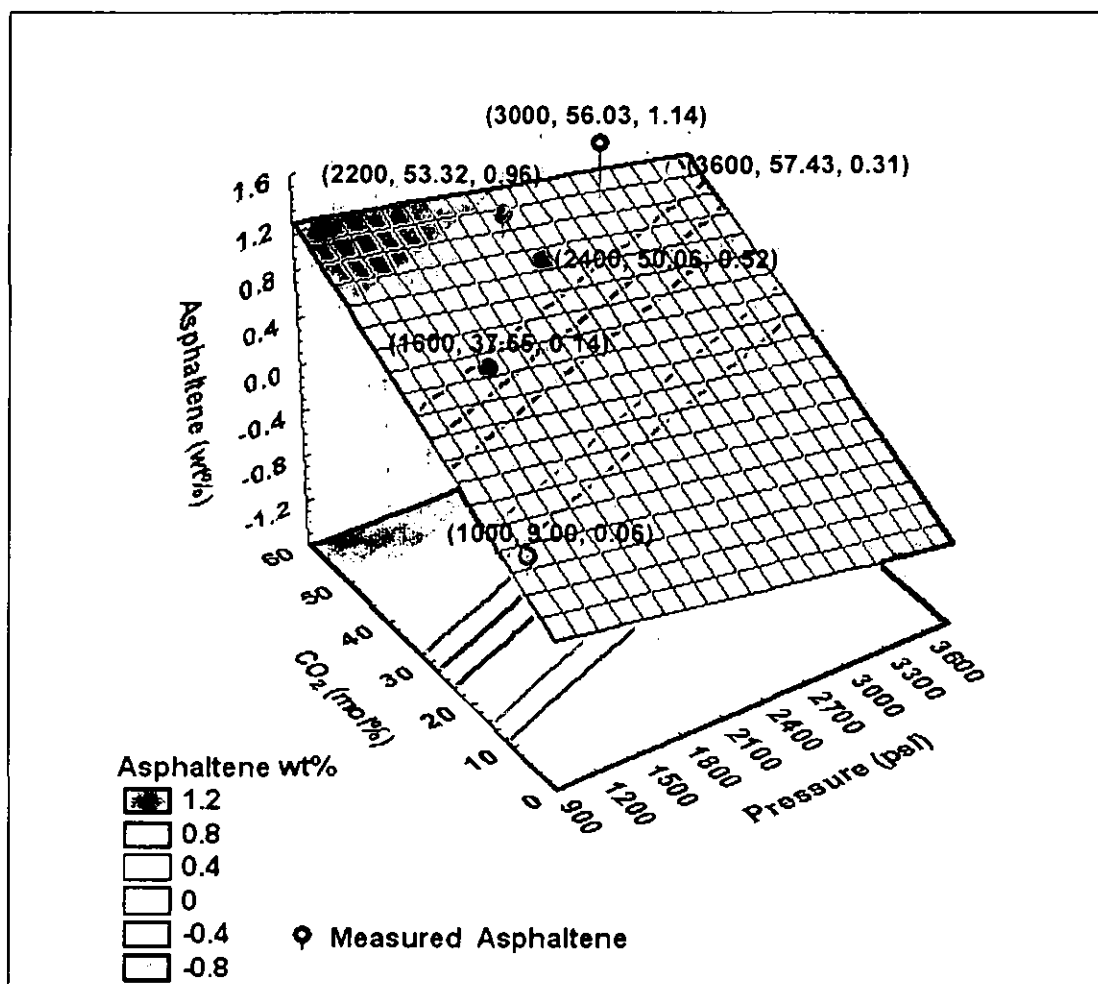


Figure 4.10 Asphaltene precipitation with different %mol of CO₂ and different pressures at 204°F

Figure 4.10 suggests that there might be a steady increase of asphaltene precipitation as CO₂ concentration increases. Similar linear relationship has also been suggested in the literature (Novosad and Constain, 1990; Parra-Ramirez *et al.*, 2001; Moghadasi *et al.*, 2006; Ying *et al.*, 2006).

At high pressure, the asphaltene precipitation increases in the presence of high CO₂ concentration. However, the amount of precipitation at these conditions (high CO₂, high pressure) is relatively less than that at lower pressure. This suggests that CO₂ concentration has bigger impact than the pressure towards asphaltene precipitation. This could be explained by the increase in the solubilizing ability of the solution at high pressure, which causes the asphaltene to remain dissolved in the

solution and only a small amount would precipitate out, even though the CO₂ concentration in the crude oil is relatively high (Muhammad Sahimi *et al*, 1997).

The observation from Figure 4.10 suggests that for Baronia RV2 oil, asphaltene precipitation increases with increasing CO₂ concentration and decreasing pressure.

For the reservoir conditions of pressure 3000 psi and temperature of 204° F, Table 4.8 shows that maximum asphaltene precipitation of 1.14 %wt occurred at 56.03 %mol CO₂. By following the asphaltene behavior for Baronia RV2 from Figure 4.10, at 3000 psi the asphaltene precipitation can be expected to exceed 1.14 %wt if the CO₂ concentration increases above 56.03 %mol. However, such situation might not occur in the reservoir because the current reservoir pressure is 3008 psi. When CO₂ is injected into the reservoir, the reservoir pressure will be raised to more than 3500 psi especially near the wellbore region. In addition, higher pressure will increase the solubility of asphaltene and cause less asphaltene to be precipitated even at high concentration of CO₂.

This observation seems to suggest that Baronia RV2 oil might not encounter severe problem of asphaltene precipitation when the reservoir pressure is above 3000 psi, even at high concentration of CO₂. However to predict the asphaltene precipitation at any concentration of CO₂ and at any pressure a correlation of asphaltene precipitation for Baronia RV2 has been developed using the data from dynamic asphaltene precipitation test.

4.5 STATISTICAL ANALYSIS FOR PREDICTION OF ASPHALTENE PRECIPITATION

This section discusses the statistical analysis correlating effect of pressure and CO₂ concentration on asphaltene precipitation for Baronia RV2 under the dynamic asphaltene conditions. The analysis used to predict the amount of asphaltene precipitation at any pressure and any CO₂ concentration and to compare them with values obtained from the dynamic asphaltene precipitation test. This correlation is based on the statistical method of regression and analysis of variance (ANOVA), which eliminated the properties of complex asphaltene.

The developed correlation of asphaltene precipitation for Baronia RV2 is a statistical analysis for the dynamic asphaltene test data. The correlation did not include the physics aspects and the properties of complex asphaltene. It is valid on the test of dynamic asphaltene precipitation for Baronia RV2 and at its conditions only.

4.5.1 Linear Regression Model

Linear regression model has been used to analyze the data of dynamic asphaltene test by using regression analysis tool of Microsoft excel software. After applying the statistical analysis of linear and polynomial regression on the gathered data from the dynamic asphaltene precipitation test, the linear regression gave the best model fitting on the gathered data. A complete analysis is shown in Appendix C. In the linear regression model, the dependent variable is assumed to be a linear function of one or more independent variables plus an error introduced to account for all other factors. The regression equation has the following form (Montgomery, 2001):

$$y = \beta_0 + \beta_1 x_1 + \beta_2 x_2 + \dots + \beta_k x_k + \varepsilon \quad (4.2)$$

In the above regression equation, y is the dependent variable, x_1, \dots, x_k are the independent or explanatory variables, β_0 defines the intercept of the plane, β_1 and β_2 are called the partial regression coefficients. β_1 measures the expected change in y per unit change in x_1 when x_2 is held constant and β_2 measures the expected change in y per unit change in x_2 when x_1 is held constant, and ε is the disturbance or error term.

Equation 4.2 called a multiple linear regression model, a linear function of the unknown parameters β_0 , β_1 , and β_2 (Montgomery, 2001).

4.5.2 Analysis of Variance (ANOVA)

Analysis of variance (ANOVA) is a statistical technique that is often used in the analysis of results from experiments containing two or more independent variables (Clarke, G.M., and Kempson, 1997; Montgomery, 2001). This method allows more than two sets of data to be examined at the same time. There are many different types of ANOVA, but they all use the same basic method of comparing the variance between different treatments (experimental data) with the variance within treatments (Clarke, G.M., and Kempson, 1997; Montgomery, 2001; Montgomery and Runger, 2002).

4.5.3 Model Fitting and Statistical Analysis

The modeling prediction of asphaltene precipitation for Baronia RV2 was done using the data of dynamic asphaltene test shown in Table 4.9. The data included pressure and CO₂ concentration as two variables acting together on asphaltene precipitation depending on the operating conditions. The linear multiple regression model was used where asphaltene represents the dependent variable y , while pressure and CO₂ %mol represented the independent variables x_1 and x_2 (Clarke, G.M., and Kempson, 1997; Montgomery, 2001).

The accuracy of the model was checked with the Analysis of Variance (ANOVA) using Fisher F-test (Clarke, G.M., and Kempson, 1997; Montgomery, 2001; Istadi, 2006). The significance test of regression was carried out to determine the relationship between the response variable (asphaltene precipitation) and a subset of the independent variables (pressure and CO₂ %mol). The response surface analyses were employed by utilizing Microsoft Excel 2003 software using the regression analysis tool.

Equation 4.3 shows the general form of the linear regression model that has been used for predicting asphaltene precipitation for Baronia RV2 (Clarke, G.M., and Kempson, 1997; Montgomery, 2001).

$$y = \beta_0 + \sum_{j=1}^2 \beta_j x_j + \varepsilon \quad (4.3)$$

Where:

y : Asphaltene Precipitation (%wt)

x_1 : Pressure (psi)

x_2 : CO₂ concentration (%mol)

β_0 : the model intercepts

β_1, β_2 : partial regression coefficients for pressure and CO₂ respectively

ε : The disturbance error term (%)

After applying the regression analysis by entering the data of Table 4.9 in the multi regression analysis using Microsoft Excel, where, y -axis represents asphaltene precipitation values, x_1 as pressure values and x_2 as CO₂ concentration values. The confidence level used in this analysis was specified as 95%.

Two trials were carried out for different assumptions of β_0 . In the first trial β_0 was assumed as not zero ($\beta_0 \neq \text{zero}$), and in the second trial β_0 was assumed as zero ($\beta_0 = \text{zero}$). When the $\beta_0 \neq \text{zero}$, the model did not give a good analysis due to low R^2 in addition to lower F -value than the F -table. However when $\beta_0 = \text{zero}$, the model gave very good results. For that reason, the β_0 is assumed to be zero in order to obtain the best results.

The results of dynamic asphaltene test were analyzed for the first trial by assuming $\beta_0 \neq \text{zero}$. Table 4.10 shows the regression analysis results by using the regression analysis tool of Microsoft excel 2003.

Table 4.10 Results of regression analysis when $\beta_0 \neq$ zero

Source	Sum of Squares	Degree of Freedom	Mean Squares	F-value
Regression	0.4849	2	0.2424	1.4655
Residuals	0.4963	3	0.1654	
Total	0.9812	5		
R^2	0.4942			
R	0.7030			

The suggested equation of asphaltene precipitation from the first trial with the assumption that $\beta_0 \neq$ zero is shown in equation 4.4

$$y = -0.1044 - 0.0002 P_{(\text{psi})} + 0.0251 \text{CO}_{2(\text{mol}\%)} \quad (4.4)$$

The results of the second trial with assumed $\beta_0 =$ zero are as shown in Table 4.11.

Table 4.11: Results of regression analysis when $\beta_0 =$ zero

Source	Sum of Squares	Degree of Freedom	Mean Squares	F-value
Regression	2.1187	2	1.0593	8.4077
Residuals	0.5040	4	0.1260	
Total	2.6226	6		
R^2	0.8078			
R	0.8988			

The correlation of asphaltene precipitation from the second trial which assumed $\beta_0 =$ zero is shown in equation 4.5

$$y = 0 - 0.0002 P_{(\text{psi})} + 0.0244 \text{CO}_{2(\text{mol}\%)} \quad (4.5)$$

The accuracy of the predicting model is judged from the determination coefficient, R^2 , which reveals total variation of the observed values of activity about its mean and is often used to judge the accuracy of a regression model. (Montgomery, 2001; Montgomery and Runger, 2002). In the case of $\beta_0 \neq$ zero (Table 4.10), the regression coefficients were estimated with a low determination coefficient of $R^2 = 0.4942$. However in the case of $\beta_0 =$ zero (Table 4.11), the regression coefficients were estimated with a satisfactory determination coefficient of $R^2 = 0.8078$.

The R^2 value indicates how much the agreement between the experimental and predicted values. For trial 1 (Table 4.10) when $\beta_0 \neq$ zero, a weak agreement is shown between the experimental and predicted values which implies that 49.42% of the total variation in the response is justified by the model. However, a fairly good agreement between the experimental and predicted values of the fitted model exists for trial 2 (Table 4.11) when $\beta_0 =$ zero. It implies that 80.7% of the total variation in the response is justified by the model.

In addition, the correlation coefficient R is a statistical measure of how well the data lies along the regression line or how well the two variables are correlated. The coefficient of correlation serves as a quantitative basis of judging how good the linear model function is for predictive purpose. The correlation coefficient R is a number between -1 and 1. A value of R which is close to 1 or -1 indicates strong correlation and a coefficient close to 0 indicates very little correlation (Lial M. L. *et al*, 2002). Comparing case 1 ($\beta_0 \neq$ zero) $R=0.7030$ and case 2 ($\beta_0 =$ zero) $R=0.898$, case 2 shows that the asphaltene precipitation model signifies a stronger correlation between the experimental and the predicted values than case 1 due to higher R value (Clarke and Kempson, 1997; Montgomery, 2001, Istadi, 2006). Thus, case 2 ($\beta_0 =$ zero) has been chosen due to the higher accuracy between the experimental and predicted results than case 1 ($\beta_0 \neq$ zero).

The accuracy of the model was checked by ANOVA method (Montgomery, 2001). The F -value for the regression is defined as the ratio of mean square due to regression to the mean square due to residual error (Montgomery, 2001). The test of significance of the fitted regression model is based on the following hypothesis:

- Null Hypothesis (H_0): $\beta_1=\beta_2=0$, [the independent variables (pressure and CO₂) have no effect on dependent variable (asphaltene)]
- Alternative Hypothesis (H_A): At least one $\beta \neq 0$, [the independent variables (pressure and CO₂) have effect on dependent variable (asphaltene)]

The (H_0) is true if the F -value $< F$ table ($F_{\alpha_s, df1, df2}$), and thus the (H_A) is rejected. Here, α_s denotes level of significance, while ($df1$) and ($df2$) express degrees of freedom with respect to regression and residual error, respectively. On the contrary, if the F -value $> F$ table ($F_{\alpha_s, df1, df2}$), the null hypothesis is rejected and the alternative hypothesis is true (Clarke and Kempson, 1997; Montgomery, 2001; Istadi, 2006). F -table values are shown in Appendix C.

In general, the calculated F -values should be equal to or greater than tabulated values for the model to be considered good (Clarke and Kempson, 1997; Montgomery, 2001). In fact, the calculated F -value corresponding to asphaltene precipitation model is 8.4077 as shown in Table 4.10, and it is greater than the tabulated F -value ($F_{0.05, 2, 4} = 6.9443$) as shown in F -value tables in Appendix C. The F -value shows a statistically significant regression at 5% level of significance (95% confidence level). In this case, the null hypothesis (H_0) is rejected at 5% level of significance based on the marked F -value (Montgomery, 2001; Istadi, 2006) implying that the independent variables contribute significantly to the model.

Figure 4.11 shows a three dimensional plot of the measured and predicted amount of asphaltene precipitation, which shows quite close results between the predicted and measured points. Figure 4.11 shows that at pressures higher than 3000 psi which it is the reservoir pressure, asphaltene precipitation existed but in small amount of less than 0.3 %wt, which might not pose significant problems in the reservoir during CO₂ injection.

The figure also shows that at low pressure, asphaltene precipitation is very low, but there is no process that will reduce the reservoir pressure to less than 3000 psi. This suggests that the solution to minimize possible asphaltene precipitation for Baronia RV2 is by injecting CO₂ at a pressure higher than 3000 psi.

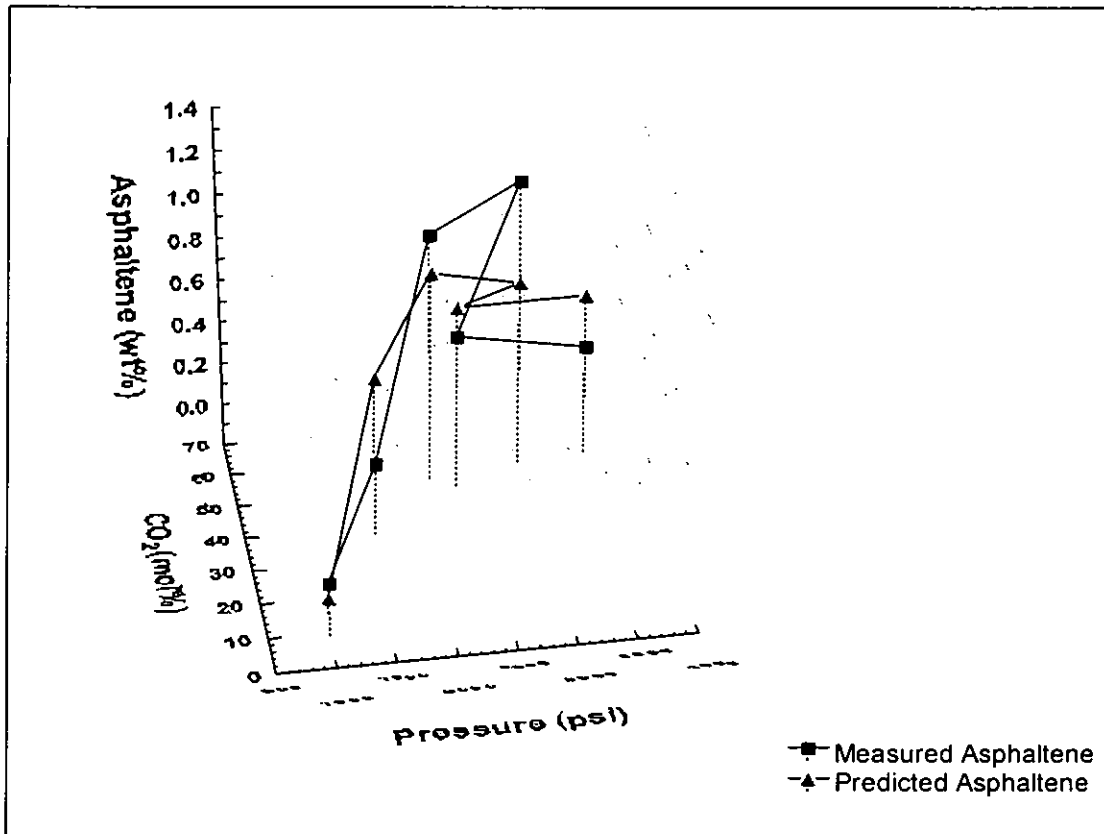


Figure 4.11 Three-dimension plot for measured and predicted asphaltene precipitation

4.5.4 Testing of Statistical Prediction of Asphaltene Precipitation

The statistical prediction equation of asphaltene precipitation was tested to check the validity of the results by applying different concentrations of CO₂ to determine the onset point of asphaltene precipitation at selected pressure then the behavior of asphaltene precipitation by changing the CO₂ concentration at different pressures would be assessed.

Figure 4.12 shows the calculated asphaltene precipitation for Baronia RV2 using Equation 4.5. The figure shows the existence of a linear relationship between the asphaltene precipitation and CO₂ concentration.

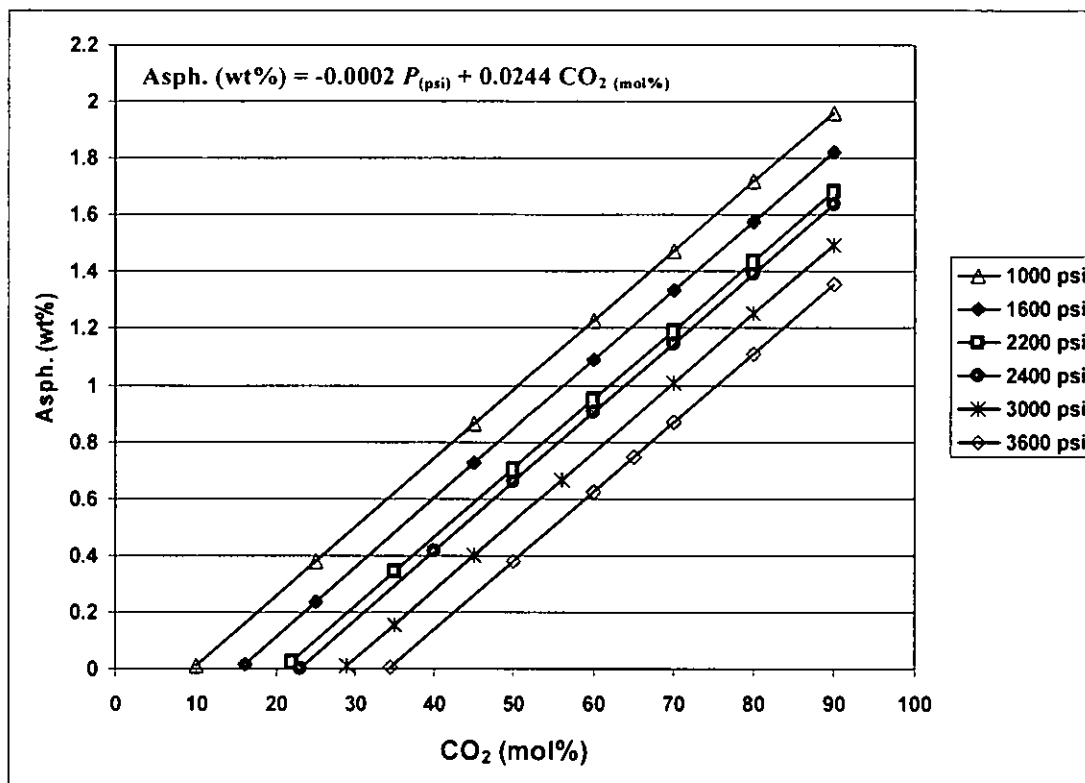


Figure 4.12 Predicted asphaltene precipitation versus. CO₂ concentration at different pressures

The figure above shows different asphaltene onset point for each pressure. The onset point increases with increasing pressure. For example at 1000 psi, the asphaltene starts to precipitate at about 10 %mol of CO₂, while at 3600 psi, the asphaltene starts to precipitate at about 35 %mol of CO₂. At pressures below the bubble point pressure, most of the light components have left the solution and evolved into the gas phase. By adding CO₂ to the live oil at low pressure, which is in a two-phase state, the light and intermediate components that still exist in the liquid phase will be extracted by the CO₂ leading to precipitation of asphaltenes. At low pressures this will happen at lower CO₂ concentrations than that at high pressure.

Results from Figure 4.12 also suggest that at certain CO₂ concentration, the amount of asphaltene precipitation is more at low pressure than that at high pressure. This could be explained by the difference in asphaltene solubility at low and high pressures (Muhammad Sahimi *et al*, 1997; Buenrostro-Gonzalez *et al.*). At high pressures more asphaltene is able to remain dissolved in the reservoir fluid due to high fluid density, thus only a small amount of asphaltene will be precipitated. However at

low pressure the solubility of asphaltene decreases due to low fluid density. In addition the large distance between the asphaltene particles and the surrounding fluid particles will lead to higher asphaltene precipitation at low pressure (Muhammad Sahimi *et al.*, 1997; Buenrostro-Gonzalez *et al.*, 2004; Speight, 2004).

Muhammad Sahimi *et al.* (1997) observed in a study on Iranian light oil, that as the pressure increases, the asphaltene precipitation decreases. However, Buenrostro-Gonzalez *et al.* (2004) reported that the pressure depletion might cause asphaltene precipitation due to reduce the density of crude oil which allows easily destabilizing the stability of asphaltene-resins micelles which lead to asphaltene precipitation.

Other correlation using same statistical method of previous correlation was developed base on the polynomial multiple regression modeling to improve the linear regression correlation of asphaltene precipitation for Baronia RV2. This correlation was more accurate to plot the measured data of dynamic asphaltene test shown in Table 4.9. The accuracy of this correlation was 96% while the accuracy for the linear regression model was 80%. However the linear regression model was justified statistically but the predicted asphaltene precipitation is little far from the measured data. The polynomial multiple regression model was tested and showed close relationship between the predicted data and measured data but statistically was not fully justified. The statistical justification was only dependent on *R*-square which it was 0.965 which is much higher than the *r*-square of the linear regression correlation which it was 0.807. But the *F* test was failed for the polynomial correlation because the *F*-calculated which was 5.67 less than less than *F*-table which was 230. The *F*-value has been calculated and compared from the table as mention previously for the linear regression model, and the *F*-table is shown in appendix C. Results from the regression analysis for the polynomial multiple regression model is shown in Table 4.12

Table 4.12: Results of the polynomial multiple regression model

Source	Sum of Squares	Degree of Freedom	Mean Squares	F-value
Regression	2.5334	5	0.5067	5.6780
Residuals	0.0892	1	0.0892	
Total	2.6226	6		
R^2	0.9659			
R	0.9828			

The correlation of asphaltene precipitation using the polynomial multiple regression model is shown in equation 4.6

$$y = 0 - 0.0012P - 0.08852CO_2 - 8.7407E-07(P)^2 + 0.0002(CO_2)^2 + 5.7318E-05(P \times CO_2) \quad (4.6)$$

Figure 4.13 shows the calculated asphaltene precipitation for Baronia RV2 using Equation 4.6. The figure shows different asphaltene precipitation amount for each different pressure and CO₂ concentration. At low pressure (1000 psi), asphaltene started to precipitate at very low CO₂ concentration. At low pressure (1000 psi) most of the light and intermediate component was already in gas phase, and when CO₂ added will extract the remaining amount of the intermediate component that still exists in the liquid phase leading to precipitate only small amount of asphaltene. However when CO₂ concentration keep increasing at low pressure (1000 psi) there was no precipitated asphaltene due to there is no intermediate component in the liquid phase to be extracted by CO₂ any more. Other pressure points above 1000 psi show the existence of a linear increase of asphaltene precipitation by increasing the CO₂ concentration with different asphaltene onset point for each pressure.

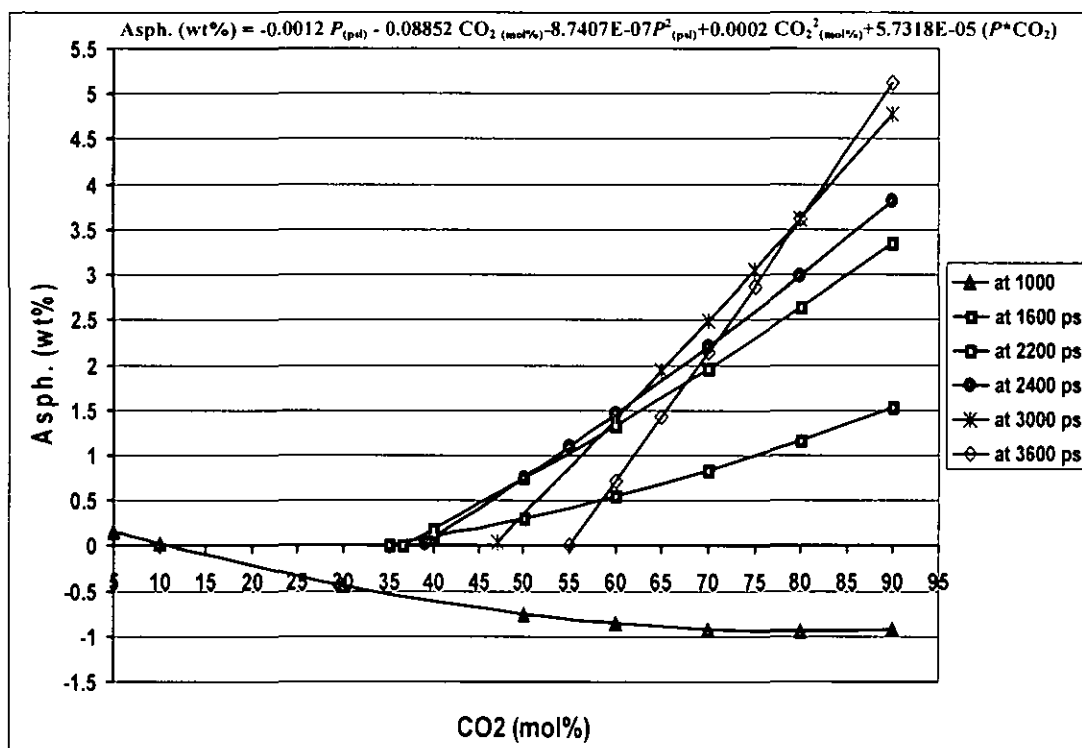


Figure 4.13 Predicted asphaltene precipitation versus. CO₂ concentration at different pressures using equation 4.6

Equation 4.6 shows more reliable results between the predicted and measured asphaltene precipitation than equation 4.5 which gave a quite far results between the predicted and measured asphaltene precipitation.

Table 4.13 shows the predicted and measured asphaltene precipitation for Baronia RV2 after applying equation 4.6. The reliable results of equation 4.6 recommended this model to predict asphaltene precipitation for Baronia RV2.

Table 4.13: Measured and predicted asphaltene precipitation

Pressure (psi)	CO ₂ (%mol)	Measured Asphaltene Precipitation (%wt)	Predicted Asphaltene Precipitation (%wt)
1000	9.00	0.06	0.05
1600	37.65	0.14	0.06
2200	53.32	0.96	0.94
2400	50.06	0.52	0.76
3000	56.03	1.14	0.98
3600	57.43	0.31	0.35

CHAPTER V

CONCLUSIONS AND RECOMMENDATIONS

5.1 CONCLUSIONS

Experiments and statistical analysis were used to investigate the possibility of asphaltene precipitation for Baronia RV2 during the contact with CO₂. The effect of CO₂ on the phase behavior has been studied and the influence of pressure and CO₂ concentration change that lead to asphaltene precipitation have been presented and discussed. The conditions of pressure and CO₂ concentration that causes minimum asphaltene precipitation have been determined. Finally, a statistical analysis to predict asphaltene precipitation for Baronia RV2 has been developed using multiple regression model.

Based on the experimental investigation on Baronia RV2 live and dead oil the followings can be concluded:

- Findings from crude oil characterization showed that Baronia RV2 has very low asphaltene content of 0.117 %wt. In spite of that Baronia RV2 has the tendency for asphaltene precipitation.
- The phase behavior of Baronia RV2 live crude was affected by the addition of CO₂. The bubble point pressure increased with increasing CO₂ concentration due to the swelling effect of CO₂. There were changes in the oil phase behavior at different concentration of CO₂.
- The EOR experiments using micro-slim tube displacement test shows that a miscible CO₂ flooding could be achieved for Baronia RV2 oil at the present reservoir conditions of 3008 psia, 204 °F since the MMP is 2435 psig.
- Static asphaltene precipitation test showed that asphaltene starts to precipitate slowly at 22% mol of CO₂ at 3008 psia, 204 °F. Then after 40% mol there was a linear increase of asphaltene precipitation with increasing CO₂ concentration. The static asphaltene precipitation test also showed that asphaltene precipitation increases with increasing concentration of injected CO₂.

-
- Dynamic asphaltene precipitation test showed that the precipitation of asphaltene would increase when the CO₂ concentration increased isobarically. Nevertheless, when CO₂ concentration was kept constant, the asphaltene precipitation increased with decreasing pressure.
 - Asphaltene precipitation increased with increasing CO₂ concentration and low pressures during the dynamic test conditions where two parameters are varied i.e. pressure and CO₂ concentration.
 - The correlation of asphaltene precipitation for Baronia RV2 oil is limited for this case study at that the specified reservoir conditions and the physical aspects and the complex properties of asphaltene have not been included. This correlation is mainly a statistical tool for predicting asphaltene precipitation for Baronia RV2 at any range of pressure and CO₂ concentration.

5.2 RECOMMENDATIONS FOR FUTURE WORK

- Before the implementation of an EOR project, it is highly recommended to conduct a full asphaltene precipitation study due to the different asphaltene behavior depending on the origin of oil and reservoir conditions.
- Bottom-hole samples are highly recommended for any asphaltene precipitation study because they are more representative samples of the reservoir fluid, thus they should contain the actual amount of asphaltene.
- Asphaltene precipitation experiments show that Baronia RV2 will have a maximum precipitation at reservoir pressure of 3008 psia, so it is recommended to maintain the pressure during the CO₂ injection.
- A complete dynamic fluid flow simulation is highly recommended to study the effect of asphaltene precipitation near the wellbore region. However, the permeability reduction, porosity alteration and the blockage in the reservoir will be studied also in the simulation to check the possibility for any formation damage might be happened due to asphaltene precipitation.
- The effect of water content and porous media should be considered for more reliable model.

REFERENCES

Alkhafeef, S. F., F. Al-Medhadi, A. D. Al-Shammari, "*A Simplified Method To Predict and Prevent Asphaltene Deposition in Oilwell Tubings: Field Case*", SPE paper 84609, presented at the 2003 SPE Annual Technical Conference and Exhibition, Denver, 5–8 October, Paper peer approved 23 February 2005.

Ashoori, S., Jamialahmadi, M., Müller-Steinhagen, H., Ahmadi, K., "*A New Scaling Equation for Modeling of Asphaltene Precipitation*", SPE 85673, presented at the 27th Annual SPE International Technical Conference and Exhibition in Abuja, Nigeria, August 4-6, 2003.

Buenrostro-Gonzalez, E., C. Lira-Galeana, A. Gill-Villegas, and J. Wu, "*Asphaltene Precipitation in Crude Oils: Theory and Experiments*", American Institute of Chemical Engineering Journal, Vol. 50, No.10, October 2004.

Clarke, G.M., and Kempson, R.E., "*Introduction to the Design and Analysis of Experiments*", London: Arnold, 1997.

Dandekar Y. Abhijit, "*Petroleum Reservoir Rock and Fluid Properties*", ISBN: 0849330432, 9780849330438, CRC Press, 2006.

Danesh, Ali, "*PVT and Phase Behavior of Petroleum Reservoir Fluids*", ISBN: 0444821961, Elsevier Science, 1998.

De Boer, R. B., K. Leerlooyer, M. R. P. Eigner, A. R. D. van Bergen, "*Screening of Crude Oils for Asphalt Precipitation: Theory, Practice, and the Selection of Inhibitors*," SPE Production & Facilities, February 1995.

Fisher, D., N. Yazawa, H. Sarma, M. Girard. A. Turta, H. Huang, "*A New Method to Characterize the Size and Shape Dynamics of Asphaltene Deposition Process in CO₂ Miscible Flooding*", SPE 84893 presented at the SPE International Improved Oil Recovery Conference in Asia Pacific held in Kuala Lumpur, Malaysia, 20-21 October 2003.

Fred I. and Stalkup Jr., "*Status of Miscible Displacement*", SPE paper 9992, April 1983.

Godbole, S. P., Thele, K. J., Reinbold, E. W., "*EOS Modeling and Experimental Observations of Three-Hydrocarbon-Phase Equilibria*", SPE paper 24936, presented at the 1992 SPE Annual Technical Conference and Exhibition, Washington, DC, Oct. 4-7 1992.

Green D. W. and Willhite G. Paul, "*Enhanced Oil Recovery*", Society of Petroleum Engineers, Richardson, Texas 1998.

Hirschberg, A., L. N. J. de Jong, B. A. Schipper, J.G. Meijer, "*Influence of Temperature and Pressure on Asphaltene Flocculation*", SPE 11202, June, 238, 1984.

Holm, LW & Josendal, VA; "*Discussion of Determination and Prediction of CO₂ MMP*", Journal of Petroleum Technology, May 1980, p870-71

Istadi, "*Catalytic Conversion of Methane and Carbon Dioxide in Conventional Fixed Bed and Dielectric Barrier Discharge Plasma Reactor*", Ph.D. Thesis, Universiti Teknologi Malaysia, 2006.

Kawanaka, S., S. J. Park, and G. A. Mansoori, "*Organic Deposition From Reservoir Fluids: A Thermodynamic Predictive Technique*," SPE Reservoir Engineering, May 1991.

Kohse, B. F., Nghiem, L. X., Maeda, H., and Ohno, K., "*Modelling Phase Behavior Including the Effect of Pressure and Temperature on Asphaltene Precipitation*", SPE paper 64465, presented at the SPE Asia Pacific Oil and Gas Conference and Exhibition, Brisbane, Australia, 16-18 October 2000.

Kokal, S. L., and S. G. Sayegh, "*Asphaltenes: The Cholesterol of Petroleum*", SPE paper 29787, presented in Middle East Oil Show, Bahrain, 11-14 March 1995.

Lars H. and C. H. Whitson, "*Miscibility Variation in Compositionally Grading Reservoirs*", SPE paper 63086, presented at the 2000 SPE Annual Technical Conference and Exhibition held in Dallas, Texas, 1-4 October 2000

Leontaritis, K. J., "*The Asphaltene and Wax Deposition Envelopes*", Fuel Science and Technology. Int., Vol. 14, 1996. 13

Leontaritis, K. J., Amaefule, J. O., and Charles, R. E., "*A Systematic Approach for the Prevention and Treatment of Formation damage Caused by Asphaltene Deposition*", SPE Production & Facilities, August 1994, 157-164

Leontaritis, K.J. and Mansoori, G.A., "*Asphaltene Flocculation during Oil Production and Processing: a Thermodynamic Colloidal Model*", SPE paper 16258 presented at the international symposium on oilfield chemistry in San Antonio, Texas, Feb. 4-6, 1987.

Lial M. L., Greenwell R. N., Ritchey N. P., "*Finite Mathematics*", Seventh Edition, Pearson Education, Inc. USA, 2002.

Mansoori, G.A., "*Asphaltene Deposition and Its Control*", The UIC Thermodynamic Research Laboratory, ChE & BioE Departments, University of Illinois at Chicago, 1997 (<http://tigger.uic.edu/~mansoori/Asphaltene.Deposition.and.Its.Control.html>).

Martin F. David and Taber J. J., "*Carbon Dioxide Flooding*", SPE paper 23564, April 1992.

McCain, William, D., Jr., "*The Properties of Petroleum Fluids*", Second Edition, ISBN: 0-87814-335-1, PennWell Publishing Company, 1990.

Michell, D.L. and J.G. Speight, "*The Solubility of Asphaltenes in Hydrocarbon Solvents*", Fuel, 53, 149-152, 1973.

Milind D. Deo "*Enhanced The Effectiveness Of Carbon Dioxide Flooding By Managing Asphaltene Precipitation*", University of Utah, Final Report, February 2002.

Moghadas, J., A. M. Kalantari-Dahaghi, V. Gholami, R. Adi, "*Formation Damage Due to Asphaltene Precipitation Resulting Form CO₂ Gas Injection in Iranian Carbonate Reservoirs*," SPE 99631 presented at the SPE Europec/EAGE Annual Conference and Exhibition held in Vienna, Austria, 12-15 June 2006.

Monger, T.G. and Fu, J.C.: "*The nature of CO₂-induced organic deposition*", paper SPE 16713 (Sept. 1987) 147.

Monger, T.G. and Trujillo, D.E.: "*Organic deposition during CO₂ and rich-gas flooding*", SPE Reservoir Engineering (Feb. 1991) 17.

Montgomery, D. C., "*Design and Analysis of Experiments*", Fifth Edition, ISBN: 0-471-31649-0, John Wiley & Sons, 2001.

Montgomery, D. C., Runger, G. C., "*Applied Statistics and Probability for Engineers*", Third Edition, ISBN: 0-471-20454-4, John Wiley & Sons, 2003.

Muhammad Sahimi, Hossien Rassamdana, and Bahram Dabir, "*Asphalt Formation and Precipitation: Experimental Studies and Theoretical Modelling*", SPE 35707, presented at the Western Regional Meeting held in Anchorage, Alaska, 22-24 May, 1997.

Mungan Necmettin, "*A Review and Evaluation of Carbon Dioxide Flooding*" Applications Report, AR-5, Petroleum Recovery Institute, April 1979.

Nghiem, L. X., "*Phase Behavior Modeling and Compositional Simulation of Asphaltene Deposition in Reservoirs*", Ph.D. Thesis, University of Alberta, 1999.

Nghiem, L. X., Hassam, M. S., and Ram Nutakki, "*Efficient Modelling of Asphaltene Precipitation*" SPE 26642 presented at the 68th Annual Technical Conference and Exhibition of the Society Petroleum Engineers held in Houston, Texas, 3-6 October 1993.

Nor Idah Kechut, "*Evaluation of EOR Gas Flooding in Baronia RV2 Reservoirs*", PETRONAS Research Sdn. Bhd. (PRSB), Final Report, 2005.

Novosad, Z. and T. G. Constain, "*Experimental and Modeling Studies of Asphaltene Equilibria for a Reservoir under CO₂ Injection*", SPE 20530 presented at the 65th Annual Technical Conference and Exhibition of the Society of Petroleum Engineers held in New Orleans, LA, September 23-26, 1990.

Parra-Ramirez, M., B. Peterson, M. D. Deo, "*Comparison of First and Multiple Contact Carbon Dioxide Induced Asphaltene Precipitation*", SPE 65019 presented at the 2001 SPE International Symposium on Oilfield Chemistry held in Houston, Texas, 13-16 February 2001.

Sarma, H. K., "*Can We Ignore Asphaltene in a Gas Injection Project for Light-Oils?*", SPE 84877 presented at the SPE International Improved Oil Recovery Conference in Asia Pacific held in Kuala Lumpur, Malaysia, 20-21 October 2003.

Sim, S. S. K., K. Takabayashi, K. Okatsu, D. Fisher, "*Asphaltene-Induced Formation Damage: Effect of Asphaltene Particle Size and Core Permeability*", SPE 95515 presented at the 2005 SPE Annual Technical Conference and Exhibition held in Dallas, Texas, U. S. A., 9-12 October 2005.

Speight, J.G., "*Petroleum Asphaltenes Part 1, Asphaltenes, Resins and The Structure of Petroleum*", Oil and Gas Science and Technology-Rev. IFP, Vol.59, No.5, pp. 467-477, 2004.

Srivastava, R. K., Huang S. S., and Mingzhe Dong, "*Asphaltene Deposition During CO₂ Flooding*", SPE 59092-PA, SPE Production and Facilities Journal, Volume 14, Number 4, pp. 235-245, November 1999.

Srivastava, R. K., and Huang S. S., "*Asphaltene Deposition During CO₂ Flooding: A Laboratory Assessment*", SPE 37468 presented at the 1997 SPE Productions Symposium, held in Oklahoma City, Oklahoma, 9-11 March 1997.

Srivastava, R. K., Huang, S. S., Dyer, S. B., and Mourits, F. M., "*Quantification of asphaltene flocculation during miscible CO₂ flooding in the Weyburn reservoir*", JCPT (Oct. 1995) 31.

Wan Nurul Adyani Wan Razak, Nor Idah Kechut, "*Advanced Technology for Rapid Minimum Miscibility Pressure Determination (Part 1)*" SPE 110265-PP presented at the 2007 SPE Asia Pacific Oil & Gas Conference and Exhibition held in Jakarta, Indonesia, 30 October–1 November 2007.

Yellig, WF & Metcalfe, RS; "*Determination and Prediction of CO₂ MMP*", Journal of Petroleum Technology, January 1980, p160-168.

Ying, J., S. Lei, S. Liangtian, H. Lei, H. Chunxia, and H. Lin, "*The Research on Asphaltene Deposition Mechanism and Its Influence on Development During CO₂ Injection*", SPE paper 104417, presented at the 2006 SPE International Oil & Gas Conference and Exhibition in China, 5-7 December 2006.

Vazquez, D. and Mansoori, G.A., "*Analysis of Heavy Organic Deposits*", Journal of Petroleum Science & Engineering, Vol. 26, Nos. 1-4, pp. 49-56, 2000.

Appendix A: Standard Method Procedure

1.0 Standard Test Method for *n*-Heptane Insoluble (ASTM D3279)

1. Scope

1.1 This test method covers determination of the mass percent of asphaltenes as defined by insolubility in normalheptane solvent. It is applicable to all solid and semi-solid petroleum asphalts containing little or no mineral matter, to gas oils, to heavy fuel oils, and to crude petroleum that has been topped to a cut-point of 343°C or higher.

1.2 The values stated in SI units are to be regarded as the standard.

1.3 This standard does not purport to address all of the safety concerns, if any, associated with its use. It is the responsibility of the user of this standard to establish appropriate safety and health practices and determine the applicability of regulatory limitations prior to use. See Section 7 for a specific hazard statement.

2. Referenced Documents

2.1 *ASTM Standards:*

C 670 Practice for Preparing Precision and Bias Statements for Test Methods for Construction Materials

3. Summary of Test Method

3.1 The sample is dispersed in *n*-heptane and filtered through a glass-fiber pad. The insoluble material is washed, dried, and weighed.

4. Significance and Use

4.1 This test method is useful in quantifying the asphaltene content of petroleum asphalts, gas oils, heavy fuel oils, and crude petroleum. Asphaltene content is defined as those components not soluble in *n*-heptane.

5. Apparatus and Materials

5.1 The assembly of the dispersing apparatus is illustrated in

The details of the component parts as follows:

5.1.1 Erlenmeyer Flask, of 250-mL capacity adapted to an Allihn-type reflux condenser, each with a 35/25 ball joint.

5.1.2 Magnetic Stirrer and Magnetic-Stirrer Hot Plate, equipped with a voltage regulator.

5.1.3 Gooch Crucible, glazed inside and outside with the exception of the outside bottom surface. The approximate dimensions shall be a diameter of 44 mm at the top tapering to 36 mm at the bottom and a depth of 20–30mm.

5.1.4 Filter Pad, glass-fiber 32 mm in diameter.

5.1.5 Filter Flask, heavy-wall with side tube, 500-mL capacity.

5.1.6 Filter Tube, 40 to 42 mm in inside diameter.

5.1.7 Rubber Tubing, or adapter for holding Gooch crucible on the filter tube.

6. Solvent

6.1 n-Heptane, 99.0 minimum mol % (Pure Grade).

7. Hazards

7.1 n-Heptane has a boiling point of 98°C and a flash point of -1°C, which means that it should be handled with care. It is recommended that both the reflux dispersion and filtration steps be conducted in a ventilated hood and away from flames or other sources of heat.

8. Procedure

8.1 Into the 250-mL Erlenmeyer flask, weigh to the nearest 0.1 mg a quantity of the sample to be tested, using 0.5 to 0.6 g for airblown asphalts, 0.7 to 0.8 g for asphalt paving binders and crude residues, and 1.0 to 1.3 g for gas oils and heavy fuel oils. Add *n*-heptane in the ratio 100 mL of solvent per 1 g of sample, using proportionally less or more solvent as dependent upon the sample size. Unless the asphalt is in a granular form, heat the flask gently and turn it to cause the sample to be distributed somewhat over the bottom or lower sides of the flask. Erlenmeyer flask is recommended. After all possible precipitate has been washed from the flask to the filtering crucible in 8.3, include the flask with the crucible for the drying, weighing, and calculation procedures in 8.3 and 9.1.

8.2 Place the Erlenmeyer flask, containing the sample plus solvent with magnetic stirrer added, on the magnetic-stirrer hot plate and secure under the reflux condenser. With the magnetic stirrer in operation, adjust for gentle refluxing for a period of 15 to 20 min when testing paving binders, fuel oils, gas oils, or crude residues. For airblown asphalts, a reflux period of 25 to 30 min is recommended. In all cases, allow the dispersed mixture to cool to room temperature for a period of 1 h. 8.3 Place the Gooch crucible plus one thickness of the glass-fiber filter pad in an oven at about 107°C for 15 min, allow to cool in a desiccator, and then weigh to the nearest 0.1 mg. Set up the filtering crucible plus filter pad in the suction flask and pre-wet with 5 mL of *n*-heptane. Warm the flask containing the sample plus solvent to 38 to 49°C on the hot plate and pour its contents (except for the magnetic stirrer) through the filter using a gentle vacuum. Filtration will proceed most rapidly if the supernatant liquid is filtered first with the insolubles transferred to the filter last. Police the beaker or flask while transferring the final precipitate, using either a rubber policeman or stainless steel spatula with a squared end. Wash the precipitate with three portions of *n*-heptane of about 10 mL each, first rinsing out the flask therewith. Place the crucible in the 107°C oven for a period of 15 min, cool in a desiccator, and weigh.

9. Calculation and Report

9.1 Calculate the mass percent of normal-heptane insolubles (NHI) as the percentage by weight of the original sample as follows:

$$\text{NHI, \%} = A/B * 100$$

where:

A = total mass of insolubles, and

B = total mass of sample.

For percentages of insolubles less than 1.0, report to the nearest 0.01 %; for percentages of insolubles of 1.0 or more, report to the nearest 0.1 %.

2.0 Paraffin Wax Content of Petroleum Oils and Asphalts (UOP-46)

SCOPE

This method is for estimating the paraffin wax content of petroleum oils and asphalts. Wax content is an empirical value dependent upon the conditions under which the wax is separated from the original material. In this method paraffin wax content is defined as the mass-percent of material precipitated when a solution of asphalt-free sample in methylene chloride is cooled to -30 C. The lower limit of detection is 5 mass percent.

OUTLINE OF METHOD

Light, clear oils are analyzed as received. Heavily colored oils and asphalts are clarified by treatment with sulfuric acid. The asphalt-free sample is dissolved in warm methylene chloride. This solution is chilled to -30 C and filtered through a cold fritted glass filter. The wax collected on the filter is removed with hot hexane. The hexane is evaporated and the wax weighed.

APPARATUS

Balance, readability, 0.1-mg.

Bath, water, Sargent-Welch Scientific Co., Cat. No. S-84215, or equivalent.

Colorimeter, ASTM, Precision, Sargent-Welch Scientific Co., Cat. No. S-66280, or equivalent.

Cylinder, graduated, 10- and 50-mL.

Desiccator, Scheibler, knob top cover, 250-mm ID, Sargent-Welch Scientific Co., Cat. No. S-25005E, or equivalent.

Desiccator plate, Scheibler form, Coors porcelain, 230-mm diameter, Sargent-Welch Scientific Co., Cat. No. S-25185F, or equivalent.

Flask, filtering, one-liter

Flask, polyethylene, foam insulated, 2-L, Sargent-Welch Scientific Co., Cat. No. S-34755-B, or equivalent
Funnel, Büchner, fritted glass, fine porosity, 60-mL capacity, Sargent-Welch Scientific Co., Cat. No. S-35590-E, or equivalent

Funnel, separatory, 250-mL

Hot plate, electric, Sargent-Welch Scientific Co., Cat. No. S-41043-50, or equivalent

Oven, gravity convection, 225 C maximum temperature, Sargent-Welch Scientific Co., Cat. No. S-64090- C, or equivalent.

Pump, vacuum, heavy duty, Sargent-Welch Scientific Co., S-71380, or equivalent.

Regulator, nitrogen, Matheson, 8-BF, CGA No. 580, or equivalent.

Sample bottles, for colorimeter, Sargent-Welch Scientific Co., Cat. No. S-8975, or equivalent

Stopper, rubber, No. 9

Tubing, glass, 122-cm, 6-mm OD, standard wall

Tubing, rubber, 3-m, 6.4-mm ID, 1.6-mm wall

Watch glass, plain, 65-mm diameter

Wax content apparatus consisting of: (see Figure)

Bath, glass, 125-mm OD, 119-mm ID, 110-mm deep, with a 20-mm diameter hole drilled in the center of the bottom, UOP Inc., or equivalent

Column clamp and clamp holder, 121-140-mm adjustable, VWR Scientific, Cat. Nos. 21572-160 and 21572-501, respectively, or equivalent

Flask, Erlenmeyer, 125-mL

Ring stand, 15 × 28-cm base, 91-cm support rod, Sargent-Welch Scientific Co., Cat. No. S-78306D, or equivalent

Stoppers, rubber, Nos. 3 and 5

Support ring, with screw clamp, 114-mm ID, 127-mm OD, Sargent-Welch Scientific Co., Cat. No. S- 73045D, or equivalent

Support shelf, with screw clamp, 127-mm diameter, VWR Scientific, Cat. No. 60125-004, or equivalent

Thermometer, ASTM 6C, Cloud and Pour, low, Sargent-Welch Scientific Co., Cat. No. S-80585, or equivalent

Thermometer clamp and clamp holder, Fisher Scientific, Cat. Nos. 05-809-10 and 05-754, respectively, or equivalent

Tubing, glass, 6-mm OD, standard wall

REAGENTS AND MATERIALS

All reagents shall conform to the specifications established by the Committee on Analytical Reagents of the American Chemical Society, when such specifications are available, unless otherwise specified.

References to water mean distilled water.

Ammonium hydroxide solution, 0.1-M

Carbon dioxide, solid (dry ice)

Desiccant, activated alumina, Sargent-Welch Scientific Co., Cat. No. SC-10486, or equivalent

Hexane, 95% minimum purity

Methylene chloride, 95% minimum purity

(CAUTION: Avoid prolonged or repeated breathing of vapor. Use only with adequate ventilation.)

Nitrogen, extra dry, 99.9% minimum purity

Phenolphthalein, indicator solution, Sargent-Welch Scientific Co., Cat. No. SC-14007, or equivalent

Sulfuric acid, concentrated, 95% minimum purity

PROCEDURE

Section A

Dry a clean 125-mL Erlenmeyer flask in an oven at 105 C for fifteen minutes, and cool in a desiccator for one hour. Weigh the flask to the nearest 0.1 mg and record the mass. Determine the ASTM color of the sample according to ASTM D 1500. If the sample is above 3 ASTM color or contains asphaltenes (cloudy to opaque in appearance), proceed to Section B. If the sample is 3 ASTM color or lighter, and clear, add 1.5 ± 0.25 g to the clean, dried, tared flask. Reweigh and record the mass to the nearest 0.1 mg. Continue the procedure as described in Section C.

Section B

Add 2.0 ± 0.25 g of the sample to the clean, dried, tared flask and record the mass to the nearest 0.1 mg. Warm the sample to aid in dissolution. Add 50 mL of hexane and carefully bring to a boil on an electric hot plate located in a hood. Add approximately 4 mL of concentrated sulfuric acid and swirl vigorously to effect intimate contact between the oil and acid. Heat the mixture gently with continued swirling over the hot plate until an acid tar is formed and there are no visible lumps. Allow the tar to settle for a minimum of 2 hours. Decant the clear asphalt-free solution into a 250-mL separatory funnel. The acid tar formed will normally adhere to the sides of the flask. Wash the tar in the flask five times with 5-mL portions of hexane warmed to 60 C. Add the washings to the contents of the separatory funnel. Add 50 mL of warm water, about 40 C, to the separatory funnel and wash the hexane solution to dilute the acid. Wash with a swirling motion to avoid the formation of emulsions. Allow the layers to settle.

Remove and discard the water. Add 15-mL of 0.1-M ammonium hydroxide solution to the separatory funnel to neutralize the remaining acid and swirl. Remove and discard the ammonium hydroxide layer. Wash the hexane solution several times, with 50-mL quantities of warm water, until the separated water shows no color change when several drops of phenolphthalein are added. Transfer the neutral hexane solution to a clean, dried, tared 125-mL Erlenmeyer flask. Wash the separatory funnel three times with 5-mL portions of hexane warmed to 60 C and add the washings to the flask. Place the flask on the water bath heated to 95 C and evaporate off the hexane. Use a nitrogen purge to aid in the removal of the last traces of hexane. Follow the procedure in *Section C*.

Section C

Dissolve the sample obtained in *Section A or B* in 20 mL of methylene chloride warmed to 35 C. If the sample is solid at room temperature, melt it before the addition of methylene chloride. Set up a methylene chloride cooling bath in the polyethylene flask. Maintain the temperature at -30 C by the addition of dry ice. (Mechanical cooling may be substituted if dry ice is not available.) Place the sample in the bath

with a swirling motion to avoid local freezing and allow it to cool for thirty minutes. Agitate the sample frequently by swirling. Set up the wax content apparatus according to the figure. Add methylene chloride to the bath and chill it to -30 C by the addition of dry ice. Cover the top of the funnel with a watch glass during the cooling process to prevent condensation of moisture. Transfer the contents of the Erlenmeyer flask to the cold fritted glass funnel. Do not allow the level of the mixture in the filter funnel to rise above the level of the liquid in the cooling bath. Use vacuum to aid in filtering. Do not allow the filter to run dry, which would cause the wax to cake. Rinse the Erlenmeyer flask five times with 5-mL quantities of methylene chloride cooled to -30 C , or until the flask and the small quantity of wax adhering to it are free from oil. Wash the wax on the filter with 30 to 35 mL of cold methylene chloride. The filtrate should be colorless and the wax white, or not darker than slightly yellow (Note 1). Remove the flask containing the filtrate and replace it with the original flask. Using a one-liter filter flask, remove by suction the methylene chloride from the cooling bath and allow the filter funnel to reach room temperature. Dissolve the wax on the filter with 20 mL of hexane warmed to 60 C . A slight vacuum may be necessary to pull the last of the dissolved wax through the filter. Do not use the vacuum at the beginning as the loss of heat by evaporation may cause the wax to solidify on the filter.

When the wax is completely dissolved from the filter, remove the flask and place it on the water bath heated to 95 C to evaporate the hexane. Purge the flask with a stream of nitrogen to aid in the removal of the last traces of hexane. Dry the flask and the wax in an oven at 105 C for 15 minutes. Allow to cool for one hour in a desiccator and then weigh it to the nearest 0.1 mg.

CALCULATION

Calculate the wax content of the sample as follows:

$$\text{Wax Content, mass \%} = 100 W/S$$

where:

S = mass of the sample, g

W = mass of the wax, g

100 = factor to convert to percentage

APPENDIX B: Calculations of CO₂ % mole

This section included the calculation of CO₂ % mole for the swelling test and asphaltene precipitation experiments.

1.0 SWELLING TEST

1.1 CO₂ Density Calculation

The calculation of CO₂ density was done by using the general gas law as following:

$$PV = znRT$$

where:

P : pressure of CO₂ in the cylinder (psia)= 5015 psia

V : volume (ft³)

z : z-factor = 0.6778 (from the table)

n : number of moles

R : general gas constant= 10.73 (ft³ psi R⁻¹ lb-mol⁻¹)

T : temperature (°R)= reservoir temperature 204 °F= 664 °R

while: $\rho = \frac{m}{V}$ and $n = \frac{m}{Mw}$

where:

ρ : density of CO₂ (lb/ft³)

m : mass (lb)

Mw : molecular weight of CO₂

So,

$$PMw = \rho zRT \longrightarrow \rho = \frac{PMw}{zRT}$$

Then, $\rho = 45.7028 \text{ lb/ft}^3 = 0.7321 \text{ g/cc}$

1.2 Calculation Number of Moles of Reservoir Fluid in The PVT Cell

Volume of reservoir fluid at 5000 psig and 204 °F = 16.978 cc

Density of reservoir fluid at 5000 psig and 204 °F = 0.689 g/cc

From the density and volume the weight of reservoir fluid has been calculated

Weight of reservoir fluid = 11.6943 g

While the molecular weight of the reservoir fluid has been calculated from the compositional analysis and it was = 76.72 g/mol

The number of moles = 0.1524 (by divided the weight on the molecular weight)

1.3 Calculation of CO₂ To Be Added To The PVT Cell

The CO₂ was added to the PVT cell at pressure of 1820 psig and at temperature of 50°C. The Table below shows the calculated number of moles of CO₂ and the volume to be added to PVT cell.

Table A.1 Calculation of CO₂ volume for swelling test

% of CO ₂	20	40	60	80
Moles of CO ₂	0.0381	0.1016	0.2286	0.6097
Wt. of CO ₂	1.6770	4.4722	10.0626	26.8336
Volume of CO ₂ in PVT cell	2.2908	6.1089	13.7450	36.6535
Volume of CO ₂ to be added	2.2908	3.8181	7.6361	22.9084

An example below to show the calculation procedure at 20 % of CO₂:

$$mole_{CO_2} = \frac{concentration_{CO_2} \times mole_{reservoirfluid}}{1 - concentration_{CO_2}}$$

$$mole_{CO_2} = \frac{0.2 \times 0.1524}{1 - 0.2} = 0.0381$$

To calculate the weight of CO₂ will be added to the PVT cell as following:

$$weight_{CO_2} = Mw_{CO_2} \times mole_{CO_2}$$

$$weight_{CO_2} = 44.01 \times 0.0381 = 1.6770 \text{ g}$$

While the density of CO₂ has been calculated before and it was 0.7321, then the volume of the CO₂ to be added to PVT cell will be calculated as following:

$$Vol_{CO_2} = \frac{weight_{CO_2}}{\rho_{CO_2}}$$

$$Vol_{CO_2} = \frac{1.6770}{0.7321} = 2.2908 \text{ cc (the volume of CO}_2 \text{ to be added to the PVT cell at 20\%)}$$

For 40% - 80% of CO₂, the calculated volume of CO₂ to be added to the PVT cell will be extracted from the volume of CO₂ in the PVT cell from previous stage.

2.0 STATIC ASPHALTENE TEST

2.1 Calculation of Number of moles of Reservoir Fluid in the PVT Cell

To calculate the CO₂ volume to be added, the number of moles of the reservoir fluid in the PVT cell has been calculated as following:

Example of calculation at 22% mol of CO₂

while:
$$\text{moles} = \frac{wt}{Mw}$$

The weight of oil has been calculated by calculating the density of oil to multiply it by the volume of oil to get the weight

$$\rho_o = \frac{62.4\gamma_o + 0.0136R_s\gamma_g}{B_o}$$

Where:

ρ_o : Density of oil (lb/ft³)

γ_o : Specific gravity for the stock tank oil = 0.8180

R_s : Solution gas oil ratio (scf/stb) = 1066 scf/stb

γ_g : Gas specific gravity = 0.7839

B_o : Oil formation volume factor@ 3008 psi = 1.502 bbl/stb

Then by applying the previous equation:

$$\rho_o = 41.5497 \text{ lb/ft}^3 = 0.6656 \text{ g/cc}$$

The measured volume of live oil in the PVT cell at pressure of 3008 psia was 67.9287cc. The weight of live oil in the PVT cell has been calculated as following:

$$\rho = \frac{\text{weight}}{\text{volume}} \longrightarrow \text{weight} = \rho \times \text{volume}$$

Then:

Weight of live oil in the PVT cell = 45.2108 g

While the molecular weight of the oil has been calculated from the compositional analysis of oil and it was 76.72 g/mol

Then:

$$\text{moles}_{oil} = \frac{wt_{oil}}{Mw_{oil}} = \frac{45.2108}{76.72} = 0.5891$$

2.2 Calculation of moles CO₂ in the PVT cell

The initial volume of CO₂ which has been transferred to the PVT was 15 cc at pressure of 5000 psig. However this volume has been converted to be at pressure of 3000 psig by using the following equation:

$$\frac{P_1 V_1}{T_1} = \frac{P_2 V_2}{T_2}$$

Where:

P_1 : Pressure at first conditions = 5000 psi = 340.1361 atm

V_1 : volume of CO₂ (cc) at 5000 psi

T_1 : temperature of CO₂ before transfer to PVT cell = 368.75 K

P_2 : pressure at second conditions = 3000 psi = 204.0816 atm

V_2 : volume of CO₂ (cc) at 3000 psi

T_2 : temperature of CO₂ after transfer to PVT cell = 368.75 K

After applying the above equation, the volume of CO₂ at 3000 psi has been calculated and it was 25 cc

To calculate the number of moles of CO₂, the volume of CO₂ at standard conditions has been calculated. That volume will be divided over the molar volume of gases which is equal 22400 cc/mol to get the number of moles of CO₂

To calculate the volume of CO₂ at standard condition the previous equation has been used and the calculated volume was 3780.3590 cc

$$\text{mole}_{CO_2} = \frac{V_{std}}{\text{molar volume}_{std}} = \frac{3780.3590}{22400} = 0.1688 \text{ mole of CO}_2 \text{ in the PVT cell}$$

2.3 Calculation of %mole of CO₂ and Oil

The number of moles of CO₂ and oil has been calculated previously where the CO₂ moles was 0.1688 and the moles of oil was 0.5891. The % mole for CO₂ and oil has been calculated as following:

$$\%mol_{CO_2} = \frac{mol_{CO_2}}{mol_{CO_2} + mol_{oil}} \times 100 = 22.265\%$$

$$\%mol_{oil} = \frac{mol_{oil}}{mol_{CO_2} + mol_{oil}} \times 100 = 77.735\%$$

For the 40, 70 and 85 %mole, the remains CO₂ volume in the PVT cell has been measured after each stage. The above calculation has been repeated to calculate the volume and % mole of CO₂ in the PVT cell.

3.0 DYNAMIC ASPHALTENE TEST

3.1 Calculation of CO₂ Volume

The oil and CO₂ has been transferred to the micro-slim tube at pressure of 3600 psi. The volume of injected CO₂ in the micro-slim tube has been calculated by multiplying the time of CO₂ contact with oil inside the micro-slim tube by the flowrate of CO₂.

Table A.2 Calculating the volume of CO₂

Pressure (psig)	Time of CO ₂ contact (Sec)	Time (min)	Q (cc/min)	Vol. of CO ₂ (cc)
3600	2409.187	40.1531	0.25	10.0383
3000	2715.093	45.2516	0.25	11.3129
2400	2707.063	45.1177	0.25	11.2794
2200	3396.141	56.6024	0.25	14.1506
1600	2544.281	42.4047	0.25	10.6012
1000	688.14	11.469	0.25	2.8673

The above Table shows that at each pressure the volume of CO₂ calculated by multiplying the time of CO₂ contact with oil by the flowrate of CO₂.

3.2 Calculation of Number of Moles of CO₂

The number of moles of CO₂ has been calculated after converting the CO₂ volume to the standard condition then divided that volume on the molar volume of 22400cc/mol as following:

By using the equation:
$$\frac{P_1 V_1}{T_1} = \frac{P_2 V_2}{T_2}$$

Where:

- P_1 : Pressure inside the micro-slim tube (atm)
- V_1 : volume of CO₂ inside the micro-slim tube (cc)
- T_1 : the temperature inside the micro-slim tube (K)
- P_2 : pressure of CO₂ at standard conditions (atm)
- V_2 : volume of CO₂ at standard conditions (cc)
- T_2 : temperature at standard conditions (K)

After applying the above equation, the volume of CO₂ at standard conditions has been calculated. The number of moles of CO₂ has been calculated by divided the volume at standard condition on the molar volume of gases 22400 cc/mol. The results are showing in the following Table:

Table A.3 Number of moles of CO₂

P_1 (atm)	V_1 (cc)	T_1 (K)	P_2 (atm)	V_2 (cc)	T_2 (K)	No. of moles of CO ₂
245.966	10.0383	368.7056	1	1828.1731	273	0.0816
205.138	11.3129	368.7056	1	1718.3141	273	0.0767
164.311	11.2794	368.7056	1	1372.2610	273	0.0613
150.701	14.1506	368.7056	1	1578.9689	273	0.0705
109.874	10.6012	368.7056	1	862.4456	273	0.0385
69.0462	2.8673	368.7056	1	146.5845874	273	0.0065

3.3 Calculation of Number of Moles of Oil

The density of oil is needed here to calculate the weight of oil by multiplying the density of oil by the volume of oil inside the micro-slim tube. The density of oil has been collected from the differential liberation data at each pressure. However the volume of oil inside the micro-slim tube was 7 cc for all the runs. By multiplying the density by the volume at each pressure the weight of oil has been calculated.

The number of moles of oil has been calculated by divided the weight of oil at each run over the molecular weight of oil which has been calculated from the compositional analysis and it was 76.72 g/mol. The table below shows the calculation of number of moles of oil:

Table A.4 Number of moles of oil

Density of Oil (g/cc)	wt of Oil	No. of moles of oil
0.6631	4.6416	0.0605
0.6620	4.6340	0.0604
0.6609	4.6265	0.0603
0.6598	4.6189	0.0602
0.6697	4.6878	0.0611
0.6764	4.7346	0.0617
0.6990	4.8929	0.0638
0.7253	5.0770	0.0662

3.4 Calculation of Oil and CO₂ % mole

The total number of moles has been calculated by the summation of CO₂ moles and oil moles. However, the mole percentage of CO₂ and oil have been calculated from the following equations

$$\%mol_{CO_2} = \frac{mol_{CO_2}}{mol_{CO_2} + mol_{oil}} \times 100$$

$$\%mol_{oil} = \frac{mol_{oil}}{mol_{CO_2} + mol_{oil}} \times 100$$

The following Table shows the calculation of % mole of CO₂ and oil

Table A.5 Calculating %mol of CO₂

Pressure (psi)	No. of moles of CO ₂	No. of moles of oil	Total no. of moles	mol% CO ₂	mol% of oil
3600	0.0816	0.0605	0.1421	57.4325	42.5675
3000	0.0767	0.0604	0.1369	56.0316	43.9684
2400	0.0613	0.0603	0.1224	50.0689	49.9311
2200	0.0705	0.0602	0.1322	53.3237	46.6763
1600	0.0385	0.0611	0.1023	37.6483	62.3517
1000	0.0065	0.0617	0.0727	9.0002	90.9998

Appendix C: Statistical Analysis

1.0 Regression Analysis

Regression is a statistical technique for investigating and modeling the relationship between variables. Regression analysis has been done using Microsoft excel 2003 using regression analysis tool. The dynamic asphaltene test data has been analyzed by regression analysis tool to calculate the regression and the residual of the asphaltene precipitation. The model coefficient, degree of freedom (df), standard error, sum of squares (SS) and mean square (MS) have been calculated from the regression analysis also.

1.1 Simple Linear Regression Model

The base of the linear regression model is the equation of straight line:

$$y = mx + b$$

The above equation could be written as:

$$y = \beta_0 + \beta_1 x$$

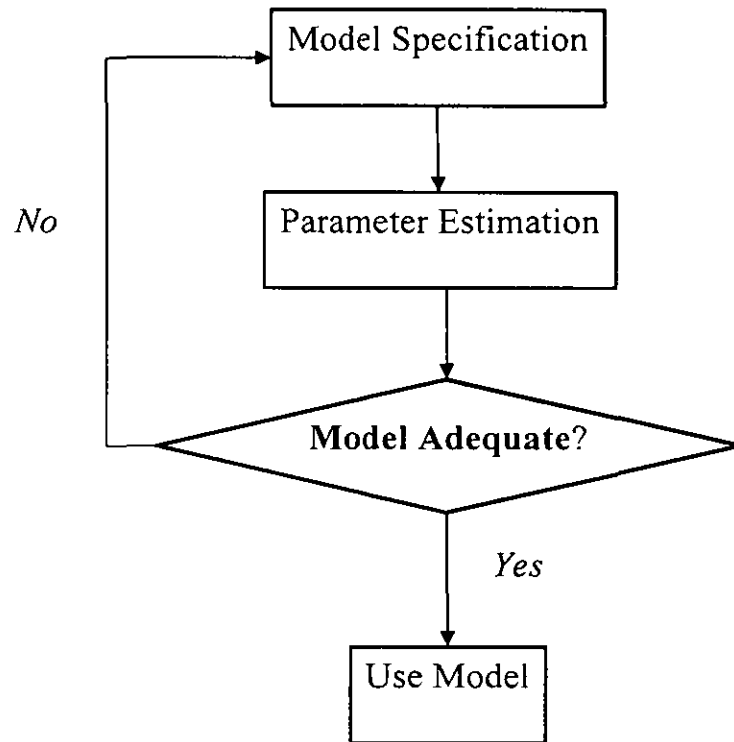
However, not all the observations will fall on the straight line, therefore there is an amount of error will be calculated. The above equation will be as following:

$$y = \beta_0 + \beta_1 x + \varepsilon$$

where: ε represent the error

It is a random variable that accounts for the failure of the model to fit the data exactly.

1.2 Statistical Modeling Procedure



1.3 Specification for Simple Linear regression Model

The simple linear regression correlation of asphaltene precipitation for Baronia RV2 is written as following:

$$y = \beta_0 + \beta_1 x_1 + \beta_2 x_2 + \varepsilon$$

where:

y : dependent (response) variable (asphaltene precipitation)

x_1, x_2 : independent (regressor/predictor) variable (pressure and CO₂ respectively)

β_0 : model intercept

β_1, β_2 : **slope**: change in the expected value of the response produced by a unit change in x

ε : random error term

1.4 Test The Significance of Regression by Analysis of Variance (ANOVA)

Analysis of variance is a powerful statistical tool used in regression analysis to show how significance is the model that derived from the data analysis. ANOVA used many tests to check the strength of the model as following:

1.4.1 Standard Error

A measure of the amount of variation there is in the model estimate. The smaller the standard error, the more precise (believable) the model estimate is.

1.4.2 Confidence Intervals

The confidence interval is to show how much the value of regression is true. As example for 95% confidence interval, means that the range of values are 95% sure that the true value lies within. The smaller the confidence interval, the more we should believe our parameter estimate. However, the larger the confidence interval, the more skeptical we should be that our estimate is “the truth”.

1.4.3 R-Square

R^2 gives the percent of variance due to between group variations. R^2 is between 0 and 1, and a larger number implies better prediction power.

$$R^2 = \frac{SS[Between]}{SS[Total]} = \frac{SSG}{SST}$$

Where:

SSG : some of square of regression

SST : some of square of total

1.4.4 *F*-Statistic

The ANOVA *F*-statistic is a ratio of the Between Group Variation divided by the Within Group Variation:

$$F = \frac{\textit{Between}}{\textit{Within}} = \frac{MSG}{MSE}$$

Where:

MSG: mean square of regression

MSE: mean square of residual

The larger the *F*-statistic, the more reliable the model is. If *F* is high it is an indication that if we ran the test again we would come to the same results (not due to chance). There is another value beside *F*-statistic called *F*-critical or *F*-table. For a good and significant model should be *F*-statistic that calculated from ANOVA equal or bigger than *F*-table at significance level (α) 0.05.

1.4.5 Null and Alternative Hypothesis

It is called hypothesis test and it is to test the significance of regression. However the hypothesis test is depending on the *F*-statistic. There is two assumptions for the hypothesis as following:

- 1- Null hypothesis (H_0): $\beta_1 = \beta_2 = 0$ (the means of all groups are equal), or in other word [(the independent variables (pressure and CO₂) have no effect on dependent variable (asphaltene)]. In case of *F*-statistic is less than *F*-critical, we accept this assumption and the regression is not significance.
- 2- Alternative hypothesis (H_A): At least one $\beta \neq 0$ (not all the means are equal), or in other word [the independent variables (pressure and CO₂) have effect on dependent variable (asphaltene)]. In case of *F*-statistic is higher than *F*-critical, we reject the null hypothesis and accept the alternative hypothesis, and the regression is significance.

The below Table shows the complete results of regression analysis and ANOVA for dynamic asphaltene data:

Table C.1 Results of regression analysis

Regression Statistics	
Multiple R	0.8988
R Square	0.8078
Adjusted R Square	0.5098
Standard Error	0.3550
Observations	6.0000

The Table above shows the R² and the overall standard error. R² is considered high and good value shows the small difference between the measured and the predicted values. However the standard error is shows a small value represent the more precise regression. The Table below shows the ANOVA analysis

Table C.2 Results of ANOVA

	<i>df</i>	<i>SS</i>	<i>MS</i>	<i>F</i>
Regression	2	2.1187	1.0593	8.4077
Residual	4	0.5040	0.1260	
Total	6	2.6226		

Where:

df: the degree of freedom for the regression, residual and total. Depending on the degree of freedom, *F*-critical will be found from the tables.

SS: some of squares for the regression and residual.

MS: means square for the regression and residual.

F-statistic: the ratio between the mean square of regression over the mean square of the residual, and it is shows higher than *F*-critical or *F*-table, therefore the regression is significance

The below Table shows the coefficients of the model and the standard error for each independent variable

Table C.3 Model coefficients and standard error

	Coefficients	Standard Error
Intercept	0.0000	#N/A
Pressure	-0.0002	0.0003
CO ₂ mol%	0.0244	0.0172

The above Table shows that:

$\beta_1 = -0.0002$, representing the coefficient of pressure

$\beta_2 = 0.0244$, representing the coefficient of CO₂ mol%

The standard error for pressure and CO₂ shows very low value, therefore the regression is significance.

1.4.6 F-table for $\alpha = 0.05$

The F-table is the standard value for F term used to compare with the F-statistic depending on the degree of freedom

Table C.4* F-table for significant 0.05

df2/df1	1	2	3	4	5	6	7	8
1	161.4476	199.5000	215.7073	224.5832	230.1619	233.9860	236.7684	238.8827
2	18.5128	19.0000	19.1643	19.2468	19.2964	19.3295	19.3532	19.3710
3	10.1280	9.5521	9.2766	9.1172	9.0135	8.9406	8.8867	8.8452
4	7.7086	6.9443	6.5914	6.3882	6.2561	6.1631	6.0942	6.0410
5	6.6079	5.7861	5.4095	5.1922	5.0503	4.9503	4.8759	4.8183
6	5.9874	5.1433	4.7571	4.5337	4.3874	4.2839	4.2067	4.1468
7	5.5914	4.7374	4.3468	4.1203	3.9715	3.8660	3.7870	3.7257
8	5.3177	4.4590	4.0662	3.8379	3.6875	3.5806	3.5005	3.4381
9	5.1174	4.2565	3.8625	3.6331	3.4817	3.3738	3.2927	3.2296
10	4.9646	4.1028	3.7083	3.4780	3.3258	3.2172	3.1355	3.0717
11	4.8443	3.9823	3.5874	3.3567	3.2039	3.0946	3.0123	2.9480
12	4.7472	3.8853	3.4903	3.2592	3.1059	2.9961	2.9134	2.8486
13	4.6672	3.8056	3.4105	3.1791	3.0254	2.9153	2.8321	2.7669
14	4.6001	3.7389	3.3439	3.1122	2.9582	2.8477	2.7642	2.6987
15	4.5431	3.6823	3.2874	3.0556	2.9013	2.7905	2.7066	2.6408
16	4.4940	3.6337	3.2389	3.0069	2.8524	2.7413	2.6572	2.5911
17	4.4513	3.5915	3.1968	2.9647	2.8100	2.6987	2.6143	2.5480
18	4.4139	3.5546	3.1599	2.9277	2.7729	2.6613	2.5767	2.5102
19	4.3807	3.5219	3.1274	2.8951	2.7401	2.6283	2.5435	2.4768
20	4.3512	3.4928	3.0984	2.8661	2.7109	2.5990	2.5140	2.4471
21	4.3248	3.4668	3.0725	2.8401	2.6848	2.5727	2.4876	2.4205
22	4.3009	3.4434	3.0491	2.8167	2.6613	2.5491	2.4638	2.3965

* Stephens L. J., "Schaum's Outlines of Theory and Problems of Beginning Statistics, Second Edition,, McGraw Hill Professional, ISBN 0071459324, pp. 302, 2006.

Appendix D: Asphaltene Deposition during Swelling Test

During the swelling test and at 80 % CO₂-Baronia RV2 recombined oil mixture the asphaltene deposition was observed formed in the PVT cell at different pressure. The pictures bellow shows the asphaltene deposition inside the PVT cell. The picture shows that asphaltene deposition increases with pressure decreased.



Figure D.1: Asphaltene precipitation at 7000 psi



Figure D.2: Asphaltene precipitation at 6500 psi

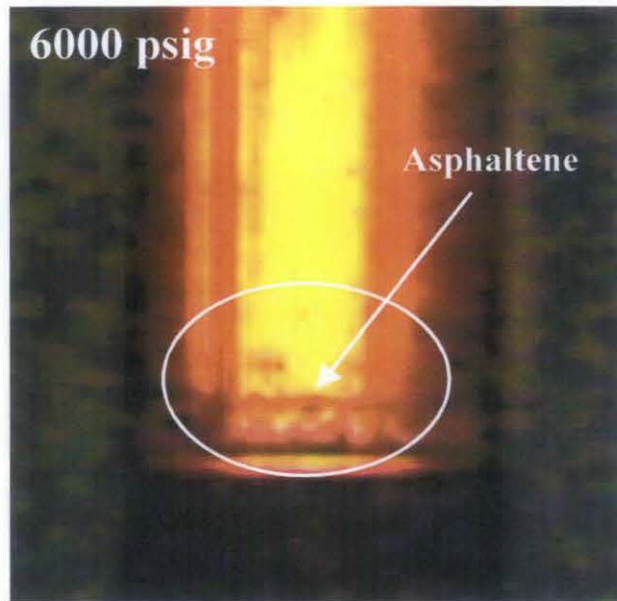


Figure D.3: Asphaltene precipitation at 6000 psi

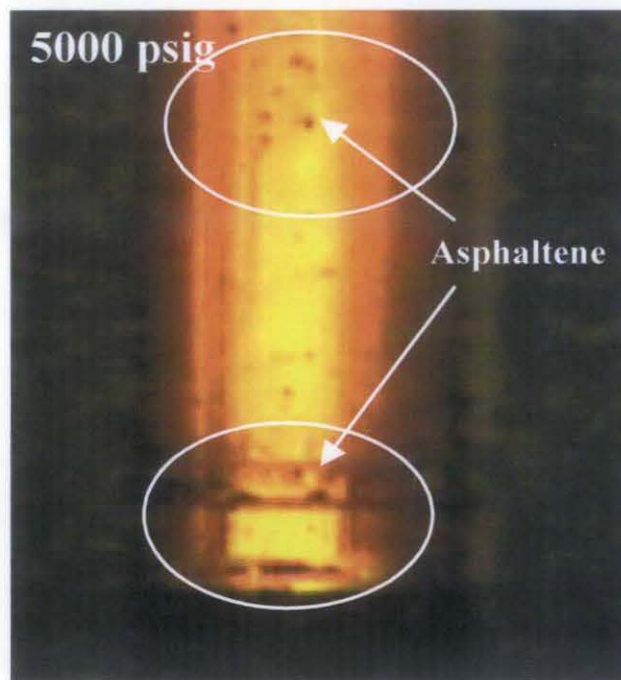


Figure D.4: Asphaltene precipitation at 5000 psi

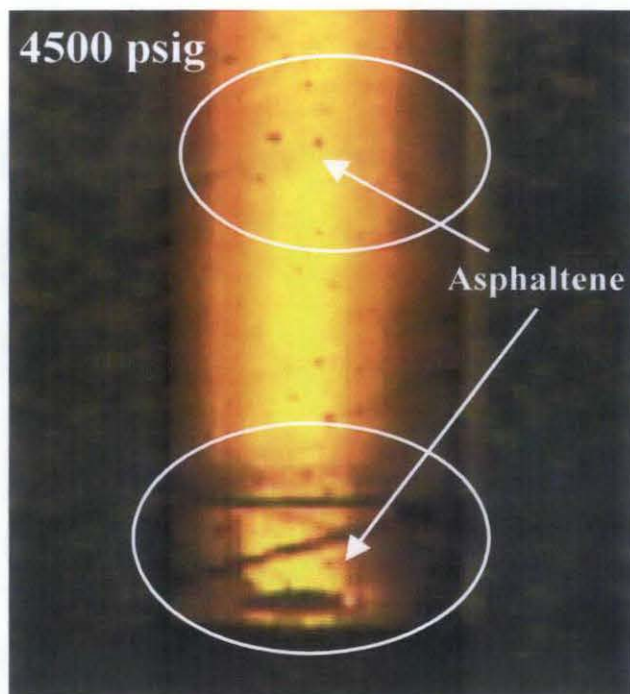


Figure D.5: Asphaltene precipitation at 4500 psi

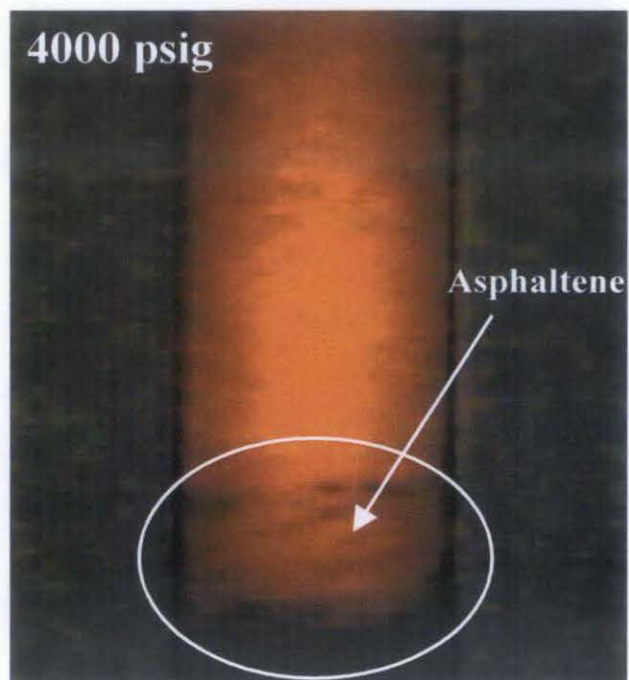


Figure D.6: Asphaltene precipitation at 4000 psi

Appendix E: The Calculated Relative Volume

1.0 Constant Composition Expansion

The relative volume has been calculated from the constant compositional expansion data during the bubble point measurement. The table below shows the relative volume and Y -function

Table B.1 Relative volume and Y -function at 0% CO₂

Pressure (psig)	Relative Volume (V/V _{sat}) (2)	Single-phase compressibility (V/V/psi)	Y -function (4)	Liquid Volume % (3)
5000	0.964			100.00
4500	0.971	1.45E-05		100.00
4000	0.978	1.46E-05		100.00
3500	0.986	1.49E-05		100.00
3200	0.99	1.60E-05		100.00
3000	0.994	1.75E-05		100.00
2900	0.996	2.00E-05		100.00
2800	0.998	2.19E-05		100.00
2700	0.999	2.29E-05		100.00
2650 (1)	1.000			
2600	1.007		2.652	99.291
2550	1.015		2.629	95.448
2500	1.023		2.606	93.349
2450	1.031		2.583	90.670
2400	1.040		2.560	90.572
2300	1.060		2.515	87.415
2200	1.082		2.469	83.108
2000	1.136		2.378	76.240
1800	1.205		2.287	67.414
1600	1.296		2.195	57.924
1400	1.42		2.104	48.237

Notes:

- (1) Bubble Point Pressure (P_b)
- (2) Relative Volume: V/V_{sat} , or volume at indicated pressure per volume at saturated pressure
- (3) Percent of the total volume of oil and gas at the indicated pressure
- (4) Y -function has been calculated from the following correlation

$$Y - \text{Function} = \frac{P_b - P_i}{P_b \times V_R}$$

Where:

P_b = Bubble point pressure

P_i = pressure at indicated pressure

V_R = Relative volume at P_i

2.0 Swelling Test

The relative volume from swelling test data has been calculated for each CO₂ concentration.

2.1 Constant Composition Expansion at 20% CO₂

Table B.2 Relative volume and Y-function at 20% CO₂

Pressure (psig)	Rel volume (V/Vsat) (2)	Single-phase compressibility (V/V/psi)	Y-function (4)	Liquid Volume % (3)
5000	0.921			100
4500	0.929	1.83E-05		100
4000	0.940	2.43E-05		100
3500	0.953	2.73E-05		100
3000	0.967	2.90E-05		100
2850	0.972	2.99E-05		100
2802 (1)	1.000			
2770	0.987		2.398	95.955
2700	1.016		2.374	92.922
2500	1.052		2.306	83.505
2000	1.186		2.135	71.598
1500	1.438		1.965	48.071
1000	1.990		1.794	27.240

2.2 Constant Composition Expansion at 40% CO₂

Table B.3 Relative volume and *Y*-function at 40% CO₂

Pressure (psig)	Rel volume (V/V _{sat}) (2)	Single-phase compressibility (V/V/psi)	<i>Y</i> -function (4)	Liquid Volume % (3)
5000	0.954			100
4500	0.964	2.06E-05		100
3500	0.975	2.24E-05		100
3400	0.987	2.43E-05		100
3300	0.989	2.61E-05		100
3200	0.992	2.70E-05		100
3100	0.998	2.85E-05		100
3025 (1)	1.000			
2950	1.008		3.110	97.376
2900	1.014		3.044	96.012
2800	1.027		2.911	96.243
2700	1.043		2.779	92.336
2500	1.083		2.514	84.599
2000	1.083		1.852	64.014

2.3 Constant Composition Expansion at 60% CO₂

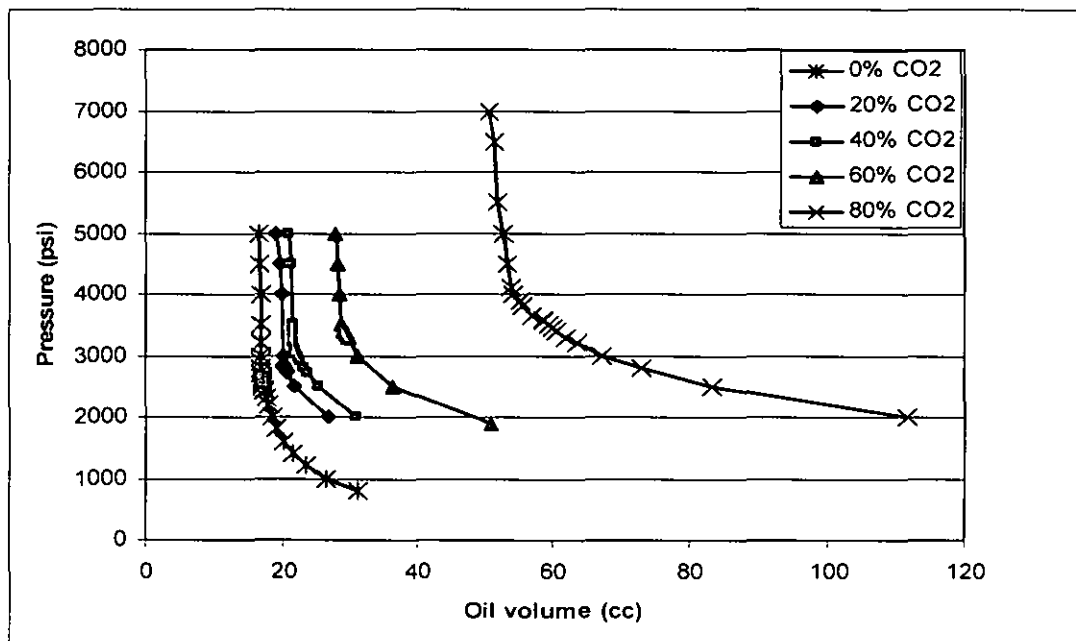
Table B.4 Relative volume and *Y*-function at 60% CO₂

Pressure (psig)	Rel volume (V/V _{sat}) (2)	Single-phase compressibility (V/V/psi)	<i>Y</i> -function (4)	Liquid Volume % (3)
5000	0.958			100
4500	0.970	2.43E-05		100
4000	0.983	2.61E-05		100
3500	0.997	2.97E-05		100
3400	0.998	3.66E-05		100
3370 (1)	1.000			
3350	1.003		2.286	99.015
3300	1.009		2.252	96.855
3000	1.060		2.052	77.194
2500	1.201		1.717	57.751
1900	1.583		1.316	34.736

2.4 Constant Composition Expansion at 80% CO₂

Table B.5 Relative volume and Y-function at 80% CO₂

Pressure (psig)	Rel volume (V/V _{sat}) (2)	Single-phase compressibility (V/V/psi)	Y-function (4)	Liquid Volume % (3)
7000	0.877			100
6500	0.898	2.30E-05		100
5500	0.910	2.70E-05		100
5000	0.954	3.31E-5		100
4500	0.944	3.88E-05		100
4100	0.964	4.28E-05		100
4000	0.988	4.79E-05		100
3880 (1)	1.000			
3800	1.007		3.043	7.094
3650	1.022		2.892	9.421
3600	1.027		2.842	9.754
3500	1.039		2.742	16.813
3450	1.046		2.692	15.878
3400	1.053		2.642	17.280
3300	1.069		2.542	19.313
3200	1.087		2.442	21.163
3000	1.130		2.241	22.866
2800	1.188		2.041	22.567
2500	1.315		1.741	24.812

Figure C.1 pressure vs. volume at different CO₂ concentration